DISSOLVING MICRONEEDLES FOR

CUTANEOUS DRUG AND VACCINE DELIVERY

A Dissertation

Presented to

The Academic Faculty

By

Leonard Yi Chu

In Partial Fulfillment

Of the Requirements for the Degree

Doctor of Philosophy in Bioengineering

Georgia Institute of Technology

October, 2009

DISSOLVING MICRONEEDLES FOR

CUTANEOUS DRUG AND VACCINE DELIVERY

Dr. Mark Prausnitz, Advisor
School of Chemical and Biomolecular
Engineering
Georgia Institute of Technology

Dr. Niren Murthy
Department of Biomedical Engineering
Georgia Institute of Technology

Dr. Richard Compans
Department of Microbiology and
Immunology
Emory University

Dr. Bruce Weniger
*Centers for Disease Control and
Prevention   (CDC)*

Dr. Valeria Milam
School of Materials Science and
Engineering
Georgia Institute of Technology

Date Approved:
October 23, 2009

ACKNOWLEDGEMENTS

My PhD has been a challenging and dramatic one. I am fortunate to work on cutting-edge technology in a world-class laboratory. Throughout the course of my scientific pursuit in the Drug Delivery Lab, I was given the opportunity to maximize my potential to strive for scientific contributions with the highest standard in all aspects under the guidance of my PhD advisor, Dr. Mark Prausnitz. Dr. Prausnitz has been a great influence on my personal development, professional communications and scientific research. His passion, patience, high standard, easy accessibility and supervision have enriched my PhD training and prepared me for future challenges. I would like to thank my advisor Dr. Mark Prausnitz and my thesis committee members Dr. Richard Compans, Dr. Valeria Milam, Dr. Niren Murthy and Dr. Bruce Weniger for their involvement, guidance and recommendations for my research and thesis.

I would like to thank Donna Bondy, our lab's administrative coordinator. Donna is the kindest and the most efficient person I have ever met. My research could not have progressed so efficiently and smoothly without her assistance. My research could not be completed without daily support from current and past lab members. I would like to thank Dr. Seong-O Choi for providing the microneedle master structure, which has served as the foundation for the development of microneedles in our lab. I would like to thank Samirkumar Patel who has devoted a tremendous amount of time ensuring proper functioning of computer hardware and software. I would like to thank Dr. Vladimir Zarnitsyn for being a great help in setting up, fixing and maintaining laboratory equipment. I would like to thank Samantha Andrews for her advice on histology. Samantha has also been a great companion in the conferences we attended together. I would like to thank Dr. Sean Sullivan and Dr. Jyoti Gupta for helpful

TABLE OF CONTENTS

LIST OF FIGURES AND TABLES

viii

LIST OF SYMBOLS AND ABBREVIATIONS

ANOVA	analysis of variance
BCA	bicinchoninic acid
BSA	bovine serum albumin
DI	deionized
ELISA	enzyme-linked immunosorbent assay
HA	hemagglutinin/hemagglutination
HAI	hemagglutination inhibition
H1N1	a subtype of influenza A virus
H&E	hematoxylin and eosin
IACUC	institutional animal care and use committee
IgG	immunoglobulin G
IIV	inactivated influenza virus
IR	infrared
LD50	lethal dose for 50% to die
MN	microneedle
NA	neuraminidase
OCT	optimal cutting temperature
P	a probability value to determine statistical significance
PDMS	polydimethylsiloxane
PLA	polylactic acid
PLGA	polylactic-co-glycolic acid
PR8	a strain of H1N1 influenza virus (A/Puerto Rico/8/34)
PVA	polyvinyl alcohol
PVP	polyvinylpyrrolidone
RBC	red blood cell
SU8	polymeric photoresist epoxy
TEM	transmission electron microscope
WSN	a strain of H1N1 influenza virus (A/WSN/33)

SUMMARY

Currently, biopharmaceuticals including vaccines, proteins, and DNA are delivered almost exclusively through the parenteral route using hypodermic needles. However, injection by hypodermic needles generates pain and causes bleeding. The needle itself poses risk of needle-stick injury. Disposal of these needles also produces biohazardous sharp waste. An alternative delivery tool called microneedles may solve these issues. Ideally, a skin delivery system should (i) deliver a broad range of therapeutics including chemical compounds, macromolecules and biologics, (ii) have a controlled dose with high bioavailability, (iii) be safe, (iv) be simple to use, and (v) be inexpensive. Current microneedle systems have addressed some of the requirements described above, but further characterizations and improvements are still needed. This project focused on one type of microneedles in which the needle tips dissolve upon insertion into the skin. The goal was to design and optimize dissolving microneedle fabrication processes for efficient drug and vaccine delivery to skin. This project also covered the formulation design and drying process for optimal vaccine stability. Finally, the microneedles were tested in vivo for influenza immunization.

The first goal was to develop new dissolving microneedle design and fabrication process for controlled drug loading, drug encapsulation and delivery with enhanced bioavailability in the skin. Due to the use of aqueous-based excipients for microneedle matrix, undesired drug diffusion within microneedles could occur during fabrication. To achieve high bioavailability, novel fabrication methods were developed to control drug diffusion by localizing the drug only in the microneedle tips. Deeper microneedle insertion was achieved by incorporating a pedestal for enhanced bioavailability.

The second part of the project focused on developing a new dissolving microneedle system called arrowhead microneedles. The key advantages of arrowhead microneedles include short administration time on the scale of seconds, full insertion of the needle tips into the skin and leaving no biohazardous sharp waste after use. Arrowhead microneedles could fully deposit the tips containing drug within the skin for expedited delivery. This rapid delivery could be achieved by two mechanisms: One relied on gradual dissolution of the tips within the skin; another one used mechanical force to separate the tips from the shafts. Upon insertion, the sharp microneedle tips were embedded within the skin while the dull shafts and backing could be quickly removed and disposed without concerns for needle stick injury and generation of biohazardous sharp waste.

After optimizing dissolving microneedle fabrication, structural design and delivery, we wanted to ensure the encapsulated molecules within microneedles remained stable. We encapsulated inactivated influenza virus within the dissolving microneedles made of a novel formulation consisting of polyvinyl alcohol and sucrose. The encapsulated vaccine samples were stored at 4°C, 25°C, 37°C, and 45°C under different packaging conditions. The results showed that the encapsulated vaccine maintained its hemagglutination potency, antigenic property and virus particle morphology over extended periods of time while the unprocessed vaccine suspended in solution lost virtually all hemagglutination activities and morphology within a few days. According to the results, we concluded that solid-state encapsulation of the vaccine in dissolving microneedles provided more potent stability over liquid-state vaccine.

Finally, based on all the optimizations of dissolving microneedles described in previous chapters, arrowhead microneedles encapsulating inactivated influenza virus vaccine were evaluated in vivo. Mice were immunized with a single dose using

arrowhead microneedles. The results showed that the immune responses as measured by virus-specific IgG levels 4 weeks after vaccination were statistically equivalent to the intramuscular injection of the same vaccine dose using hypodermic needles. The immunized mice were protected from lethal virus challenge.

We envision the newly developed dissolving microneedle system can be a safe, patient compliant, easy-to-use and self-administered method for rapid drug and vaccine delivery to the skin.

CHAPTER 1

INTRODUCTION

Skin offers an attractive site for drug and vaccine delivery. Being the largest organ of the body, skin is easily accessible and allows both local and systemic treatment. Unlike the oral administration, transdermal delivery bypasses poor absorption, enzymatic degradation in the gastro-intestinal track and metabolism in the liver [1, 2]. Transdermal drug delivery is mainly hampered by the presence of stratum corneum, the outermost layer of the skin. This tissue barrier prevents molecules larger than about 500 Da or hydrophilic drugs from entering into the body [3]. To deliver macromolecules or skin impermeable compounds effectively across the skin, the stratum corneum has to be altered, removed or disrupted.

The most commonly used tool for delivering therapeutics by injection is hypodermic needles. Although hypodermic needles can overcome the skin barriers effectively, these needles create pain, cause bleeding and generate sharp biohazardous waste. These issues decrease the willingness of patients to receive medication. Extreme cases of such fear can create needle phobia [4-6]. Incidents of needle-stick injury are common. Disposal of the needles can be costly and environmentally burdensome. Developing countries in particular have high incidence of needle misuse [7]. Due to lack of medical resources, sharing and reuse of needles are commonly seen. Such mishandling of needles promotes the transmission of blood-born pathogens including hepatitis B, HIV and other diseases.

To address the issues and limitations of hypodermic needles, we developed an alternative delivery tool called microneedles. Microneedles are micron-size needles that disrupt stratum corneum in a minimally invasive manner [8, 9]. The needles

target the epidermis and superficial dermis of the skin where abundant immune cells are present while keeping the deeper tissue undamaged. Some methods of drug delivery using microneedles have already been developed. For example, the skin can first be treated with microneedles followed by drug application at the treatment site [10-14]. Alternatively, the drug can be coated onto solid microneedles [15-17] or encapsulated within biodegradable [18, 19] or dissolving microneedles [20-23]. The drug is then released within the skin upon insertion.

The primary choice of microneedle in this project is dissolving microneedle. Dissolving microneedles are made of water-soluble excipients. The molecules of interest are encapsulated within the needles. Upon insertion, the microneedles dissolve and then release the encapsulated molecules within the skin. To study drug and vaccine delivery to skin using dissolving microneedles, the project covers four main areas:

1. To optimize the fabrication process of dissolving microneedles with controlled drug encapsulation, enhanced drug loading capacity with minimal drug wastage, and more complete insertion of the needle tips into skin for improved bioavailability.

2. To develop a novel microneedle system that requires a short administration time, results in complete insertion of the needle tips, and produces no sharp waste after use.

3. To study the stability of encapsulated vaccines in microneedles during microneedle processing and post-processing storage under different temperatures and different packaging conditions over extended periods of time.

4. To immunize mice using the newly developed microneedle system and evaluate the immune response.

CHAPTER 2

BACKGROUND

2.1 Drug Delivery

2.1.1 Overview of Drug Delivery

The U.S. annual sales of advanced drug delivery systems are approaching $20 billion and are growing rapidly [1, 24]. As new drugs and biopharmaceuticals continue to emerge, development of drug delivery systems for achieving optimal therapeutic effects is receiving increasing attention in the pharmaceutical, biotechnology and medical community.

Drug delivery system is a broad term for technology that sends drugs to the appropriate target site for generating therapeutically desirable effects. The technology can be largely divided into two categories: macro delivery systems that use medical devices, tools or various dosage forms to deliver drugs into the body; and particulate delivery systems that use micro- and nano-vehicles to encapsulate drugs and provide functionalities for delivery at cellular and molecular level. The scope of the thesis primarily focuses on the macro delivery systems, although the microneedles themselves are of micron dimensions.

Scientists have been exploring various delivery systems that send drugs into the body via different routes to achieve local and systemic prevention and treatment of diseases. Each route of delivery has its own advantages and disadvantages. Some methods of delivery are more invasive than the other. Oral administration of small molecules by swallowing oral dosage forms is the most common practice of medical

treatment due to its noninvasive nature. Because of the varying degree of absorption, metabolism and excretion from the body, a great deal of effort has been spent on controlled release of drug to achieve sustaining drug levels in the desirable therapeutic range. However, biopharmaceuticals taken orally face major challenges including poor absorption and enzymatic degradation in the GI track, and metabolism in the liver [1, 2]. To avoid these obstacles, biopharmaceuticals in particular are delivered through other routes including pulmonary, parenteral and transdermal.

Pulmonary delivery is another example of a noninvasive delivery method. Delivering drugs and biopharmaceuticals to the lung has been used to treat respiratory diseases such as asthma [25, 26] and cystic fibrosis [27]. The therapeutic effect of pulmonary delivery can be local in the upper respiratory tract and the lung or systemic if absorbed into the alveoli. The main advantage of delivery through the lung is the large absorption surface area with thin tissue lining and limited presence of proteolytic enzymes [28, 29]. One of the greatest challenges for pulmonary delivery is the reproducibility of delivery and delivery efficiency. The delivery efficiency typically lies between 20-50% of the drug administered to the lung [30].

The parenteral route is the most direct way of getting molecules into the body circulation. Injection of therapeutics through the skin into the blood stream or surrounding tissues produces high delivery efficiency within very a short administration time. This method of delivery is accomplished almost exclusively by needle-syringe system. However, the system's sharp hypodermic needle generates bleeding and pain, leading to low patient compliance and needle phobia, a symptom characterized by frightening reaction which includes plunging blood pressure and fainting [4-6].

Sending drugs into the body circulation while avoiding the first pass effect, skin offers an attractive option. Being the largest organ of the body, skin is very accessible

for local and systemic treatment. However, due to the presence of the outermost dominant barrier of the skin, the stratum corneum, only a limited number of drugs are able to pass through the skin passively. These transdermal drugs are subject to constraints including molecular size less than about 500 Da and octanol-water partition coefficients that highly favor lipids and small required dose up to miligrams [31]. To deliver chemical compounds or macromolecules beyond the constraints across the skin, chemical or physical methods that alter or remove the stratum corneum are required. Various methods and devices have been designed to facilitate the transport of molecules across the skin non-invasively or with minimal invasiveness. More details will be discussed in the following sections.

Other delivery routes include nose, vagina, eye, etc. These delivery routes are less commonly used due to accessibility. However, they are important and effective routes for local treatment of diseases.

2.1.2   Skin Anatomy
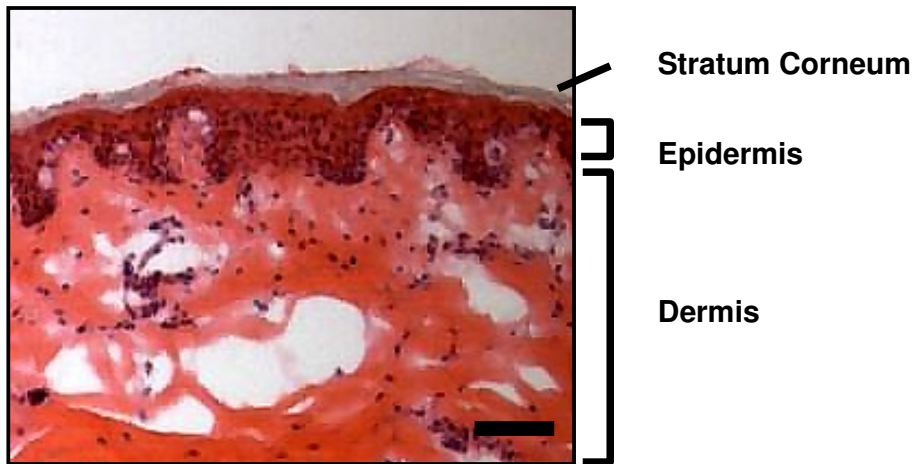
Fig. 2.1. Porcine cadaver skin stained with hemotoxilyn and eosin showing stratum corneum, epidermis and dermis. (Bar= 50 µm)

Skin is comprised of three distinct layers: stratum corneum, viable epidermis and dermis. Stratum corneum is the topmost layer of the skin. This layer consists of dead keratinocytes, also known as corneocytes, forming a 10~20 µm thick stack. Stratum corneum serves as the dominant barrier in limiting the passage of molecules from entering the skin. The structural arrangement of corneocytes in lipid bilayers is often described as the bricks and mortar of a brick wall [32]. Viable epidermis is the next deeper section of the skin. It is roughly 0.1 mm thick mainly consists of keratinocytes. The keratinocytes linked by desmosomes offer both structural strength to epidermis and resistance for passage of molecules across the epidermis [33, 34]. Beneath the epidermis layer is a 2 to 3 mm dermis layer containing capillaries, nerves, hair follicles and sweat glands. Below dermis is called the hypodermis where fat is the primary constituent [35].

Within the viable epidermis, there is an abundance of antigen presenting cells

including Langerhans cells, CD8+ and CD4+ T lymphocytes, mast cells and macrophages [36-39]. Langerhans cells, comprising about a quarter of the skin surface area, are believed to play a major role in cutaneous immunization upon stimulation [40]. Dermal dendritic cells, upon activation, bring antigen from the skin to draining lymph nodes and present the antigen to T helper lymphocytes for subsequent immune responses [35]. However, the specific mechanisms of the resulting immune response remain unclear.

2.1.3   Transdermal Delivery

Transdermal delivery represents an attractive alternative to needle-syringe system for several reasons. Transdermal delivery is a noninvasive method that sends drugs directly to the body circulation without going through the first pass effect. Earlier generation of transdermal delivery involves liquid spray, gel, topical formulation or patch, which serve as the reservoir for extended release of drugs into the skin. Examples of such products include testosterone gels, estradiol spray and contraceptive patches. The limitation of topical application lies upon the barrier function of the stratum corneum which permits only molecular size less than approximately 500 Da and highly lipophilic drugs to enter [3]. The new generation of transdermal delivery seeks to overcome the barrier function of stratum corneum by adding chemical enhancers that reversely alter the stratum corneum or introduce driving force to facilitate transport of molecules across the skin [41]. Chemical enhancers disrupt the organization of stratum corneum lipid bilayer by inserting amphiphilic molecules [42, 43]. Other chemical enhancers use supramolecular structures such as liposomes and denrimers to increase skin permeability and drug partition to the skin. More recently, biochemical enhancers use peptides to enhance

7

the skin permeability by forming transient pores in the stratum corneum [44, 45].

Iontophoresis uses a different approach that enhances transdermal delivery by applying an electrical current to drive molecules across the skin barrier [46, 47]. The delivery rate scales with the electrical current. Therefore, the drug release profile and dosing can be controlled for small molecules or larger highly charged molecules delivery [48]. Applications of iontophoresis include delivery of lidocaine and fentanyl for local anesthesia [49, 50] and pilocarpine to induce sweat for the diagnosis of cystic fibrosis [51, 52]. In addition to enhance skin permeation by electrical means, ultrasound, an oscillating pressure wave also has shown to enhance the flux of small molecules like lidocaine [53] and large biomolecules like insulin, heparin and vaccine [54, 55]. Ultrasound promotes the transdermal delivery by generating cavitation resulting from the oscillation and collapse of bubbles at the skin surface.

Stratum corneum can also be removed by physical means including thermal ablation, tape stripping, microdermabrasion using sandpaper and device. Thermal ablation uses heat to selectively perforate skin for microseconds to milliseconds without damaging deeper tissue [3, 56]. Animal studies have shown the thermal ablation successfully delivered human growth hormone and interferon alpha-2b into the skin [57, 58]. A repetitive stripping of stratum corneum using adhesive tape has shown to enhance the permeability of macromolecules such as low molecular weight heparin across the skin [59]. Similarly, abrasion using sandpaper against the skin has also shown to remove stratum corneum effectively for enhanced transdermal drug and vaccine delivery [60, 61]. Recently, studies have demonstrated that physical methods can remove stratum corneum selectively and completely using a microdermabrasion device in a more controlled and precise manner for an enhanced skin permeability [62].

Another physical method which does not involve removal, rather perforation of

stratum corenum is the use of microneedles. Microneedles are minimally invasive transdermal delivery tools that create micron-size channels in the skin, thereby allowing a wide range of drugs and biomolecules to pass through the skin. Details about microneedles are discussed in the next section.

2.2 Microneedles

2.2.1 Development of Microneedles
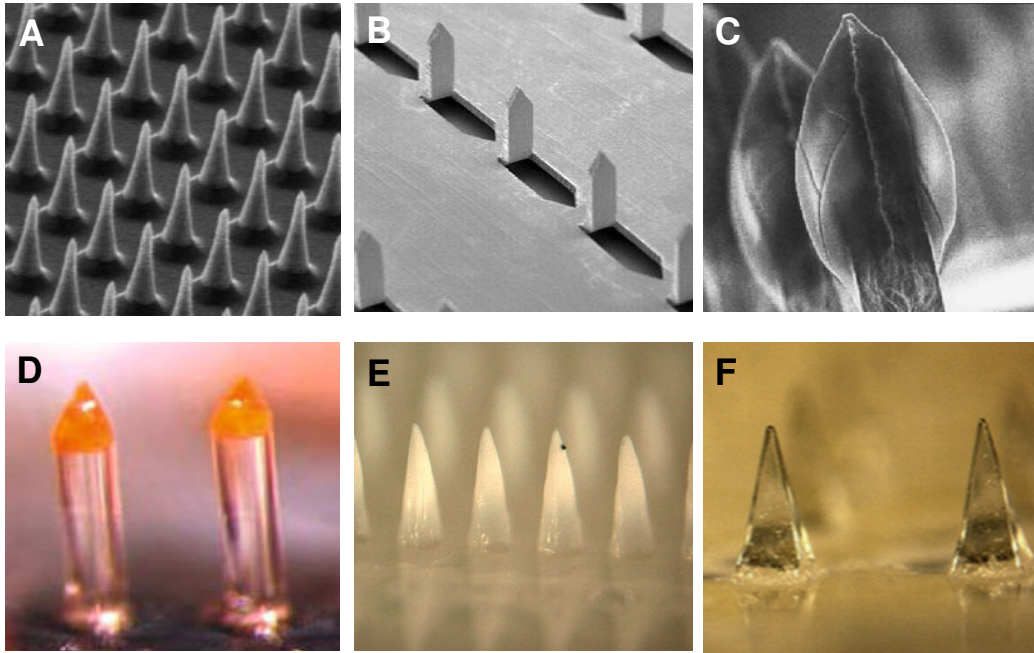
Fig. 2.2. Different types of microneedles: (A) Silicon microneedles [63]. (B) Metal microneedles [15]. (C) Coated metal microneedles [16]. (D) Biodegradable polymer microneedles [19]. (E) Dissolving PVP microneedles [22]. (F) Dissolving CMC microneedles [23].

Microneedles are arrays of microscopic needles that enable active delivery of a wide range of molecules into the skin. The concept of microneedles is a combination of hypodermic needles and transdermal patches. Microneedles contain sharp tips that disrupt the stratum corneum but are not long enough to cause damage to the deeper tissue. Microneedles are also assembled and applied like a patch onto skin as a minimally invasive delivery method. Studies have shown that the microneedle insertion on human subjects can have minimal sensation of pain [64, 65].

There are several types of microneedles that adopt different mechanisms of

delivery. Solid microneedles can be used to enhance skin permeation by creating holes for subsequent drug application on the microneedle-treated skin site [10-14, 66]. Drugs can also be directly coated on the solid microneedles and are released within the skin upon insertion [15-17]. Hollow microneedles, similar to hypodermic needles except the needles are fabricated into micron size, contain channels for drug solution to flow through. In this project, solid microneedles are of primary interest; hollow microneedles will not be mentioned further, because they are more difficult to make and use.

Solid microneedles were first introduced as microfabricated needles etched out of a silicon substrate. Those needles are extremely sharp with radius of curvature < 1 µm which facilitates piercing into the skin [63, 67]. Since silicon is brittle, not biodegradable and not proven biocompatible in the human body [68], any fracture of silicon microneedles in the skin may raise health concerns. Metal has been used as an alternative material to silicon for microneedle fabrication [69-71]. Needles made of metals are mechanically robust, and some are known to be biocompatible [72], although metal needle breakage in the skin is still undesirable. Lasers can pattern microneedles on metal sheets into rows of in-plane needles or arrays of needles that will be bent out-of-plane. A wide range of molecules from chemical compounds to biomolecules can be coated onto the needle substrate [15, 73]. Since metal needles are made sharp and not degradable, for safety reason proper disposal of the sharp waste is required.

To address the non-biodegradable disposal problem, biodegradable polymer microneedles have been introduced. These polymer microneedles are made by molding at high temperature. The drugs of interest are encapsulated within, instead of coated on, the biodegradable needles. Upon insertion, the polymer slowly degrades within the skin for controlled release [19, 74]. Needle fracture within the skin would

11

not pose a concern since the chosen polymers used for microneedle fabrication are biodegradable into safe degradation products and will ultimately be excreted from the body. However, fabrication of biodegradable polymer microneedles requires high temperature, which can damage the encapsulated heat-sensitive drugs and biomolecules. In addition, biodegradable polymer microneedles (e.g. poly (lactic) acid) require weeks to months to degrade. Continuous wearing of biodegradable microneedle patch for months is unappealing. Nevertheless, biodegradable polymer microneedles are expected to be safe to administer and pose little environmental waste hazard.

2.2.2 Dissolving Microneedles

Another type of polymer microneedles is made entirely of water-soluble excipients. These water-soluble microneedles, also known as dissolving microneedles, dissolve rapidly upon insertion into skin, leaving no biohazardous sharp waste. Since drugs or biomolecules are encapsulated within the water-soluble matrix, the drug release profile largely depends on the dissolution rate of the microneedles within the skin. There are a number of ways to fabricate dissolving microneedles using different materials and adopting different fabrication techniques. Molten-based dissolving microneedles are made by melting excipients at an elevated temperature and then cooling to form a solid structure [20, 75]. Dissolving polymer microneedles can also be made by drying long-chain polymer solution using desiccants, centrifugal force or ventilation [21, 23, 76]. These fabrication processes are carried out at ambient temperature, which avoids thermal damage to the encapsulated drugs or biomolecules. Other method of fabricating dissolving microneedles involves the use of UV light to polymerize monomers into polymers in the absence of water or other solvents [22].

The main advantage of dissolving microneedles is the safety of use.   Because the sharp needle tips dissolve and disappear upon insertion, there are no concerns for fracture of the needle tips within the skin, and reuse or sharing of the needles among patients. However, the key limitation for dissolving microneedles is their mechanical properties. High-aspect ratio structure increases the chance of premature needle fracture upon insertion into the skin [18] whereas low-aspect ratio needles may not insert into the skin completely [23]. To address the limitations of microneedles in general, this thesis devotes two chapters to discuss new findings regarding the improvements on dissolving microneedle design, fabrication and delivery.

2.3 Formulations

2.3.1 Pharmaceutical Excipients

An excipient is an inactive ingredient added to the active ingredients of a medication to aid the delivery. For example, many medications in powder form are difficult to administer orally, exicipients can bulk up the size of the medications into oral dosage form for the ease of dosing, handling and swallowing. In some cases, the medications may not be easily absorbed or be able to reach the target site in the body. In this case, excipients can facilitate absorption, offer protection against environmental change and control release profile of drugs in the body. The classification of excipients into functional categories depends on the roles they serve in the given route of administration and the form of medication. Due to the presence of a vast number of excipients and functionalities, the following sections only address excipients and functionalities that pertain to this project's microneedle fabrication and design.

2.3.2 Binders

The term "binder" is used to describe an excipient that holds the active and inactive ingredients together. This is common in pharmaceutical oral dosage forms in which the binders help the formation of tablets or granules for the ease of handling and ingestion. Another principle role of binders is to offer mechanical strength to the dosage form. Formulations used for microneedle coating solution and dissolving microneedle fabrication contain binders such as carboxymethyl cellulose, dextrin and

xanthan gum as the mechanical support [21, 23, 73]. For coated microneedles, long chain polymers such as methyl cellulose, hydroxypropyl cellulose, polyethylene glycol and polyvinyl alcohol also serve as the viscosity enhancers for successful control of coating and dosing [15].

In this project, the chosen binder for making dissolving microneedles is polyvinyl alcohol (PVA). PVA is a water soluble synthetic polymer. Its physical characteristics depend on the degree of hydrolysis of polyvinyl acetate during manufacturing. In general, the polymer is considered harmless. It has been used widely since the 1930s in industrial, commercial, pharmaceutical and food applications. Moreover, it is approved in several medical applications including transdermal delivery, oral administration and ophthalmic solution such as synthetic tears. PVA is included in the FDA Inactive Ingredient Guide [77] for topical application, transdermal delivery, intramuscular injection, ophthalmic solution, and oral tablet. The solubility in aqueous solution and biodegradability of PVA make this polymer an excellent candidate for formulation preparation and medical device fabrication.

Disposal of medical parts made of PVA is environmentally harmless. Several microorganisms with ubiquitous presence in artificial and natural environments have shown to degrade PVA by enzymatic processes [78]. The absorption, distribution and excretion of orally administered PVA (MW < 50,000) in rats have also been evaluated. Studies found that greater than 98% of ingested PVA was recovered in feces within 48 h, less than 0.2% was found in urine and accumulation in the tissue was not detectable [79]. Toxicological studies of oral administration including acute toxicity, genotoxicity and reproductive toxicity all have shown that PVA is relatively harmless even at relatively high doses [80-83].

2.3.3 Fillers

Fillers in pharamaceutical terms means the excipients used for bulking up the size and providing the shape to a dosage form. The proper size and shape is important for the convenience of patients to handle the medication. Fillers also provide proper filling of the microneedle mold during dissolving microneedle fabrication. Fillers are generally very water soluble; they can be prepared into highly concentrated solution without much viscosity contraint. Therefore, fillers offer a complementary role to the binders when the formulated solution is approaching its solubility and viscosity limit. Fillers used in this project include polyvinylpyrrolidone (PVP) and sugar molecules (sucrose, trehalose, maltodextrin).

PVP is a water-soluble polymer made from monomer N-vinylpyrrolidone. It readily dissolves in water. It is a poor viscosity enhancer; therefore it can be prepared into highly concentrated polymer solution. PVP has been used in a number of industries including pharmaceuticals, food, beverage, cosmetic, toiletry and photography [84]. According to the FDA Inactive Ingredient Guide [77], PVP is used in transdermal delivery, oral dosage forms, inhalation, and ophthalmic solution. The toxicity of PVP K-30 (average MW ~ 40,000) has been evaluated in rats by topical application to the skin, inhalation and oral administration. PVP is considered safe and no significant toxic effects were reported [85]. However, there have been some concerns for PVP retention in the body. Studies have shown that injection of high dose of PVP with molecular weight > 100,000 can cause labeled PVP thesaurosis or PVP storage disease [86]. Injection of PVP with molecular weight < 20,000 resulted in better body clearance; greater than 90% is excreted in the urine and feces within 48 h and only less than 1% PVP is left at the injection site [87].

Sugars are essential to human nutrition.   This project used three types of sugar as the fillers for dissolving microneedle fabrication, namely sucrose, trehalose and maltodextrin. Sucrose is a disaccharide of glucose and fructose. Trehalose is also a disaccharide formed by an α, α-1, 1-glucoside bond between two α-glucose units. Maltodextrin is a short chained soluble starch sugar made from hydrolysis of starch. All three sugars are absorbed and metabolized into glucose, the primary energy source for cells and proper function of human body. Sucrose and Trehalose are known for their high water retention capabilities. In addition to serving as additives in the food industry, these sugars have been used in many pharmaceutical formulations. For example, bevacizumab, marketed as Avastin, contains α,α-trehalose dihydrate.

2.4 Influenza Vaccine

2.4.1 Influenza Virus
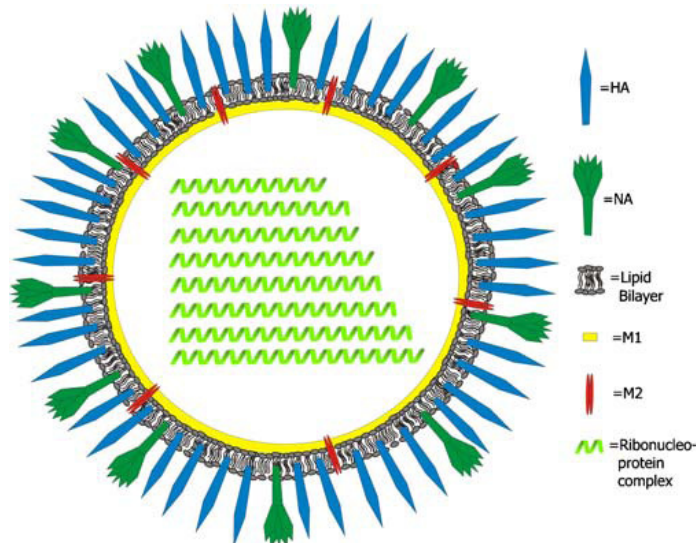
Fig. 2.3. A schematic drawing of an influenza virus. HA: hemagglutinin; NA: Neuraminidase; M1: Matrix protein; M2: Proton channel. [88]

Influenza spreads rapidly and imposes considerable burdens in economy and health care cost. The annual epidemics are thought to cause three to five million cases of severe illness and 250,000 ~ 500,000 deaths annually around the globe [89]. Most deaths currently associated with influenza in industrialized countries occur among the elderly over 65. Not much is known about the impact of influenza in the developing world. However, there are cases indicating that influenza outbreaks can result in massive deaths within a short period of time [89].

Influenza viruses are divided into three groups, A, B and C. The surface of influenza viruses is coated with spike-like antigens, namely hemagglutinin and neuraminidase. Due to frequent minor genetic changes in the viruses, known as the

antigenic drift, annual reformulation of vaccines is necessary to fight specifically against influenza subtypes [90].

Various influenza vaccines have been used for more than 60 years such as inactivated vaccines. A more recently used influenza vaccine includes live, attenuated vaccines. The inactivated whole-virus form is the chosen vaccine for this project. The amount of vaccine given to patients typically is one dose; equivalent to 15 µg of vaccine [91]. For trivalent vaccine containing three strains, 45 µg of antigen is given [92].

2.4.2   Influenza Vaccine Stability

Almost all influenza vaccine today is formulated into liquid. The presence of dynamic chemical and physical interaction in aqueous solution leads to a limited life-time of vaccine stability. There are a number of factors that can be used to determine the stability of influenza vaccine, including hemagglutinin content, presence of neuraminidase, pH and visual appearance of the vaccine solution [93]. Hemagglutination potency is a sensitive parameter for stability determination [94]. Long term stability studies are typically carried out by following the ICH guidelines [95, 96]. Due to temperature sensitivity of inactivated influenza vaccine, either elevated temperature or freezing can damage and denature the vaccine antigens [93, 97, 98]. Therefore, inactivated influenza vaccine must be stored at temperature from 2°C to 8°C for maintenance of its optimal quality. This narrow temperature range poses a major challenge for keeping the vaccine stable during transport and distribution.

2.4.3 Cold Chain

Cold chain is defined as a series of temperature controls during transport, storage and distribution of shipments from the site of manufacturing to the final destination of delivery. In many cases, cold chain involves constant monitoring of the goods and requires special packaging. For example, vaccine vial monitors (VVMs), a type of time-temperature indicator, prevent the usage of vaccines that have had prolonged exposure to elevated temperature. For influenza vaccines, as well as many other drugs and biopharmaceuticals, the temperature is typically set between 2 °C to 8 °C (-30°C to 5°C for some) [99]. Cold chain is critical for transport of vaccines to distant regions with hot climates, particularly in the developing world. Disruption of cold chain can lead to mass vaccine wastage. Historically there were cases in which the cold chain was disrupted by wars. Vaccine wastage may also result from other causes such as the expiration of vaccine or thermal damage (including freezing) due to improper handling or equipment failures in the cold chain [100].

2.4.4 Drying Methods

Ideally, influenza vaccines that are stable at freezing condition, room temperature, and even transient elevated temperatures would reduce the reliance on cold chain. In an attempt to produce a more stabilized vaccine formulation, one method is to convert liquid vaccine into dry powder form. The methods of drying biopharmaceuticals including proteins, vaccines and macromolecules for enhanced stability have already been established and practiced. Much evidence has supported the general statement that biopharmaceuticals in a dry state are more stable than in a liquid state. The reasons for better stability in solid state can possibly be attributed to

less mobility and vibration of the molecules, absence of actively mobile degradative enzymes and hydrolysis. However, the process of drying (and/or freezing) may induce stress to the structural integrity, thereby changing the conformation and thus the activity of the molecules.

There are a number of drying methods; each has its own advantages and disadvantages. Although the quality of drying method also depends on the vaccine formulation, the details of incorporating stabilizers in the formulation for drying will be discussed in the next section. When given vaccination using a needle-syringe system, dried powder vaccines need to be reconstituted into solution. On the other hand, dried powder vaccines can be used directly in alternative delivery methods including nasal, pulmonary or epidermal delivery by means of inhalation or PowderJet-injection [101, 102]. In this project, two drying methods have been adopted. These methods are described below:

Freeze drying, also known as lyophilization, is a process involves freezing of sample and then removing solvent (most cases are water) by sublimation (direct transition from solid to gas phase) under high vacuum. Generally, lyophilization is the preferred method of drying biopharmaceuticals [103]. Lyophilization can be divided into three stages: freezing, primary drying and secondary drying [104]. The rate of freezing is critical; generally it is preferred to freeze the sample instantly instead of gradual cooling. Slow freezing can increase the chance of protein degradation due to prolonged exposure to phase separation. Slow freezing also encourages biomolecular degradation as the solute becomes more and more concentrated [105]. The next stage is primary drying. Primary drying is a process that removes water from the frozen sample by sublimation. During the drying cycle, the ice is transferred from the sample to the condenser where the pressure is well below the vapor pressure of ice. Majority of water is removed by the end of the primary drying cycle. Next, the secondary

drying further reduces the residual moisture left from the primary drying to achieve a moisture level less than 1%. During the secondary drying process, more energy is required to remove the residual water by desorption. Thus, this drying process typically operates at a much higher temperature than the primary drying.

Other speedier drying processes other than air-ventilation that are applicable to drying microneedles are vacuum drying and desiccation. Vacuum drying is a process of reducing the pressure such that the boiling point of water becomes lower than the sample temperature. Desiccation involves drying samples with a hygroscopic substance such as dry silica gel or anhydrous caustic soda (desiccants) in a sealed container (desiccator). The advantages of these two processes are low cost and can be carried out at ambient temperature without subjecting to heat or freezing stress.

2.4.5   Stabilizers

Solely drying vaccines into solid state does not guarantee the long-term stability, even if the drying process itself does not cause damage to the vaccines. Vaccine formulation also plays a critical role in long-term stability. This project used trehalose and sucrose as the primary stabilizers for lyophilizing the encapsulated influenza vaccine. Numerous studies have shown that sugars offer stability to proteins [106-109], liposomes and viruses [110, 111] during drying and subsequent storage. When properly dried with sugars, the molecules become embedded in the amorphous sugar in its glassy state. Studies have offered several explanations to the enhanced stability of biopharmaceuticals in sugar glass. The sugar glass acts as a coating that provides the barrier to prevent molecules from aggregating [112]. The sugar glass matrix also reduces the lipid diffusion and molecular mobility (vitrification), thereby preventing degradation [113]. During the drying process, the sugars replace water

molecules for the hydrogen bond interactions with the active ingredients to preserve

their structural integrity [114].

2.5　Immunization with Influenza Vaccine

2.5.1　Methods of Immunization

Injection using hypodermic needles is still the primary method of vaccination of inactivated virus vaccines or split vaccines. But this method has some issues including pain, potential disease transmission if misused, needle-stick injury and disposal of biohazardous sharp waste. To address these issues, other delivery methods such as tape stripping, microneedles, thermal ablation, electroporation, and jet injection have been used to deliver vaccines [35]. The scope of this project only covered cutaneous immunization using microneedles.

Microneedle's ability to target immune cells in the epidermis makes it an excellent candidate for cutaneous vaccination. Modified vaccinia virus (a virus particle representative of some vaccines) has been shown to be uniformly coated on stainless steel microneedles [15]. Ovalbumin, a well-characterized antigen, has been coated with different doses on the Macroflux solid microneedle array for immunization studies in hairless guinea pigs. These immunization studies have shown that the induced immunization by microneedle arrays was comparable with intradermal vaccine delivery by hypodermic needles. At low doses the microneedle immunization was superior to IM delivery [115]. Influenza vaccination in rats has been carried out using a 34 Ga single hollow microneedle with a total exposed length of 1 mm. Dose sparing was achieved in some cases but the extent of dose sparing varied depending on the vaccine employed and the strain of influenza virus [116]. Recently, immunization of mice using solid microneedles coated with inactivated influenza virus has shown to generate an equivalent immune response compared to

intramuscular injection using hypodermic needles [117, 118]. However, more in vivo studies still need to be carried out to determine whether or not "microneedle vaccination" is superior to intramuscular vaccination using hypodermic needles.

2.5.2   Vaccination in Developing Countries

In 1974, the World health Organization (WHO) initiated the Expanded Program on Immunization (EPI) that aimed to immunize the world's children against six diseases (diphtheria, tetanus, whooping cough, poliomyelitis, measles, and tuberculosis). The initiative was particularly challenging in the developing world at that time because less than 5% of the children were fully immunized and health infrastructure was missing [119]. In 1991, WHO and UNICEF announced that 80% of the world's children were immunized with the EPI vaccines. While some regions, particularly in Africa, remained below the average of global immunization, the efforts of immunization programs have been shown effective, especially in Latin American where polio has been eliminated [119, 120]. According to the 1993 World Development Report compiled by the World Bank and WHO, communicable and perinatal diseases caused 60% of the disease burden of children under 14 and 80% of deaths of children under 5 in developing countries [121]. Although many of those diseases could be prevented by vaccines, the vaccines were not readily available in developing countries. Therefore, it is clear that developing countries are in need of vaccination for infectious disease prevention. However, the lack of trained personnel, facilities and capital impedes access to appropriate medical care. Three major problems associated with mass vaccination in the developing world are identified: vaccination cost, unsafe use of hypodermic needles, and vaccine storage.

High vaccination cost is one of the primary reasons for shortage of vaccine

supply to the developing world. The cost is a comprehensive sum of vaccine manufacturing cost, delivery tool cost, transport and storage expenses, and trained personnel wages. A breakdown of immunization costs shows that out of the total cost of US $15 every full immunization against the six mentioned diseases, more than $14 are spent on infrastructure including personnel and only less than $1 for the vaccines [119]. Based on the cost breakdown, elimination of infrastructure and personnel cost would drastically reduce the cost burden of vaccination.

To avoid any additional cost, unsafe practices such as needle sharing or reuse in the developing world are common. It is estimated that 8-12 billion injections are given in health care settings globally each year [122, 123]. Unsafe practices account for more than 50% of the injections in developing countries [7]. Consequently, disease transmission such as hepatitis B and C, human immunodeficiency virus and other blood-borne pathogens has given rise to another health care issue.

Another vaccination issue comes from transport and storage. From manufacturing to actual vaccine administration, the process is not a simple shipment of goods. Most vaccines require a storage temperature ranging from 2°C~8°C [124]. Exposure to heat will reduce the vaccine shelf life [125]. Freezing will also cause irreversible damage to the vaccines that cannot be frozen [126, 127]. Cold chain, defined as a process carried out at a certain temperature range, is adopted for vaccine storage and transport. This process requires cold rooms and refrigerators for proper storage. Additional monitors and freeze indicators are often included in shipments. As a result, cold chain is an expensive process that shows no guarantee to the vaccine quality due to the vulnerability of liquid formulated vaccine to external temperature variation.

To lower the cost of vaccination, to eliminate biohazardous sharp waste and needle reuse, and to store vaccine without specialized facilities or equipments, this

project aimed to improve and design new microneedle systems that address all of

these problems for the benefit of health care in both industrialized and developing

world.

CHAPTER 3

Fabrication of Dissolving Polymer Microneedles

for Controlled Drug Encapsulation and Delivery:

Bubble and Pedestal Microneedle Designs

Leonard Y. Chu[1], Mark R. Prausnitz[1,2,*]

[1] Wallace Coulter Department of Biomedical Engineering,
Georgia Institute of Technology, Atlanta, GA 30332
[2] School of Chemical & Biomolecular Engineering,
Georgia Institute of Technology, Atlanta, GA 30332
* corresponding author (prausnitz@gatech.edu)

3.1 Abstract

Dissolving microneedle patches offer promise as a simple, minimally invasive method of drug and vaccine delivery to the skin that avoids the need for hypodermic needles. However, it can be difficult to control the amount and localization of drug within microneedles. In this study, we developed novel microneedle designs to improve control of drug encapsulation and delivery using dissolving polymer microneedles by (i) localizing drug in the microneedle tip, (ii) increasing the amount of drug loaded in microneedles while minimizing wastage, and (iii) inserting microneedles more fully into the skin. Drug localization in the microneedle tip was achieved by either casting a highly concentrated viscous polymer solution as the needle matrix or incorporating an air bubble at the base of the microneedle to prevent drug diffusion into the patch backing. As another approach, a pedestal was introduced to elevate each microneedle and thereby increase its drug loading capacity. The pedestal also enabled more complete microneedle penetration into the skin to ensure a greater percentage of the drug encapsulated in the microneedle was delivered into the skin. Altogether, these novel microneedle designs provide a new set of tools to fabricate dissolving polymer microneedles with improved control over drug encapsulation, loading and delivery.

3.2   Introduction

Transdermal delivery as an alternative route to parenteral administration has gained increasing attention. A number of different transdermal patches delivering molecules less than approximately 500 Da and high lipophilicity such as nicotine, fentanyl and estrogen have been introduced commercially with significant clinical impact [3]. However, delivering biologics in the form of proteins or whole micro-organisms across intact skin is extremely difficult due to the presence of stratum corneum, i.e., the outer most layer of the skin. To overcome this skin barrier, microneedles offer a minimally invasive method that disrupts the stratum corneum in a relatively painless way [8, 128, 129]. Skin offers an excellent site for drug and vaccine delivery partly because delivering molecules via the skin bypasses intestinal and hepatic first-pass metabolisms. Moreover, the abundant presence of dendritic cells and Langerhans cells also makes skin an attractive site for vaccine delivery. Numerous studies have shown that the delivery of vaccines to the skin using intradermal injection or other methods that overcome the stratum corneum barrier effectively triggered immune response in animal models [130, 131].

Ideally, a skin delivery system should (i) deliver a broad range of therapeutics including small molecule drugs, macromolecules and biologics, (ii) have a controlled dose with high bioavailability, (iii) be safe, (iv) be simple to use, and (v) be inexpensive. Traditional non-invasive transdermal patch systems are simple to use and inexpensive, but the choice of therapeutics is limited to small molecules due to the presence of stratum corneum. In some cases, chemical enhancers have been used to facilitate the transport of molecules across the skin, but skin irritation can be a limitation [42, 132]. Other approaches have included supramolecular structures, such

as liposomes and emulsions, as well as physical approaches, such as iontophoresis, ultrasound, and thermal ablation [9, 133]. However, each method has shortcomings and has made only limited clinical impact to date.

Recently, microneedles have shown the capability of delivering a variety of molecules into the skin, including drugs and vaccines [10, 14-16, 21, 75, 134-136]. Microneedles are micron-scale needles that are produced by adapting the tools of the microelectronics industry. Microneedles pierce across the stratum corneum and into the epidermis and/or superficial dermis to administer compounds into the skin for local or systemic administration. Microneedles can be assembled into patches, which offers simplicity of use and low cost similar to conventional transdermal patches. Studies have shown that coated microneedles can carry a controlled dose by coating the drug only onto a defined region on the needle substrate surface [15, 16, 117]. The coated drug is released from the microneedle upon insertion into the skin. A drawback of this approach, however, is that such microneedles leave behind sharp, biohazardous waste after use, which may present safety concerns and special disposal needs.

Dissolving polymer needles have been developed by making microneedles out of water-soluble polymer that encapsulates drug within the needle matrix and fully dissolves upon insertion into the skin, thereby eliminating sharp biohazardous waste [20, 21, 23, 137, 138]. Thus, dissolving microneedles appear to be an attractive drug delivery system, because they are designed to deliver a wide range of therapeutics, are easy to use, are inexpensive, and leave no sharp waste after use. However, it can be difficult to control the dose encapsulated and delivered from polymer microneedles due in part to drug diffusion within the water-soluble microneedle matrix during fabrication.

This study seeks to improve upon dissolving microneedle design by better controlling drug encapsulation and delivery. More specifically, we seek to overcome

the difficulties of controlling, loading and delivering a specified drug dose with dissolving microneedles using novel approaches that (i) localize drug only in the microneedle tip, (ii) increase the amount of drug loaded in microneedles while minimizing wastage, and (iii) insert microneedles more fully into the skin. To localize drug only in the microneedle tip, we prevented drug diffusion out of microneedles during fabrication by either using a highly concentrated polymer solution to increase viscosity or introducing an air bubble at the base of the needle that constrained the drug from diffusing into the backing. To increase the amount of drug loaded in microneedles while minimizing wastage, we added a pedestal at the base of the microneedle to provide extra volume to each microneedle, thereby increasing their overall drug loading capacity. Finally, to insert microneedles more fully into the skin, we again used the pedestal design to provide higher aspect-ratio microneedles capable of inserting more fully into the skin, but with sufficient mechanical strength to avoid failure during insertion.

3.3   Materials and Methods

3.3.1   Fabrication of Microneedles

3.3.1.1   Microneedle Molds

Pyramid microneedle mold. A mold of a 10 x 10 array of 300 x 300 x 600 µm
(W x L x H) pyramidal microneedles was fabricated using photolithography and
molding techniques described previously [139, 140]. Briefly, a pyramidal microneedle
mold was created by exposing SU-8 photoresist (SU-8 2025, Microchem, Newton,
MA) to ultraviolet light. A microneedle master structure made out of
polydimethylsiloxane (PDMS) (Sylgard 184, Dow Corning, Midland, MI) was
molded off the SU-8 mold and coated with gold. Next, a PDMS mold replicate was
created from the gold-coated master structure. Then, polylactic acid (PLA) (L-PLA,
1.0 dL/g; Birmingham Polymer) was melted at 195°C under vacuum to fill the mold
replicate and make a PLA master structure replicate. Finally, a PDMS mold replicate
was made from the PLA master structure replicate.

Pedestal microneedle mold. A pedestal microneedle mold was made by aligning
a PDMS microneedle mold containing a 10 x 10 array of 300 x 300 x 600 µm (W x L
x H) pyramidal cavities with two laser-cut stainless steel sheets each containing a 10 x
10 array of 340 x 340 x 150 µm (W x L x H) non-tapered through-holes. The pattern
of the non-tapered through-holes was first drafted in AutoCAD software (Autodesk,
Cupertino, CA) and then cut into 150 µm stainless steel sheets (McMaster-Carr,
Atlanta, GA) using an infrared laser (Resonetics Maestro, Nashua, NH) at a cutting
velocity of 1 mm/s with 10% attenuation of laser energy. The laser-cut metal sheets
were electropolished (E399 electropolisher, ESMA, South Holland, IL) for 10 min at
2 A in a 74°C mixture of glycerin, 85% ortho-phosphoric acid and water (6:3:1 by

volume) (Fisher Scientific, Fair Lawn, JN). The electropolished metal sheets were washed briefly with 30% nitric acid solution at room temperature and blow-dried with nitrogen gas. Individual metal arrays patterned with 10 x 10 through-holes were detached from their mother electropolished metal sheet. Each metal array was then coated with a thin PDMS film by dipping into a pre-cured PDMS and spinning at 672 x g for 1 min (GS-15R, Beckman, Fullerton, CA). Two 150 µm-thick metal arrays coated with PDMS were aligned and stacked on top of the PDMS mold. An integrated metal-PDMS composite mold was formed as the PDMS coating adhered the metal sheets and PDMS mold together upon curing at 150°C for 10 min.

Extended pyramidal microneedle mold. Extended pyramidal microneedle master structure was made by trimming off the projected portion of the 340 x 340 x 300 µm pedestal into a tapered structure with an extended microneedle base of 300 x 300 x 300 µm (W x L x H) using a razor blade (VWR). Polyvinyl alcohol (PVA) (MW 2000, ACROS Organics) was dissolved in DI water (50 wt %) and was used to smoothen the rough surfaces of the tapered needle structure. The viscous polymer solution was applied and then coated onto the tapered microneedle structure by centrifuge at 3200 x g at 25°C for 1 hr. After the polymer film was centrifuge dried, extended pyramidal microneedle mold was made by curing the PDMS on top of the extended microneedle structure coated with a PVA film at 37°C overnight.

3.3.1.2 *Preparation of Microneedle Matrix Material*

The microneedle matrix material was a polymer blend consisting of polyvinyl alcohol (PVA, MW 2000) (ACROS Organics) and polyvinylpyrrolidone (PVP) (BASF, K17, Aktiengesellschaft, Ludwigshafen, Germany) (ratio 3:1). To make a 50 wt % polymer solution, 3 g PVA was dispersed in 4 ml DI water and heated at 60°C for 3 h.

Then, 1 g PVP was added to the PVA solution and mixed thoroughly using a spatula. The polymer blend was incubated at 37°C in a sealed glass bottle overnight. Similarly, 30 and 40 wt% polymer solutions were also prepared. Unless indicated, a 50 wt% polymer solution was used to fabricate the microneedles.

3.3.1.3 Drug Loading into the Mold

Sulforhodamine B (Molecular Probes, Eugene, OR) was used as the model drug and was dissolved in DI water to prepare stock solutions at concentrations of 1 mg/ml and 10 mg/ml. Two methods of drug loading were used for different studies. The first method was a two-step process that first loaded and dried the drug solution in the mold cavities and then cast the polymer solution into the mold. This method created a drug gradient in which the tip of the microneedle had the highest concentration. Sulforhodamine stock solution was pipetted onto the top of a PDMS mold to cover the cavities and then was vacuumed at room temperature to – 91 kPa for 3 min. After vacuuming, residual sulforhodamine on the mold surface was pipetted off and recycled for reuse. The PDMS mold filled with sulforhodamine was then dried under centrifugation at 3200 x g at room temperature for several minutes. Dried sulforhodamine adherent to the mold surface was removed by Scotch tape (3M, St. Paul, MN). The second method involved the direct casting and drying of a pre-mixed drug and polymer solution, as described below. Using this method, the drug was uniformly distributed within the microneedle matrix upon drying.

3.3.1.4 Polymer Casting into the Mold

Approximately 150 µl PVA/PVP blend solution was applied to cover the entire array of microneedle cavities in the mold. The mold covered with polymer solution was vacuumed at room temperature to – 91K Pa for 5 min. To fabricate solid microneedles, the residual polymer on the mold surface was left to dry at room temperature. To make bubble microneedles, the residual polymer was spun off by centrifuging at 3200 x g at room temperature for 5 min and then dried at room temperature.

3.3.1.5 Backing Assembly

The backing layer was assembled differently for solid and bubble microneedles. To assemble the backing for bubble microneedles, a small piece of office paper (approx. 1 cm x 1cm) was coated with a thin film of a highly concentrated PVA/PVP solution and placed on top of the mold after polymer casting and drying. The assembled mold was then dried at room temperature over night. For solid needles, no additional backing assembly was done, because the residual polymer left on the mold surface was used as the backing after drying. In both cases, after the microneedles and backing were both dried, the resulting microneedle array was detached from the mold using double-sided adhesive tape (444 Double-Sided Polyester Film Tape, 3M,). The microneedle array was then attached to a SEM mount (Structure Probe, West Chester, PA), which served as the handle to facilitate manual handling and insertion into the skin.

3.3.2   In Vitro Microneedle Insertion Assessment

3.3.2.1   Microneedle Insertion into Skin

Porcine cadaver skin (Pel-Freez, Rogers, AR) was shaved using a razor (Dynarex, Orangeburg, NY). The skin's subcutaneous fat was removed by a scalpel (Feather, Osaka, Japan). The processed skin was laid flat on a cutting board at room temperature. The surface of the skin was dried with a paper towel. Microneedles were manually inserted into the skin while positioning two fingers on either side of the intended insertion site to keep it under mild tension. These microneedles were inserted by pushing against the skin with a distance of approximately 1 cm from the skin surface. Pyramidal, extended pyramidal and pedestal microneedles containing sulforhodamine were each manually inserted into the skin for 30 s, 2 min and 10 min. Each subset of microneedles for each insertion time had at least 3 replicates. The microneedles were microscopically imaged before and after insertion (Olympus SZX16, Pittsburgh, PA).

3.3.2.2   Imaging and Histology

The microneedle insertion sites were excised from the bulk skin with a scalpel. The isolated skin pieces were placed in cryostat molds embedded in optimum cutting temperature (OCT) media (Tissue-Tek, Torrance, CA). The skin was fixed in OCT by freezing the sample on dry ice. Frozen skin samples were sliced into 12-μm thick sections (Cryo-star HM 560MV, Microm, Waldorf, Germany). The skin sections were stained with hematoxylin and eosin using an automated staining machine (Leica Autostainer XL, Nussloch, Germany). After staining, the sections were covered with

glass slides sealed with cytoseal 60 (low viscosity, Richard-Allan Scientific, Kalamazoo, MI). The sections were dried overnight before taking images under the microscope (Nikon E600, Tokyo, Japan).

3.3.3   Bioavailability

3.3.3.1   Spectrofluorometer

The amount of drug delivered into the skin was determined based on a mass balance of three parameters: the total amount of drug encapsulated in microneedles before insertion into skin, the amount of drug remaining in needles after insertion and removal from skin, and the residual drug left on the skin surface. After the needles were removed from the insertion site, adhesive tape (3M, St. Paul, MN) was used to strip off the residual dye left on the skin surface. The microneedles and skin-stripped tapes were then soaked in DI water in separate containers for 30 min at room temperature. The samples were transferred into cuvettes and measured by spectrofluorometry (Photon Technology International, Lawrenceville, NJ). The excitation wavelength of sulforhodamine was set at 565 nm. Area under the curve from 580 nm to 620 nm was calculated using Felix software (Photon Technology International). This reading was fitted into the sulforhodamine standard curve to obtain the actual amount of sulforhodamine by mass. The amount of sulforhodamine delivered into the skin was determined by subtracting the amount of sulforhodamine left in the needles and on the skin surface from the amount originally encapsulated in the microneedles.

3.4 Results

3.4.1 Microneedle Fabrication

In this study, we introduced new fabrication processes to better control drug encapsulation within dissolving microneedles. Microneedles with pyramidal geometry were fabricated by a series of molding and casting techniques. In this process, drug was loaded selectively into the microneedles (i.e., and not in the backing). We did not want to spread the drug solution to cover the entire microneedle mold and then dry it because this method could result in non-uniform drug loading or large amounts of drug wastage in the backing. Instead, we loaded the drug into the microneedle cavities of the mold (Fig. 3.1A) and then recycled the residual drug solution on the mold surface using pipettes to avoid wastage (Fig. 3.1B). To keep the drug localized in the microneedle cavities of the mold, we evaporated the drug solution to leave a solid drug film in the tips of the mold cavities prior to casting the polymer solution (Fig. 3.1C and 3.1D).

We next formed the microneedle base and backing using different methods to produce microneedles of two different designs: solid microneedles and bubble microneedles. Solid needles were made by casting sufficient polymer solution to form the microneedle base and backing after drying (Fig. 3.1E1). The dried microneedles were then peeled off from the mold (Fig. 3.1F1). To make bubble needles, the polymer solution outside the mold cavities was spun off the mold surface. Upon drying, the polymer solution in the mold cavities solidified with a meniscus-like shape in each microneedle cavity (Fig. 3.1E2). Upon applying a second layer of polymer solution to the mold surface, surface tension effects prevented it from filling the empty space in the mold cavities defined by the polymer meniscus. After drying, this

left a void – i.e., a bubble -- between the backing layer and the microneedles (Fig. 3.1F2).
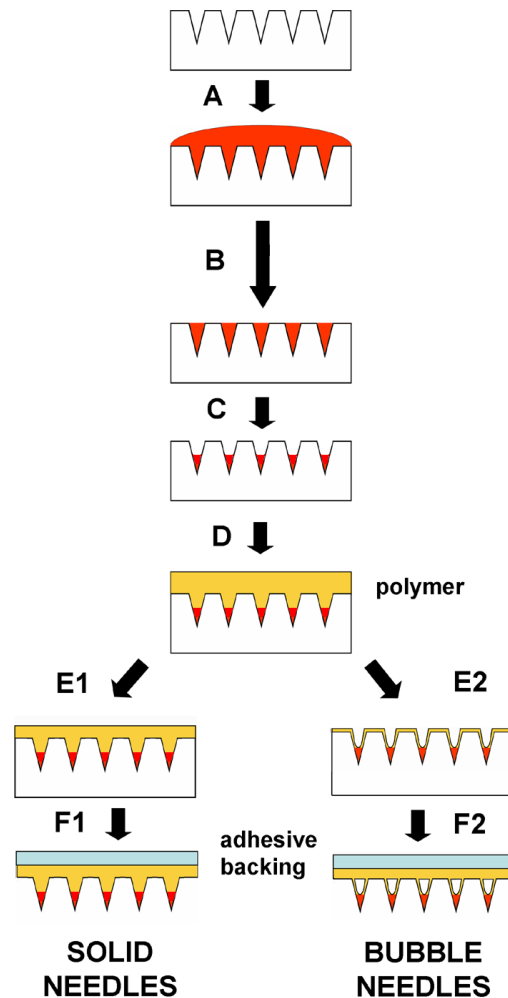
Fig. 3.1. Schematic of solid and bubble needle fabrication process. (A) A PDMS microneedle mold [140] was filled with drug solution under vacuum; (B) Residual drug solution was removed from the surface by a pipette and later reused; (C) Drug solution in the mold cavities was dried under centrifugation; (D) Drug-free polymer solution was cast onto the mold and filled under vacuum; (E1) The polymer solution was either air-dried or dried under centrifugation at low speeds; (F1) Dried solid needles were peeled off the mold by an adhesive backing; (E2) The polymer solution was either physically scraped off the mold surface and then air-dried or dried under centrifugation at high speeds; (F2) A backing coated with a thin film of concentrated polymer solution was placed on top of the mold and then air dried. After drying, the bubble needles were peeled off.

Using this fabrication approach, the maximum amount of drug loaded into each microneedle is the produce to the microneedle cavity volume times the drug solubility in its carrier solvent. One approach to increase drug loading per microneedle would be to use a solvent that increases drug solubility, although choice of solvents is also limited by safety considerations. Another possibility would be to overcome the solubility limit by using particulate systems in which drug particles are suspended in the carrier solvent. However, particle size must be much smaller than microneedle size and such systems can lead to non-uniform needle-to-needle loading. As another alternative, we increased loading capacity of microneedles by effectively increasing microneedle mold cavity volume by adding a pedestal at the base of each mold cavity. To accomplish this, the pyramidal PDMS mold was reverse-molded from a master microneedle needle structure (Fig. 3.2A). We then aligned PDMS-coated laser-cut stainless steel sheets with the PDMS mold (Fig. 3.2B and 3.2C). In this way, each pyramidal cavity in the mold was positioned immediately below a hole in the stacked metal sheets above. This created enlarged microneedle mold cavities consisting of a non-tapered pedestal at the base of the pyramidal needle tip. Pedestal microneedles were then fabricated in a manner similar to above (Fig. 3.2E and 3.2F).
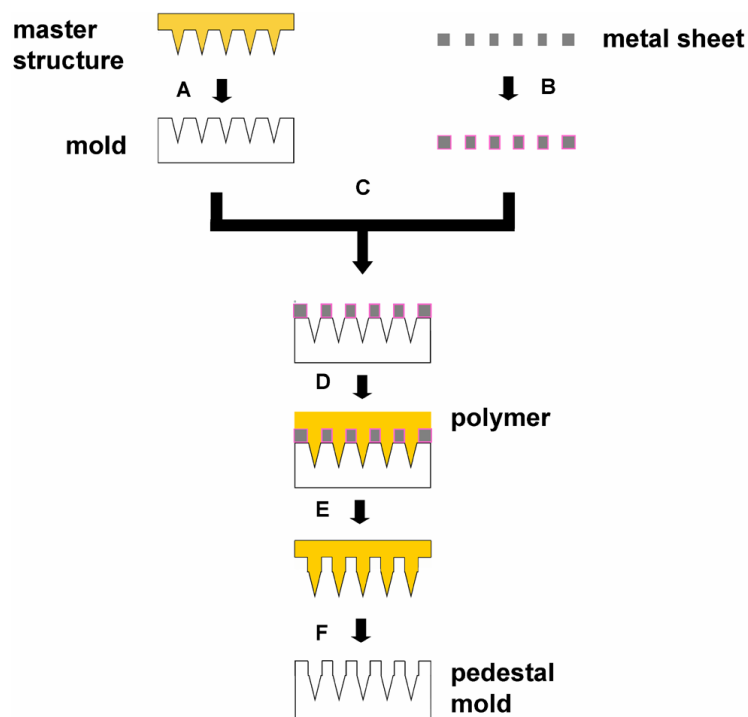
Fig. 3.2. Schematic of pedestal microneedle mold fabrication. (A) A PDMS mold was created from a master microneedle structure. (B) An infrared laser-cut metal sheet was coated with PDMS; (C) A composite mold was formed as the coated metal sheet(s) were placed on top of the PDMS mold and cured under heat; (D) Molten polymer was cast onto the composite mold by vacuum; (E) After cooling, microneedles with pedestal structure were peeled off the composite mold; (F) The pedestal microneedles were then used as the master structure for making pedestal PDMS mold replicates (see Fig. 3.1).

3.4.2 Drug Localization and Delivery Efficiency

One of our goals was to develop methods to load and localize drug in the tips of the microneedles. Using the solid microneedles, we found that polymer concentration in the casting solution had an important effect. As shown in Fig. 3.3A, using a low concentration casting solution (30 wt %) led to distribution of the model drug, sulforhodamine, throughout the needle and into the backing. We believe that the low viscosity of the low concentration casting solution allowed sulforhodamine to diffuse out of the microneedle mold cavity through the microneedle matrix during drying in the microneedle mold. Consistent with this hypothesis, increasing viscosity by increasing the polymer concentration (40 wt %) better kept the sulforhodamine within the needle (Fig. 3.3B). Casting at a still higher polymer concentration (50 wt %) localized the sulforhodamine even more to the microneedle tip (Fig. 3.3C).

Because microneedle formulations are subject to many constraints such that sufficiently increasing casting solution viscosity may be problematic, we developed another approach to keeping drug in the microneedle tip by introducing an air bubble at the base of the microneedle. Using this approach, sulforhodamine was contained within the microneedle independent of polymer concentration (Fig. 3.3D, 3.3E and 3.3F). We believe this was because the bubble formed a physical barrier that prevented diffusion out of the microneedle. As an aside, the bubble also decreased the mechanical strength of the microneedles, which could be a limitation in some situations. However, under the conditions used in this study we found that bubble microneedles inserted reliably into skin and did not ever break.
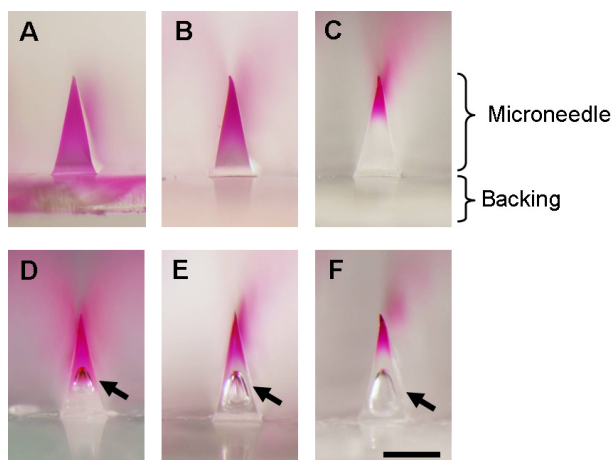
Fig. 3.3. Solid and bubble microneedles loaded with model drug localized to the tips imaged by bright field microscopy. Top row: Solid needles loaded with 1 mg/ml sulforhodamine B encapsulated in (A) 30 wt %; (B) 40 wt %; (C) 50 wt % PVA/PVP blends. Bottom row: Bubble needle counterparts loaded with 1 mg/ml sulforhodamine B encapsulated in (D) 30 wt %; (E) 40 wt %; (F) 50 wt % PVA/PVP blends. The arrows indicate the location of air bubbles. Bar = 300 μm.

We were motivated to keep sulforhodamine localized in the tips of the microneedles because we expected that to enable more efficient drug delivery into the skin (i.e., leaving less drug remaining in the microneedle device). To test this expectation, we inserted solid and bubble microneedles made using different polymer concentrations into porcine cadaver skin and monitored drug release over time. As shown in Fig. 3.4, delivery efficiency was highly correlated with drug localization. Microneedles with drug localized in the microneedle tip (i.e., Solid 50%, Bubble 50% and Bubble 40%) showed an initial burst release of sulforhodamine within the first 30 s resulting in approximately 80% drug release within 10 min. Microneedles with sulforhodamine distributed throughout the needle matrix but not in the backing (i.e., Solid 40% and Bubble 30%) had a smaller burst release, but then delivery efficiency increased over time to approximately 70% drug release, probably due to continued microneedle matrix dissolution. Finally, microneedles with sulforhodamine distributed into the backing demonstrated low delivery efficiency corresponding to

only about 20% drug release. The delivery did not significantly increase with time, suggested that 10 min was insufficient time for the sulforhodamine in the backing to diffuse into the skin, and was therefore wasted.
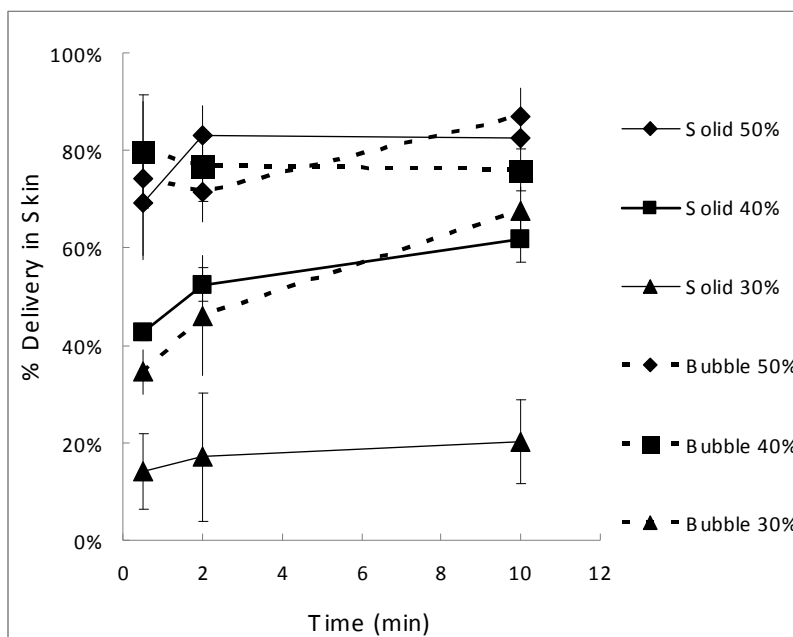
Fig. 3.4. Percentage delivery of sulforhodamine B over the time during microneedle insertion into porcine cadaver skin. Solid lines are for solid microneedles and dashed lines are for bubble microneedles made using different polymer solution concentrations. Data points represent averages of n = 3 replications, with standard deviation bars shown.

3.4.3   Drug Loading Capacity and Variability

Our second goal was to increase drug loading in the microneedles without wastage in the backing. To achieve a higher loading in the microneedles, we made larger microneedle mold cavities, which enabled more drug solution to be cast into each cavity and resulted in larger microneedles. We did not change the tip geometry,

because it is critical to microneedle insertion into the skin. Instead we elongated the base portion of the needle either in a tapered fashion, which resulted in "extended pyramidal" microneedles or with a non-tapered structure, which generated "pedestal" microneedles. The original pyramidal needle has a volume of 18 nl. Elongating the base in the extended pyramidal needle increased the volume to 45 nl, which is two and a half times larger than the pyramidal needle. The pedestal microneedle volume was increased to 53 nl, which is almost three times larger than the pyramidal needle. As an example, casting with a solution containing 10 mg/ml of drug results in 0.53 µg of drug encapsulated per needle (i.e., 53 µg in 100 needles or 530 µg in 1000 needles). These doses are sufficient for many vaccines and protein therapeutics [141, 142].

We made measurements of drug loading dose to assess reproducibility and wastage. As shown in Table 3.1, the amount of sulforhodamine encapsulated within microneedles was determined at two different drug concentrations in the casting solution and using the three different microneedle designs. We found that the amount encapsulated within the microneedles was close to that predicted as the product of microneedle mold cavity volume times drug concentration, although there was some deviation especially when lower drug concentration was used. The device-to-device variability ranged from 0.1 µg to 0.92 µg per 100 microneedles on an absolute basis, which corresponded to 8 to 2 % on a percent basis.

Table 3.1. Drug loading using three different microneedle designs

	Pyramidal		Extended Pyramidal		Pedestal	
Miconeedle mold cavity volume (per 100 microneedles)	1.80 µl		4.50 µl		5.30 µl	
Drug concentration in the coating solution	1 mg/ml	10 mg/ml	1 mg/ml	10 mg/ml	1 mg/ml	10 mg/ml
Drug loaded after encapsulation (per 100 microneedles)	1.33 ± 0.1 µg	18.10 ± 0.74 µg	4.16 ± 0.45 µg	40.55 ± 0.62 µg	6.37 ± 0.44 µg	54.30 ± 0.92 µg
Drug wastage during fabrication (per 100 microneedles)	0.11 ± 0.09 µg	1.13 ± 0.29 µg	0.19 ± 0.03 µg	1.36 ± 0.63 µg	0.08 ± 0.1 µg	1.28 ± 0.3 µg

Drug wastage, as assessed by the amount of drug left on the mold surface (i.e., not inside a mold cavity), scaled with drug concentration and was relatively independent of mold geometry. Wastage ranged from 0.08 µg to 0.19 µg when casting with 1 mg/ml sulforhodamine and from 1.13 µg to 1.36 µg when casting at 10 mg/ml. This corresponds to a residual volume on the mold surface on the order of 100 nl per 100-needle array. Because the absolute wastage amount was relatively independent of mold geometry, drug wastage was just 4 – 3 % for the extended pyramid needles and 1 – 2 % for the pedestal needles. We expect that these values could be further reduced with additional optimization and automation of the protocol.

3.4.4   Microneedle Insertion Depth

Our third goal was to achieve a more complete insertion of microneedles into the skin. We hypothesized that by inserting microneedles more fully would result in higher drug bioavailability in the skin. The extended pyramid and pedestal microneedles achieved greater drug loading by elongating the needle base, which makes the needles longer. Because skin deflection during microneedle insertion can result in a significant fraction of the needle remaining outside the skin [23, 143], the original pyramidal microneedles are not expected to fully insert. However, mounting them on a pedestal or on an elongated based should facilitate full insertion of the microneedle tip, in which the drug is encapsulated. Clearly, there is a limit to how far this strategy can be carried forward. Still longer microneedles should encapsulate more drug and insert more fully into the skin. However, if the microneedles become too big, then they will hurt, which should reduce patient acceptance.

To study this issue, pyramidal microneedles, extended pyramidal microneedles and pedestal microneedles were fabricated as shown in Fig. 3.5A, 3.5B and 3.5C. The pyramidal microneedles were 600 µm long and the extended pyramidal and pedestal needles were 900 µm long. We determined the depth of microneedle insertion and its impact on the amount of drug delivered to the skin in three ways. First, we examined the histological cross sections of skin at the insertion sites. As shown in the representative images in Figs. 3.5A1, 3.5B1 and 3.5C1, pyramidal microneedles inserted to a depth of approximately 150 µm, whereas both the extended pyramidal and pedestal needles inserted to a depth of approximately 250 µm into the porcine cadaver skin, which was similar to 250 µm length of the drug-loaded tip portion of the needles. Although the pedestal needles had a bulkier base than the extended pyramidal needles, the pedestal did not appear to hamper insertion, perhaps because the base

portion of the microneedle was primarily used to overcome skin deflection and did not insert into the skin itself.
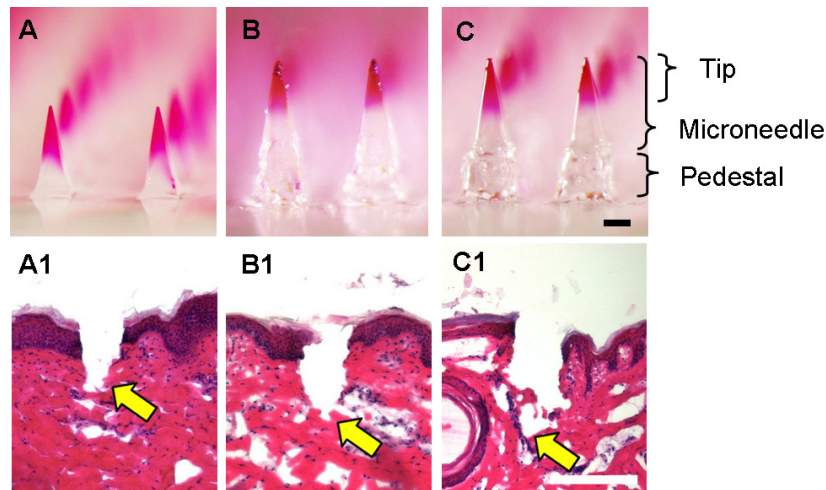
Fig. 3.5. Skin insertion depth of three different microneedle structures imaged by bright field microscopy. (A) Pyramidal microneedles (base width x base depth x needle height: 300 x 300 x 600 µm); (B) Extended pyramidal microneedles (300 x 300 x 900 µm) and (C) Pedestal microneedles (340 x 340 x 900 µm). Corresponding H&E-stained histology cross sectional images of insertion sites in porcine cadaver skin: (A1) Pyramidal microneedles; (B1) Extended pyramidal microneedles and (C1) Pedestal microneedles. The arrows indicate the depth of the microneedle insertion track. Bar = 200 µm.

As a second assessment, we determined how the insertion depth affected the dissolution of the microneedles. As determined by microscopic examination of needles after 10 min insertion, we found that pyramidal needles lost approximately 50% of their original length from 600 µm to 300 µm (Fig. 3.6A and 3.6A1). Because of the tapered geometry, this corresponds to a 12% loss in microneedle volume. In contrast, both the extended pyramidal needles and pedestal needles lost almost 80% of their lengths, reducing from 900 µm to 450 µm (Fig. 3.6B, 3.6B1, and 3.6C, 3.6C1). This corresponds to complete dissolution of the upper 450 µm containing the drug-loaded tip.
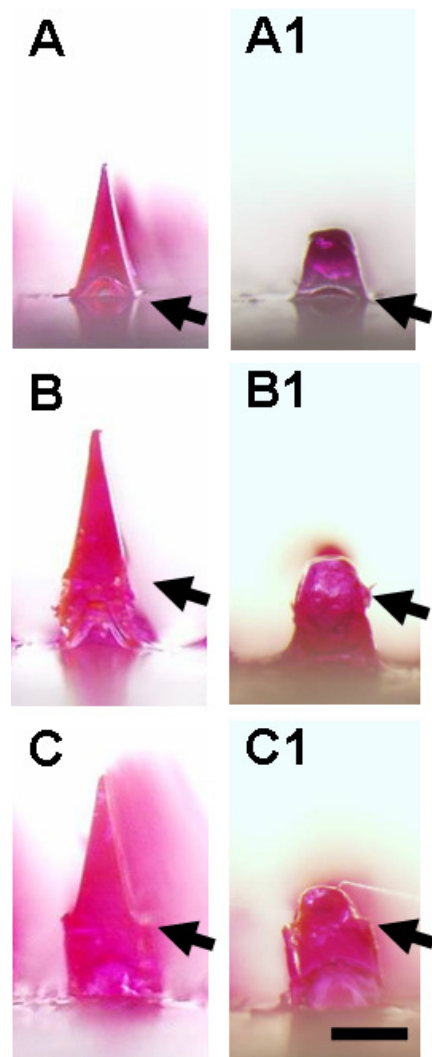
Fig. 3.6. Microneedle dissolution after insertion into porcine cadaver skin imaged by bright field microscopy. Left column shows microneedles uniformly loaded with 1 mg/ml sulforhodamine before insertion into skin. (A) Pyramidal microneedle; (B) Extended pyramidal microneedle; (C) Pedestal microneedle. Right column shows corresponding microneedles after a 2 min insertion into skin. The arrows indicate the base of the primary 600 µm microneedle structure at its interface with the extended pyramidal portion or pedestal portion. Bar = 300 µm.

Third, we further determined the amount of delivery by quantifying the efficiency of microneedle insertion and dissolution in the skin based on the amount of encapsulated drug released during the insertion. To facilitate this analysis, we encapsulated the model drug, sulforhodamine, uniformly throughout the microneedle rather than localizing it in the tips. A mass balance on the amount of sulforhodamine initially encapsulated and that remaining after insertion showed that the pyramidal needles lost almost 10% of their original volume, where as both the extended pyramidal and pedestal needles lost almost 50% of their microneedle matrix (Fig. 3.7). Altogether, these three methods of assessment reach the common conclusion that the elongated microneedle geometries enable a deeper insertion and more efficient delivery of drug into the skin.
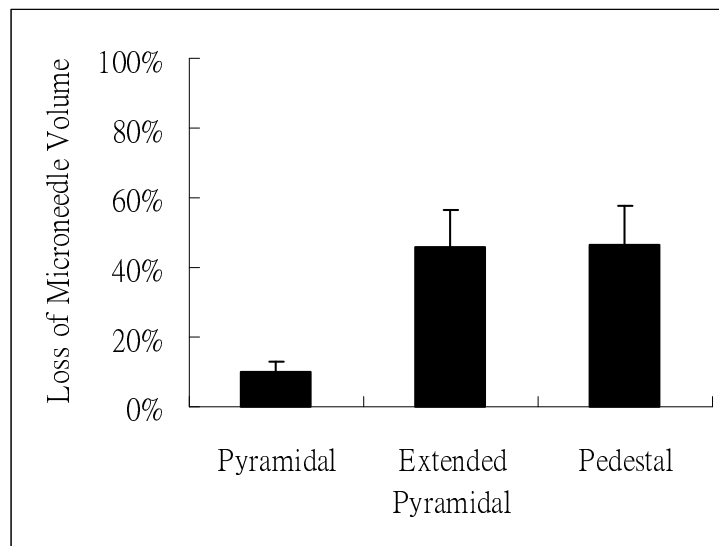
Fig. 3.7. Microneedle dissolution after insertion into porcine cadaver skin as determined by a quantitative mass balance. Loss of micronneedle volume was determined based on the amount of sulforhodamine encapsulated in microneedles before and after insertion in skin. Data points represent averages of n = 3 replications, with standard deviation bars shown.

3.5   Discussion

Dissolving polymer microneedles offer a simple, safe, and minimally invasive delivery method to the skin. Yet, due to the need for water-based casting of the polymer when molding the needles, drug encapsulation, loading and delivery can be difficult to control. We addressed these issues by (1) localizing drug only in the microneedle tip, (2) increasing the amount of drug loaded in microneedles while minimizing wastage, and (3) inserting microneedles more fully into the skin.

Localizing drug only in the microneedle tip required control of drug deposition in the tip during casting as well as minimizing drug diffusion out of the tip during drying. When the drug and polymer matrix material were premixed and cast onto the microneedle mold together, the volume of this mixture would take up too much space in the microneedle mold upon drying and thereby make localization in the microneedle tip difficult. In this study, we showed that drug localization in the tip can be better achieved by first casting a solution containing drug with little or no added excipients and then drying the drug into the tip of the microneedle mold under centrifugal force. As a second step, this was followed by casting and drying the polymer solution to form the rest of the microneedle matrix.

During this second step, diffusion of drug out of the tip can take place as the dried drug makes contact with, dissolves in and diffuses through the aqueous polymer solution. As shown in Fig. 3.3, drug diffusion during this step is affected by polymer concentration, such that a higher concentration solution inhibited diffusion and helped maintain drug localization in the tip. However, use of highly concentrated polymer solutions can be constrained by their physical characteristics including high viscosity, poor solubility or gelation, which can make processing during fabrication difficult.

As an alternative to blocking diffusion through the use of concentrated polymer solutions, we introduced a new technique in which dilute polymer solution could be used and drug diffusion from the tip was blocked by incorporating a bubble at the base of each microneedle. In this approach, the excess polymer was spun off the mold surface and, after drying, a concave drug film was formed in the base of each microneedle mold cavity, as shown in Fig. 3.1E2. Instead of refilling the hollowed cavity, which could re-dissolve the drug, the hollow cavity was left unfilled and capped with a backing layer containing little moisture. The outcome of this technique was an entrapped air bubble that blocked drug diffusion. Comparing the bubble needles with their solid needle counterparts, the bubble needles had more defined drug localization even in microneedles made up of dilute polymer solutions. Moreover, microneedles with better drug localization showed greater delivery efficiency compared to the ones with less effective drug localization.

In addition to localizing drug into the microneedle tip, we also sought to maximize the dose encapsulated in a microneedle while avoiding the wastage of drug. Any drug that dried on the mold surface was considered wasted because it could not be recycled or delivered into the skin easily. To minimize drug wastage, we only loaded drug solutions in the microneedle mold cavities, which resulted in the dose encapsulated per needle being constrained by the volume of the needle itself. To address this limitation, we modified the pyramidal needles by introducing two additional structures: extended pyramidal needles and pedestal needles. These new microneedle structures bulked up the original pyramidal needle volume from 0.018 μl to 0.045 and 0.053 μl respectively. The amount of drug wastage was independent of the microneedle structure. Rather, the wastage was determined by the amount of unrecycled drug left on the mold surface. As a result, encapsulating larger doses was preferred because the relative percent wastage of drug became less significant as we

increased the dose (Table 1).

Skin deflection and elasticity is one of the main causes for incomplete insertion of microneedles. The degree of skin deflection depends on a variety of factors including microneedle tip sharpness, microneedle aspect ratio, needle-to-needle spacing, microneedle length and insertion speed. Because the matrix of dissolving polymer microneedles is weaker (i.e., has a smaller Young's modulus) than, for example, metal microneedles, dissolving microneedle geometry must provide added mechanical strength, which usually results in a wide needle (i.e., smaller aspect ratio). This geometry makes dissolving microneedles more difficult to insert fully into the skin compared to, for example, the slender, high-aspect ratio metal needles used in other studies [15, 18, 115, 144].

As the needles are inserted into the skin, the insertion stops as the deflected skin surface hits the backing of the needle array, which prevents the needles from further piercing. To reduce the impact of this issue, we elevated the microneedles by adding a pedestal to the base of the microneedle. According to Fig. 3.5, we found that the additional 300 μm offered by the pedestal only resulted in an additional 100 μm insertion depth. This may be because the pedestal only partially overcame the skin deflection without the presence of physiological skin tension in our in vitro apparatus. In principle, needle length could be extended longer, but in practice, it would be difficult to remove dissolving microneedles longer than 1 mm from the PDMS mold and pain caused by such long needles may become a concern [145].

Controlled dosing administered by dissolving microneedles plays a critical role in their eventual use in medicine. Some compounds such as biotherapeutics and vaccines are relatively expensive to produce. A controlled drug encapsulation process with minimal wastage reduces the overall cost of a microneedle patch, especially for costly drugs. In some cases, when a drug has a narrow therapeutic window, controlled

dosing becomes crucial to avoid over-or under-dosing. Another important aspect of this study is the more complete insertion of microneedles. People in different age groups and in different weight categories have different skin mechanical properties. The ability to insert microneedles more fully into the skin reduces the likelihood of delivery failure due to variable skin types. Overall, the new fabrication techniques introduced here bring dissolving polymer microneedle technology closer to practical use.

3.6   Conclusions

We have introduced new methods to fabricate dissolving microneedles for controlled drug encapsulation and delivery. These new microneedle designs and drug loading techniques enabled more drug to be loaded and localized into the microneedle tip with minimal drug wastage. By incorporating a pedestal at the base of the microneedle, microneedles could insert more fully. More complete insertion of the microneedles allowed a higher fraction of the encapsulated drug to be delivered into the skin. Overall, these technical advancements of controlled encapsulation and delivery provide an important step toward developing dissolving microneedles to serve as a reliable, versatile and safe delivery tool for administering a wide range of therapeutics.

3.7   Acknowledgements

CHAPTER 4

Rapid Cutaneous Delivery

Using Separable Arrowhead Microneedles

Leonard Y. Chu[1], Mark R. Prausnitz[1,2]

[1] Wallace Coulter Department of Biomedical Engineering,
Georgia Institute of Technology, Atlanta, GA 30332
[2] School of Chemical & Biomolecular Engineering,
Georgia Institute of Technology, Atlanta, GA 30332

4.1 Abstract

To overcome the pain and risk of biohazardous sharp waste associated with hypodermic needles, we introduce a novel delivery tool called separable arrowhead microneedles. These needles are featured by capping micron-size sharp tips onto blunt shafts. Upon insertion into the skin, the tips containing drug or vaccine dissolve or are mechanically separated from the shafts on the scale of seconds. After administration, the needle shafts become dull and can not be reused. As a result, concerns for biohazardous sharp waste disposal and needle-stick injury are reduced. Thus, drug and vaccine delivery using arrowhead microneedles can be a quick, convenient, safe and potentially self-administered method.

4.2 Introduction

Currently, biopharmaceuticals and vaccines are delivered almost exclusively by subcutaneous or intramuscular injection using hypodermic needles. While hypodermic needles have a long history of use in clinical practice, many issues such as patient incompliance due to needle phobia, sharing and reuse of needles, as well as disposal of sharp waste exist. Patient incompliance due to needle phobia is prevalent [4]; it presents impediments to clinical practice as the fear of injection reduces the willingness to be treated or vaccinated [5, 146]. Unsafe injection practices such as needle sharing and reuse accounted for more than 50% of the total injections in developing countries [7], leading to transmission of blood-born pathogens including hepatitis B, C and HIV. In addition to safety concerns of disposing hypodermic needles, handling and proper disposal of such biohazardous sharp waste can also be economic burdensome [147]. Summing all the costs from the societal perspective including device purchase and usage, medical costs and lost productivity, conventional disposable needle-and-syringe systems are one of the most expensive injection devices compared to other automated injection systems and jet-injectors [148].

There has been a wave of effort to seek alternative methods other than using hypodermic needles to deliver drugs and vaccines through the skin. Non-invasive approaches using transdermal patches primarily deliver small molecules less than approximately 500 Da or highly lypohilic molecules passively through the skin [3]. To deliver macromolecules across the skin, stratum corneum, the outermost barrier of the skin, needs to be altered or removed. Tape stripping [59], dermabrasion [60, 61] and thermal ablation [3, 56] have shown to remove stratum corneum selectively without

damaging deeper tissues. However, administration using such methods requires a two-step process that involves stratum corneum removal and subsequent drug application.

Microneedles are microscopic needles that create tiny channels in the skin upon insertion. Recently, molecules have been incorporated into microneedles forming an all-in-one delivery device which requires only a single application to deliver a full dose. For example, molecules were coated onto sharp, mechanically robust substrates for subsequent release in the skin [15-17]. These drug-coated microneedles minimize the risk of needle-stick injury due to their miniaturized size, but concerns for sharp waste disposal and needle reuse still remain. Molecules can also be encapsulated within dissolving microneedles made of water-soluble materials. When inserting dissolving microneedles into the skin, their water-soluble sharp tips dissolve and then release the encapsulated molecules within the skin [20-23]. While dissolving microneedles do not generate sharp waste, they have lower young's modulus compared to, for example, coated metal needles. Weaker mechanical properties of dissolving microneedles pose some limitations: high-aspect ratio needles may risk mechanical failure during insertion while low-aspect ratio needles may result incomplete insertion of needles due to skin deflection [18, 23].

Considering all the advantages and disadvantages of current cutaneous delivery tools including hypodermic needles and different microneedle designs, we introduce a novel type of microneedles called arrowhead microneedles. These needles are featured by capping sharp dissolvable or biodegradable tips onto mechanically robust dull shafts. This study covers step-by-step fabrication process of arrowhead microneedles. We also evaluated the insertion of arrowhead microneedles into cadaver skin and tested the safety of the device after use.

4.3 Materials and Methods

4.3.1 Microneedle Fabrication

4.3.1.1 Microneedle Mold

A 10 x 10 array of polydimethylsiloxane (PDMS, Sylgard 184, Dow Corning, Midland, MI) pyramidal microneedle mold was fabricated by Choi et al using photolithography and molding techniques [140]. Each pyramidal microneedle cavity was 600 μm deep with a 300 μm x 300 μm square base. Polylactic acid (PLA) microneedle master structure was made by casting molten PLA (L-PLA, 1.0 dL/g; Birmingham Polymer, Pelham, AL) onto the PDMS mold by vacuum at – 91k Pa for 1 h at 195°C. PDMS mold replicates were made by curing PDMS mixture on top of the PLA master structure at 37°C overnight.

4.3.1.2. Fabrication of Microneedle Shafts and Backing

A 125 μm-thick stainless steel sheet (McMaster-Carr, Atlanta, GA) was cut using infrared laser (Resonetics Maestro, Nashua, NH) at a cutting velocity of 1 mm/s with one pass, 20% attenuation of laser energy, and air purge at a constant pressure of 140 kPa based on AutoCAD (Autodesk, Cupertino, CA) drawings. Laser-patterned shafts on the metal sheet were bent 90° out-of-plane using a razor blade (VWR) while viewing under a microscope. The processed metal pieces with bent shafts were electropolished using electropolishing solution (E972, ESMA Inc., South Holland, IL) in E399 electropolisher (ESMA Inc.) for 15 min at 2 A at 45°C. The electropolished

metal pieces were briefly rinsed in 30% nitric acid solution, cleaned with DI water and blow-dried with nitrogen gas.

4.3.1.3. Microneedle Matrix and Formulation Preparation

Model drug sulforhodamine B (Molecular Probes, Eugene, OR) was dissolved in DI water at a concentration of 5 mg/ml. To encapsulate sulforhodamine B, a polymer blend consisting polyvinyl alcohol (PVA) (ACROS Organics, MW 2000) and polyvinylpyrrolidone (PVP) (BASF, K17, Aktiengesellschaft, Ludwigshafen, Germany) (ratio 1:1) was prepared. PVA was dispersed in DI water at 25°C and then heated to 90°C for 1 h. PVP was added and mixed homogeneously with the PVA solution. The polymer blend was incubated at 60°C for a few hours and cooled to room temperature before use. To encapsulate vaccine (inactivated influenza virus in PBS) (A/Puerto Rico/8/34, Emory Vaccine Center, Atlanta, GA), a blend of PVA and sucrose (Sigma-Aldrich, St Louis, MO) was used (ratio 1:1). Similarly, sucrose was mixed homogeneously with the PVA solution at 60°C and cooled to 25°C before use.

4.3.1.4. Drug Loading and Polymer Blend Casting

Sulforhodamine B or inactivated influenza virus was loaded into the PDMS mold by vacuuming to – 91k Pa for 3 min. The residual drug or vaccine on the mold surface was recycled by pipettes. The mold filled with drug or vaccine was centrifuged at 3200 x g at room temperature for 3 min. The drug-free polymer blend was cast onto the mold by vacuuming to -91k Pa for 3 min, and centrifuged again at 3200 x g at room temperature for 5 min.

4.3.1.5 Shaft Alignment and Drying

Before the polymer blend cast on the mold became completely dried, electropolished shaft array was aligned manually to the mold cavities under a stereo microscope (Olympus SZX16, Pittsburgh, PA). Gentle force was applied onto the metal backing against the mold until the stoppers located in adjacent to the shaft array hit the mold surface. For needles encapsulating sulforhodamine B, PVA/PVP blend was dried at room temperature overnight. For needles encapsulating inactivated influenza vaccine, PVA/Sucrose blend was freeze-dried in a lyophilizer (VirTis Wizerd 2.0 freeze dryer, Gardiner, NY). The samples were frozen to -40°C for 1 h, and then vacuumed at 2.67 Pa at -40°C for 10 h. While the pressure was kept constant at 2.67 Pa, the temperature was gradually ramped up to 0°C for 1 h, 20°C for 1 h and 25°C for another 10 h. After the drying process, the molded pyramidal polymer tips connecting to the shaft array were removed from the mold. Prior to inserting microneedles into the skin, stoppers in adjacent to the shaft array were bent down.

4.3.2   In Vitro Test

4.3.2.1   Microneedle Insertion and Evaluation

Prior to microneedle insertion, porcine cadaver skin (Pel-Freez, Rogers, AR) was processed by removing hair using razors (Dynarex, Orangeburg, NY) and subcutaneous fat using a scalpel (Feather, Osaka, Japan). The processed cadaver skin was dried with paper towels. The skin was held steadily with a mild tension by two fingers. Microneedles were manually pushed against the skin from a distance of

approximately 1 cm. To deliver drug by dissolution, the needles were inserted in the skin for a designated time. To deliver drug by mechanical separation, manual oscillatory shear force was applied onto the needles against the skin immediately after insertion. The needles were removed from the skin immediately or waited for a designated time after shearing. Each insertion was done in four replicates.

Human cadaver skin was obtained from the Emory University School of Medicine (Atlanta, GA, USA) with approval from the Georgia Tech IRB. To prepare human cadaver skin for insertion test, subcutaneous fat was removed by a scalpel. Microneedle insertion on human cadaver skin was performed in the same way as was done in porcine cadaver skin. To evaluate the damage of metal shafts to human cadaver skin, blunt metal shafts without sharp polymer tips were applied against the skin in the same manner as were done using microneedles with sharp tips. After applying the shafts, the applied region was stained with tissue marking dye (Electron Microscopy Sciences, Hatfield, PA) for 5 min. The residual dye was removed from the skin surface using paper towels and alcohol swabs (Becton-Dickinson, Franklin Lakes, NJ). All images of the microneedles and the application sites on the skin were taken using a stereo microscope (Olympus SZX16, Pittsburgh, PA).

4.3.2.2. *Imaging and Histology*

Microneedle insertion sites were excised from the bulk skin using a scalpel. The isolated skin piece was embedded in Optimum Cutting Temperature (OCT) media (Tissue-Tek, Torrance, CA) in a cryostat mold. The sample was fixed by freezing the OCT sample on dry ice. Frozen OCT samples were sliced into 12-μm thick sections using a cryostat (Cryo-star HM 560MV, Microm, Waldorf, Germany) and imprinted on glass slides. Fluorescent images were taken (Nikon E600, Tokyo, Japan) prior to

staining. The same skin sections were subject to hematoxylin and eosin staining using an automated staining machine (Leica Autostainer XL, Nussloch, Germany). A few drops of cytoseal 60 (low viscosity, Richard-Allan Scientific, Kalamazoo, MI) were applied onto the stained skin sections. The samples were then covered with glass cover slips and dried in fume hood over night. The images of the stained skin sections were taken under bright field using the Nikon microscope.

4.4   Results

4.4.1   Arrowhead Microneedle Fabrication

Arrowhead microneedles were fabricated by combining two components: dissolvable or biodegradable tips encapsulating drug or vaccine, and mechanically robust shafts and backing. We first loaded the drug into a PDMS mold (Fig. 4.1A), recycled the drug on the mold surface (Fig. 4.1B) and then dried the drug to the tips of the mold cavities (Fig. 4.1C). We performed a second mold-filling step by casting polymer solution onto the mold. Encapsulation took place as the polymer solution mixed with the model drug loaded in the mold cavities (Fig. 4.1D). Next, we removed the excess polymer on the mold surface to avoid contact with the metal shafts during alignment and drying (Fig. 4.1E).

Metal shafts were fabricated and prepared separately from the drug loading and polymer casting process. After the metal shafts were bent out-of-plane and electropolished, we aligned the metal shafts to the mold cavities before the polymer dried out. As shown in Fig. 4.1, stoppers located next to the metal shafts prevented the shafts from dipping all the way into the bottom of the mold cavities during alignment (Fig. 4.1F). The length difference between the shaft and the stopper defined the degree of overlap between the shaft and the microneedle tip. After drying, the shafts were removed along with the dried polymer tips from the mold (Fig. 4.1G). Finally, the stoppers were bent down manually (Fig. 4.1H).
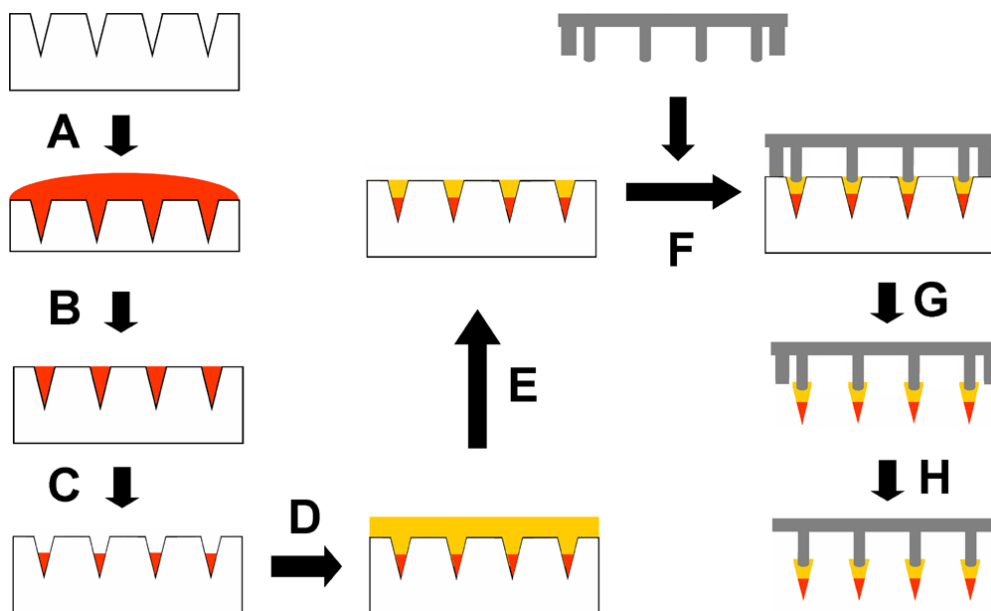
Fig. 4.1. Schematic of arrowhead microneedle fabrication process. (A) A PDMS mold was filled with the drug of interest by vacuum. (B) Excess drug on the mold surface was removed and recycled. (C) Drug loaded in the mold cavities was dried by centrifugation. (D) Polymer solution was cast into the mold cavities by vacuum. (E) Residual polymer solution was spun off by centrifugation. (F) Metal shafts were aligned to the mold cavities. (G) The whole device was air-dried at room temperature or freeze-dried overnight. After drying, the dried polymer tips connected to the metal shafts were removed from the mold. (H) Metal stoppers in adjacent to the shafts connected to polymer tips were bent down.

A 5 x 5 array of arrowhead microneedles encapsulating sulforhodamine B was fabricated (Fig. 4.2A). The needle shaft's front dimension was made wider (Fig. 4.2A1) to offset the mechanically weaker and thinner side of the shaft determined by the metal sheet thickness (125 μm) (Fig. 4.2A2). The number of needles in an array could be varied. We increased the number of needles to fifty (5 x 10 array) (Fig. 4.2B) for inactivated influenza virus encapsulation within the needle tips. The needles containing influenza virus appeared to be colorless and opaque (Fig. 4.2B1).
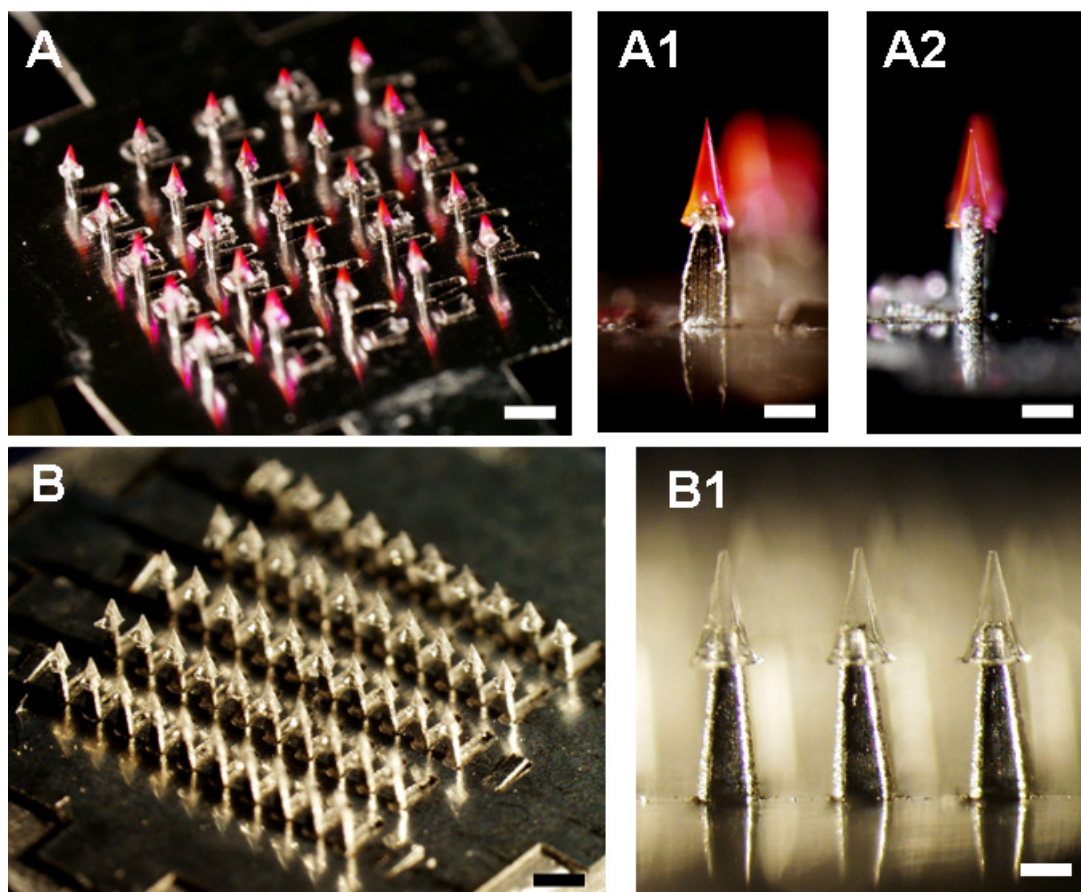
Fig. 4.2. Arrowhead microneedles. (A) An array of 5 x 5 arrowhead microneedles consisting 600 µm metal shafts capped with 600 µm water-soluble PVA/PVP pyramidal tips encapsulating sulforhodamine B (Bar = 1 mm); Individual needle's front view (A1) and side view (A2) (Bar = 300 µm). (B) An array of 10 x 5 arrowhead microneedles consisting 700 µm metal shafts capped with 600 µm water-soluble PVA/Sucrose pyramidal tips encapsulating inactivated influenza virus (Bar = 1 mm); closeup view of individual needles (B1) (Bar = 300 µm).

4.4.2   In Vitro Delivery of Sulforhodamine B in Porcine Cadaver Skin

Next, we evaluated arrowhead microneedle insertion and drug release in porcine cadaver skin. After 3 min insertion, sulforhodamine B was barely visible on the skin surface (Fig. 4.3A1) but glowed immensely at the inserted spots under fluorescent microscopy (Fig. 4.3A2). We believe that majority of the sulforhodamine was delivered within the skin but not on the skin surface. We also examined the

microneedle insertion from the side by obtaining histological cross sections. We found that the microneedle tips (600 μm) were fully inserted into the skin, creating approximately 600 μm cavities (Fig. 4.3B1). Drug release from the dissolved microneedle tips was local at the insertion cavities (Fig. 4.3B2).
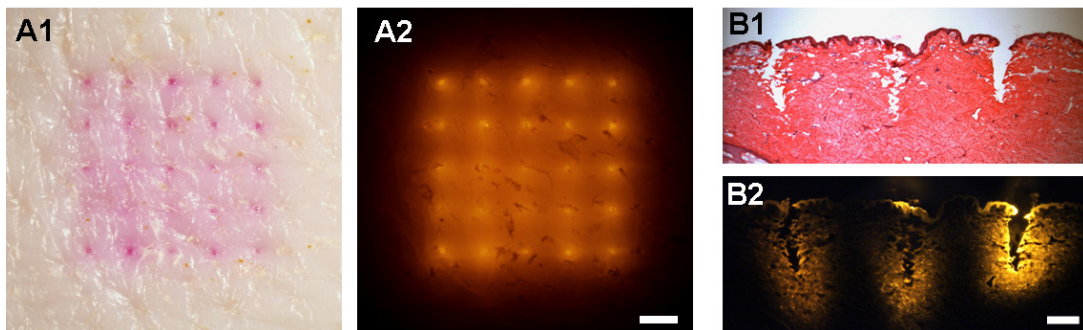
Fig. 4.3. Porcine cadaver skin insertions. En face view of skin imaged by bright field (A1) and fluorescence (A2) optics (Bar = 1 mm); Histological cross section of a row of microneedle insertion sites (B1) and the corresponding fluorescent image of sulforhodamine B released from the arrowhead microneedles prior to H&E staining (B2) (Bar = 300 μm).

We have already shown that arrowhead microneedles could insert the tips completely into the skin. Next, we sought to examine the correlation between the length of the needles and the insertion depth in porcine cadaver skin. We kept the length of microneedle tip constant at 600 μm while varying the length of metal shaft. We investigated three different lengths of microneedles: 900, 1200 and 1500 μm (Fig. 4.4A, 4.4B, and 4.4C). After insertion, fluorescent images showed local release of sulforhodamine at the insertion cavities (Fig. 4.4A1, 4.4B1 and 4.4C1). The H&E stained histological cross sections showed cavities generated by the corresponding needles in the skin with distinct layers of stratum corneum, viable epidermis and dermis (Fig. 4.4A2, 4.4B2 and 4.4C2). Based on the results, we found that although longer needles generated deeper insertions, the insertion depths did not match the full length of the needles, presumably due to skin deformation.
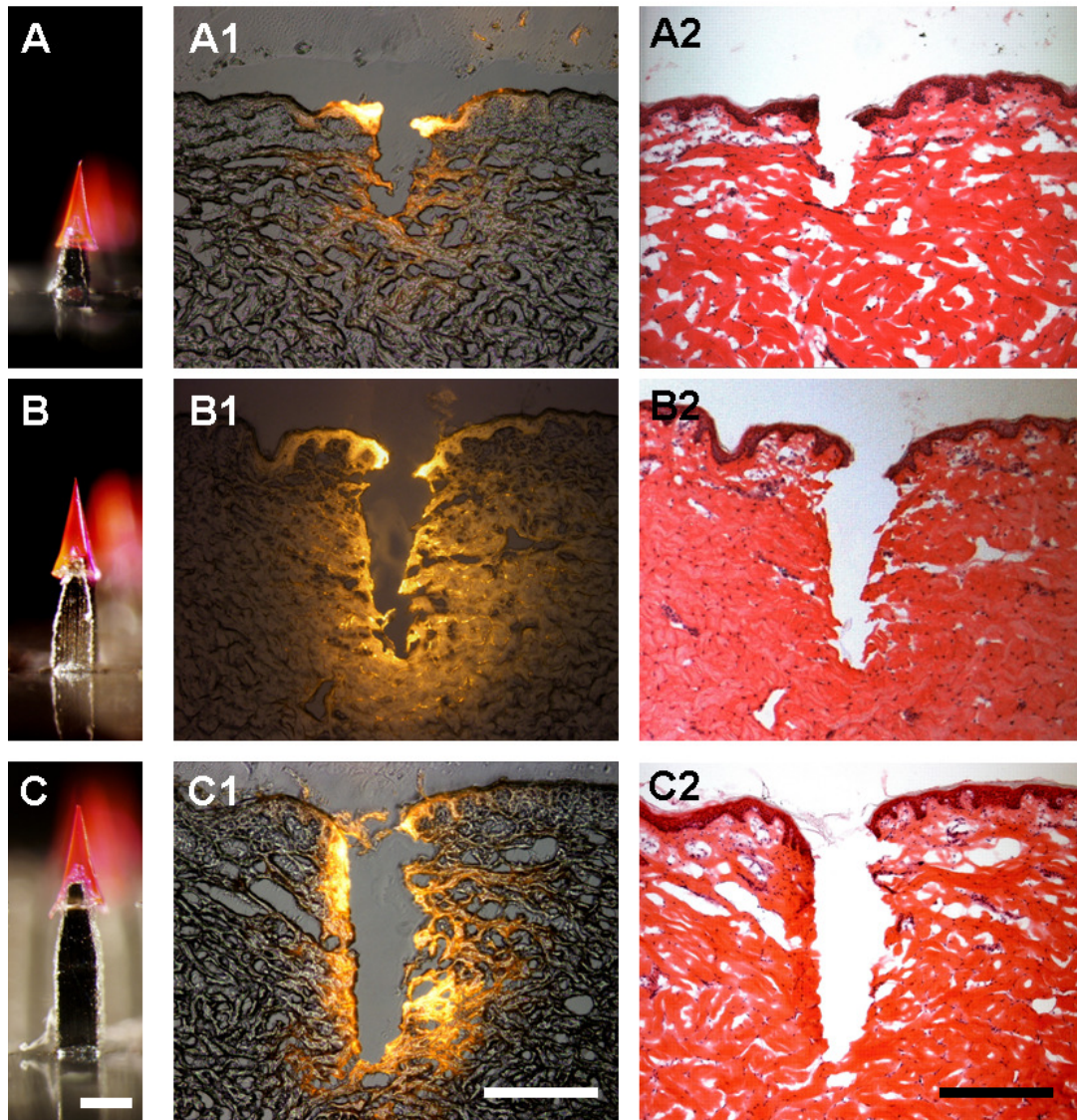
Fig. 4.4. The effect of arrowhead shaft length on porcine cadaver skin insertion depth. (A) A 900 μm needle its corresponding insertion depth under fluorescence (A1) and H&E staining (A2); (B) A 1200 μm needle and its corresponding insertion depth under fluorescence (B1) and H&E staining (B2); (C) A 1500 μm needle its corresponding insertion depth under fluorescence (C1) and H&E staining (C2). Bar = 300 μm

Arrowhead microneedles were capable of delivering drug on the scale of seconds. We evaluated two different mechanisms of delivery: The first mechanism involved dissolution of the polymer tips. The needles were applied and remained inserted in the

skin for subsequent dissolution of the tips by skin's interstitial fluid. The encapsulated drug was released as polymer tips dissolved. A burst release of sulforhodamine up to approximately 70% was achieved within 5 s of delivery (Fig. 4.5A). By extending the insertion time to 60 s, the delivery efficiency was increased to 90%. The second mechanism relied on mechanical separation of polymer tips from metal shafts. Upon insertion, an oscillatory shear force was applied to the needles against the skin. With one second of administration time after applying the shear force followed by removal of the needle backing, the delivery efficiency had reached approximately 90% (Fig 4.5B). Leaving the needles inserted in the skin longer after shearing did not significantly increase the delivery efficiency. As shown in Fig.4.5, both delivery approaches were able to achieve high delivery efficiency within seconds.
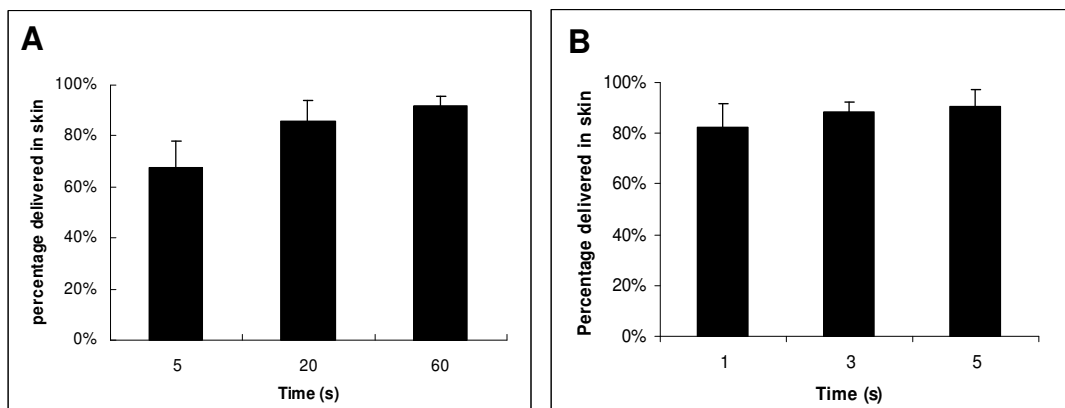
Fig. 4.5. Delivery efficiency of sulforhodamine B in porcine cadaver skin using arrowhead microneedles. (A) Dissolution-based delivery over 60 s. (B) Delivery facilitated by mechanical shear in seconds.

Arrowhead microneedles also allowed rapid delivery of drug encapsulated within materials that are biodegradable (i.e. not dissolvable). Using arrowhead microneedles, PLGA needle tips could be rapidly deposited within the skin for controlled release of drug. This rapid administration of biodegradable polymer tips did not rely on the

process of biodegradation, which could take weeks to months. Rather, the polymer

tips were mechanically separated from the shafts by shear force upon insertion. As

oppose to dissolvable tips, the PLGA tip encapsulating sulforhodamine B remained

physically intact for subsequent controlled release of drug within the skin (Fig. 4.6).
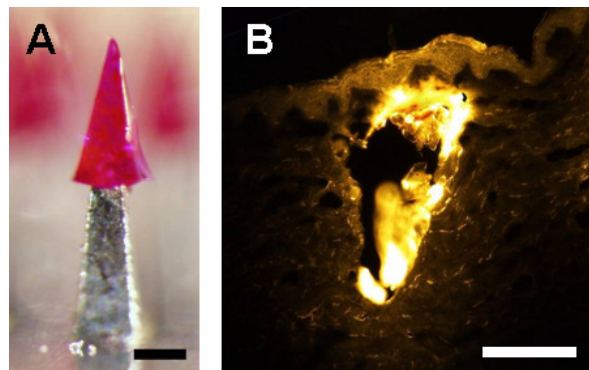
Fig. 4.6. Deposition of biodegradable PLGA tips using arrowhead microneedles. (A) A 1200 µm arrowhead microneedle encapsulating sulforhodamine B; (B) Histological cross section of a PLGA microneedle tip deposited within porcine cadaver skin under fluorescent microscopy. (Bars = 200 µm)

4.4.3 Safety Evaluation of Microneedles Post-Insertion

To study the safety of arrowhead microneedles after use, we compared three sets

of devices: arrowhead microneedles with intact sharp tips, microneedle shafts without

tips as mimicries of post-insertion needles in which the tips have been dissolved, and

sharpened shafts as the negative control for skin piercing test. First, we inserted an

array of 1200 µm tall arrowhead microneedles with sharp polymer tips containing

sulforhodamine B into human cadaver skin (Fig. 4.7A). The resulting insertion

showed 50 red sulforhodamine marks on the skin (Fig. 4.7A1). The

sulforhodamine-dotted skin illustrated that the needles were capable of inserting and

releasing the drug into human cadaver skin. After insertion, the sharp polymer tips

dissolved and left with the blunt metal shafts. To test the safety of used arrowhead microneedles, we applied clean blunt metal shafts as the mimicries of post-insertion needles onto the skin (Fig. 4.7B). The tissue marking dye did not permeate into the skin at the application site (4.7B1). In contrast, if we sharpened the blunt shafts used for arrowhead microneedles and applied onto the skin with the same force as applying the arrowhead microneedles, the skin was damaged as indicated by dots of permeabilized marking dye (Fig. 4.7C and 4.7C1). The study demonstrated that arrowhead microneedles become non-sharp after use, thus the needles can not be reused and shared, and pose no sharp waste disposal concerns.
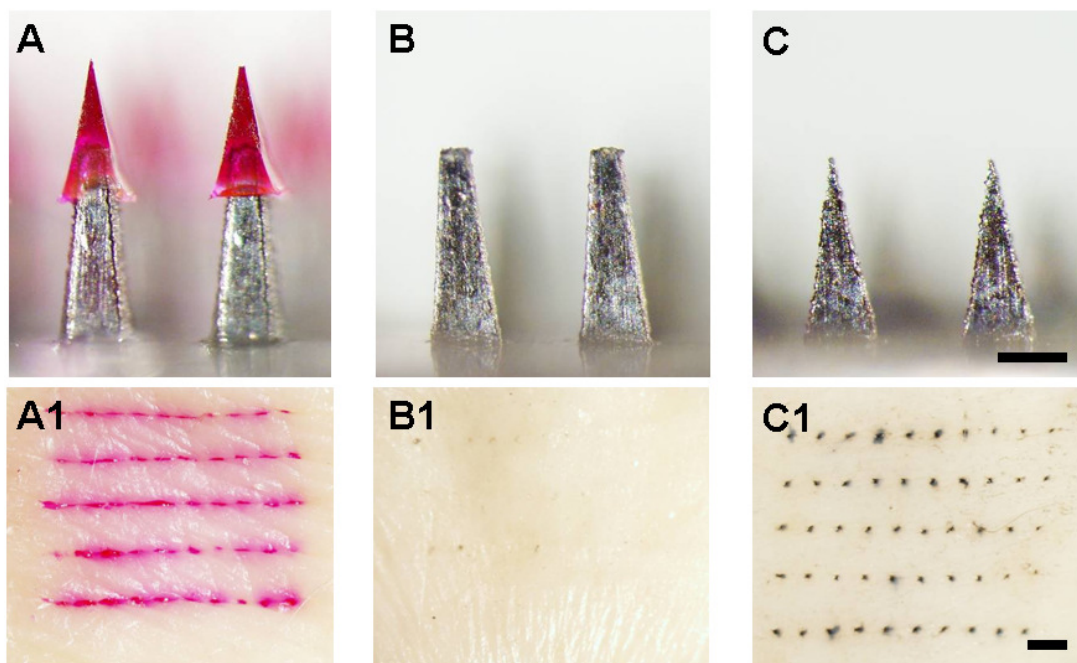
Fig. 4.7. Evaluation of arrowhead needle's safety in human cadaver skin (A) 1200 μm arrowhead needles with exposed 600 μm shafts, and the corresponding insertion (A1); (B) Representative 700 μm arrowhead shafts as mimicries of post-insertion needles, and the corresponding application of the shafts on the skin stained with tissue marking dye (B1); (C) Sharp 700 μm arrowhead shafts with the same aspect-ratio as in (B), and the corresponding insertion stained with dye (C1) (Top Row: Bar = 300 μm; Bottom Row: Bar = 1 mm).

4.5   Discussion

Over the past years, development of microneedles has been progressed at a rapid pace to address different drug delivery needs. For the first time, dissolvable or degradable microneedle tips containing drug or vaccine can be rapidly separated from microneedle backing and remained embedded within the skin upon insertion. The backing can then be removed quickly after administration without needing of extended patch wearing time. The novelty of arrowhead microneedles including the needle's unique geometry and delivery mechanisms is based in part on the existing microneedle designs. For example, arrowhead microneedle shafts supporting the tips are made of mechanically robust materials similar to coated microneedle's substrate, except the arrowhead shafts are made blunt. Unlike coated microneedles, the sharp edges of arrowhead microneedles are replaced by dissolvable or biodegradable materials similar to dissolving polymer microneedles, except the dissolvable/biodegradable arrowhead tips are physically spaced apart from the microneedle backing by the shafts.

Microneedles coated with or encapsulating drugs can not achieve reliable and consistent delivery simply by disrupting the stratum corneum; these needles have to penetrate into the skin with a certain depth for drug release within the tissue. In this case, the amount of drug delivered into the skin is largely determined by the depth of microneedle penetration. However, variable skin properties pose some challenges in achieving a uniform microneedle piercing. Studies have shown that age and regional differences account for the variable skin biomechanical properties [149, 150]. Although clinical study in human will need to validate the delivery, we believe arrowhead microneedles can overcome variable skin properties with the needle's

versatile insertion depth. We have shown also arrowhead microneedles were capable of delivering drugs into a variety of mammalian skin, including pig cadaver skin, human cadaver skin and mouse skin (data not shown). During the skin insertion studies, skin deflection was inevitable and the degree of skin deformation was dependent on skin properties. Discrepancies between the needle length and its corresponding insertion depth in pig skin indicated that additional needle length was required to overcome the skin deflection (Fig. 4.4). However, longer needles are associated with greater pain [145]. Therefore, a balance between delivery efficiency, delivery uniformity and pain needs to be considered.

Administration time is an important consideration especially when the target patient population is large and under time constraints [151]. Conventional transdermal patch requires long hours of wearing time due to slow passive transport of drug across the skin barrier. Long patch wearing time could generate problems such as premature removal of the patch. Literature on dissolving microneedles has reported delivery times from minutes to hours for the needles to be fully dissolved [22, 23]. Studies on coated microneedles required patch wearing time up to 15 min [16] but needle application time as short as one minute has been reported [15]. In our study, arrowhead microneedles have shown to deliver drug to porcine cadaver skin as fast as one second with over 80% delivery efficiency. The time required to administer drug using arrowhead microneedles is comparable to hypodermic needles. This rapid administration is favorable in clinical practice when the hospital traffic is severe or when conducting a mass vaccination campaign.

Biohazardous sharp waste continues to pose burdens on public health as well as our environment. Arrowhead microneedles solved this problem by using dissolvable or biodegradable sharp tips. After administration, these sharp tips become embedded within the skin and ultimately were disintegrated and secreted from the body. Without

presence of the sharp tips, the microneedle shafts could not easily penetrate into the

skin. Thus, it is safe to dispose the backing after use without worrying about

needle-stick injury or sharp waste disposal.

4.6 Conclusions

We introduced a novel delivery tool called arrowhead microneedles for rapid cutaneous delivery of drug and vaccine. Using arrowhead microneedles, drugs could be delivered into the skin via two mechanisms: microneedle tips containing drug could be dissolved and then separated from the shafts within the skin. Alternatively, the tips could be mechanically separated from the shafts by shear force while remaining embedded within the skin. The administration time using arrowhead microneedles was on the scale of seconds. After insertion, the needles became dull and could not be reused. Therefore, there would be no concerns for biohazardous sharp waste disposal or needle-stick injury by the contaminated needles. We envision drug and vaccine delivery using arrowhead microneedles can be a safe, quick, convenient, patient compliant and potentially self-administered method.

4.7 Acknowledgements

CHAPTER 5

Evaluation of the Stability of Influenza Vaccine

Encapsulated in Dissolving Microneedles

Leonard Y. Chu[1], Ling Ye[2], Ke Dong[2], Richard W. Compans[2], Chinglai Yang[2], Mark R. Prausnitz[1,3]

1. Wallace H. Coulter Department of Biomedical Engineering**,**
Georgia Institute of Technology, Atlanta, GA 30332, USA.
2. Department of Microbiology and Immunology and Emory Vaccine Center,
Emory University School of Medicine, Atlanta, GA 30329 USA
3. School of Chemical & Biomolecular Engineering,
Georgia Institute of Technology, Atlanta, GA 30332, USA.

5.1 Abstract

To achieve a delivery system that does not require reconstitution of dried vaccine when given a vaccination, we incorporated influenza vaccine (A/Puerto Rico/8/34) into dissolving microneedles as part of the delivery device. The purpose of this study was to investigate the stability of encapsulated vaccine in dissolving microneedles during microneedle processing and post-processing storage. We evaluated the effect of different drying techniques as well as the effect of formulation on hemagglutination (HA) potency of the encapsulated vaccine. After processed into microneedles, the encapsulated vaccine was stored at four different temperatures (4°C, 25°C, 37°C and 45°C) under different packaging conditions. We found that drying the encapsulated vaccine by lyophilization maintained the most HA potency. Inclusion of sucrose in the formulation also protected the vaccine from drying stresses. The HA assay showed that the encapsulated vaccine was more thermally stable than the unprocessed vaccine over prolonged periods of time. The finding was consistent with the HA antigenic activity measured by ELISA and the virus particle's morphological structure captured using transmission electron microscopy. In conclusion, the encapsulated influenza vaccine was more thermally stable than the unprocessed vaccine in solution over long-term storage.

5.2 Introduction

Influenza is a contagious disease with high morbidity, especially in elderly population [152] . Vaccination is the most effective way to prevent and control the spread of the disease. Today, almost all influenza vaccines are formulated in liquid form, which must be kept at a temperature range of 2°C~8°C to maintain the vaccine quality. Due to this narrow temperature requirement, vaccine management typically adopts cold chain, a series of temperature control during transport, distribution and storage. However, even cold chain does not guarantee the quality of vaccine; any accidental exposure to heat or unintentional freezing of vaccines by frozen packs during transport and storage can result in vaccine wastage. In addition to the thermal instability of liquid vaccine, stock piling of liquid vaccine for the purposes of mass distribution and emergency use also requires substantial protection and careful handling, and refrigerated warehouse space [153].

To minimize the dependency on cold chain and the required storage space, vaccines are dried into solid powder form. The most commonly used technique for drying vaccines is freeze-dry (lyophilization). Sugar glass technology, an inclusion of sugar into vaccine formulation, is used to protect vaccines from freezing stress during lyophilization. Amorphous sugar in its glassy state is believed to enhance the stability of vaccines by preventing biomolecules from aggregating [112], reducing the diffusion and mobility of lipids (vitrification) [113] and replacing water molecules' hydrogen bond interaction with the biomolecules [114]. Current vaccination method using needle-syringe system requires reconstitution if the vaccine is dried into powder form. However, since reconstitution is an additional preparation step, administration error or expiration of reconstituted vaccine can occur if not handle properly [154].

Many alternative delivery methods have taken the advantage of more stable dry vaccine without needing of reconstitution. Influenza vaccine in powder form has been delivered using a needle-free helium-powered PowderJect device into the skin [155]. Influenza vaccine can also be delivered intranasally by spraying vaccines into the nostrils [156]. Other method involves intradermal delivery of vaccines, which uses arrays of microscopic needles that insert vaccines into the epidermis and dermis of the skin in a minimally invasive way [117, 118]. Dissolving microneedles, for example, deliver molecules of interest by inserting the dissolvable needle tips encapsulating the molecules into the skin. Dissolving microneedles have demonstrated the capability of encapsulating proteins such as Erythropoietin (EPO), beta-galactosidase, lysozyme without causing significant damages to the proteins' functionalities [21-23].

In this study, we encapsulated inactivated influenza virus (A/Puerto Rico/8/34) in dissolving microneedles primarily made of polyvinyl alcohol (PVA) and sucrose. PVA is a harmless synthetic polymer that has been evaluated in numerous toxicity studies [157]. PVA is included in the FDA Inactive Ingredient Guide for topical application, transdermal delivery, intramuscular injection, ophthalmic solution, and oral tablet. PVA was used as a binder that offers mechanical strength to the microneedles whereas sucrose served as a microneedle matrix filler and a vaccine stabilizer.

The stability of encapsulated vaccine in microneedles at different storage temperatures under different packaging conditions was investigated. We first evaluated the influence of drying techniques and formulation on vaccine stability during encapsulation and processing into microneedles. By following the ICH guidelines to carry out post-processing storage for long-term stability studies [95, 96], we investigated four storage temperatures: 4°C as the control, 25°C, 37°C as the accelerated temperature and 45°C as the stress condition. To determine vaccine stability, we assessed the hemagglutination (HA) activity based on the maximum

dilution of vaccine that exhibits hemagglutination. We also investigated the antigenic

activity of HA using capture ELISA. In addition, we used electron microscopy to

examine the morphological integrity of influenza virus particles subject to different

temperatures.

5.3   Materials and Methods

5.3.1   Microneedle Fabrication

5.3.1.1   *Microneedle Mold*

A polydimethylsiloxane (PDMS, Sylgard 184, Dow Corning, Midland, MI) microneedle mold was fabricated by Choi et al using photolithography and molding techniques [140]. The mold contains 10 x 10 pyramidal microneedle cavities, each cavity was measured 600 x 300 x 300 µm (H x W x L). Polylactic acid (PLA) (L-PLA, 1.0 dL/g; Birmingham Polymer, Pelham, AL) microneedle master structure was made by casting molten PLA (195°C) onto the PDMS mold and vacuuming at – 91k Pa for 3 h. The reverse molded PLA structure was peeled off the PDMS mold after cooling to room temperature. New PDMS mold replicates were mass produced by curing PDMS mixture on top of the PLA master structure at 37°C overnight.

5.3.1.2   *Vaccine and Microneedle Formulation Preparation*

Inactivated influenza virus (IIV) (A/Puerto Rico/8/34) was supplied by Emory Vaccine Center (Atlanta, GA). The unprocessed vaccine solution was diluted with PBS to 0.5 mg/ml. Trace amount of trehalose (D-(+)-Trehalose dehydrate, Sigma-Aldrich) was added into the vaccine solution.

To prepare microneedle formulation, polyvinyl alcohol (PVA) (ACROS Organics, MW 2000) was dispersed in DI water at room temperature. The dispersed PVA solution was heated to 90°C for 1 h until PVA became fully dissolved. Sucrose

(≥99.5%, Sigma-Aldrich) was added into the PVA solution while the solution was still warm and mixed uniformly using a spatula. After 1 h of heating, the hot PVA/sucrose mixture was centrifuged at 1500 x g for 1 h to remove air bubbles in the mixture. To prepare PVA/Sucrose blend containing maltodextrin (dextrose equivalent 4.0 – 7.0, Sigma-Aldrich), same procedure was followed except maltodextrin was mixed with the PVA solution at 90°C before adding the sucrose. The de-bubbled mixture was cooled to room temperature overnight. The formulation used for long-term stability study was composed of a mixture of PVA, sucrose, maltodextrin dissolved in DI water (ratio 3 : 1 : 0.5 : 4 by weight).

5.3.1.3 *Vaccine Loading and Encapsulation*

The PDMS molds were loaded with vaccine solution containing trace amount of trehalose by vacuuming to – 91k Pa for 3 min. The residual vaccine solution was recycled using a pipette. The molds filled with the vaccine were placed in uncapped conical tubes (VWR) and were immediately centrifuged (GS-15R, Beckman, Fullerton, CA) at 3200 x g at 20°C for 3 min. After centrifugation, the mold surface was cleaned by tape stripping (Scotch Tape, 3M, St. Paul, MN). Next, the viscous excipient blend was applied onto the molds using a spatula. The molds covered with the excipient blend were vacuumed at – 91k Pa for another 5 min. After vacuuming, the molds were placed in capped conical tubes and centrifuged at 3200 x g at 20°C for 5 min. Finally, the molds were stored temporarily in 4°C and ready to be lyophilized.

5.3.1.4 Drying Process

The mold cast with vaccine and excipient blend were freeze-dried in a lyophilizer (VirTis Wizerd 2.0 freeze dryer, Gardiner, NY) for approximately 24 h. The freeze-drying steps were programmed as follows: The molds were frozen to -40°C for 1 h, and then vacuumed at 2.67 Pa at -40°C for 10 h. While the pressure was kept constant (2.67 Pa), the temperature was gradually ramped up to 0°C for 1 h, 20°C for 1 h and 25°C for another 10 h. After lyophilization, the microneedle array was removed from the mold using a double-sided tape (444 Double-Sided Polyester Film Tape, 3M, St. Paul, MN).

5.3.2 Microneedle Packaging and Storage

The microneedles were stored under three different packaging conditions. The first set of microneedles was placed in beakers without any control of humidity. The second set of microneedles was stored in sealed vials with controlled humidity. The vial used for microneedle containment consisted of a 3.7 ml uncapped glass vial (Fisher Scientific) placed in a 20 ml glass vial (Fisher Scientific). The 3.7 ml vial was loaded with 1 g of desiccants (Calcium Sulfate, Drierite, Xenia, OH) to control the humidity inside the sealed 20 ml vial. The microneedles were placed in the space between the wall of the 3.7 ml vial and the wall of the 20 ml vial. After placing the microneedles, the 20 ml vials with desiccants inside were capped tightly and further sealed with wrappings of parafilm (Fisher Scientific) around the vial cap. The thrid set of microneedles was also sealed in the 20 ml vials with controlled humidity as described previously except the air in the vial was replaced by nitrogen gas. The 20 ml vials containing the microneedles and the desiccants were loosely capped and were

repeatedly vacuumed to – 91k Pa and filled with nitrogen gas three times in a vacuum desiccator (Pequannock, NJ). All of the microneedles under different packaging conditions were allotted to 4°C, 25°C, 37°C and 45°C for long-term storage. Data points were collected on Day 0, 1, 3, 7, 14, 30 and 60.

5.3.3   Sample Preparation

Each microneedle array was dissolved in 1 ml of DI water. The dissolved microneedle solution containing vaccine and excipients was transferred to an eppendorf tube and centrifuged at 29,000 x g (Eppendorf centrifuge 5804) at 4°C for 30 min. The supernatant was removed and the vaccine pellet was re-suspended with PBS to 100 µl. The re-suspended vaccine solution was used for stability analyses.

5.3.4   Characterization of Vaccine Structural Integrity and Antigenic Property

5.3.4.1   Hemagglutination Assay

A total of 100 µl re-suspended vaccine solution was added to the U-shaped 96-well plate (Corning Costar Corp, Cambridge MA). The control was prepared by diluting 1.7 µl of 0.5 mg/ml unprocessed vaccine solution with PBS into 100 µl. The vaccine solutions were serially diluted by two-fold with PBS. Chicken red blood cell (RBC) (Lampire, Pipersville, PA) was diluted to 0.5 % and added to each well containing the diluted vaccine solution (1:1 ratio by volume). After 1 h of incubation at 25°C, the HA potency was recorded based on the maximal dilution that exhibited hemagglutination.

5.3.4.2 Capture ELISA

Goat-anti Flu H1N1 (USSR strain, from US biological Co.) was used as the capture antibody. The antibody was coated on 96-well plates by incubating 100 μl of the antibody solution at a dilution of 1:500 in each well overnight at 4°C. The solution was aspirated from each well. The plate was washed with PBS-T three times. After washing, the plates were blocked by adding 150 μl of PBS containing 2% BSA. The plate was incubated at room temperature for 2 h. The 2% BSA solution was aspirated and the plate was washed repeatedly. The vaccine samples were obtained from re-suspension of the vaccine pellet described previously. One hundred microliter of the re-suspended vaccine samples and the unprocessed vaccine standards were transferred into the wells and were incubated 2 h at room temperature. After incubation, the solutions were aspirated and the plate was washed repeatedly. The serum from the influenza HA expressing DNA construct immunized mice was added at a dilution of 1:500 to each well. After aspiration and washing, anti mouse IgG-HRP (Southern Biotech, Birmingham) was incubated in each well for 1 h at room temperature. After washing the plate five times, 50 μl of Tetramethylbenzidine (TMB) (Sigma-Aldrich) was added as the substrate solution. Fifty microliter of 0.2N HCl was added to stop the reaction. The optical density of each well was determined by a microplate reader set at 450 nm.

5.3.4.3 Negative Staining and Electron Microscopy

To examine the morphology of encapsulated vaccine, 10 μl of re-suspended vaccine solution was applied to a formvar carbon coated grid at room temperature for 3 min. Extra vaccine suspension was absorbed by filter paper. The grids were

immediately stained with 2% phosphotungstic acid for 30 sec. Excess stains were removed by filter paper. The samples were examined on a Hitachi 7500 transmission electron microscope.

5.4 Results

5.4.1 Microneedle Fabrication

To investigate the stability of vaccine encapsulated within dissolving microneedles, unprocessed vaccine was reformulated and dried into microneedles. Fig. 5.1 showed a 10 x 10 array of solid dissolving microneedles made of PVA/Sucrose blend encapsulating influenza vaccine. The back side of the array was immobilized on a double-sided tape for the ease of handling and portability. Each pyramidal needle was 600 μm tall with a 300 x 300 μm base (Fig 5.1B). The needles encapsulating vaccine appeared to be opaque. Although not visually distinguishable, the vaccine was encapsulated only within the microneedles but not in the array backing.
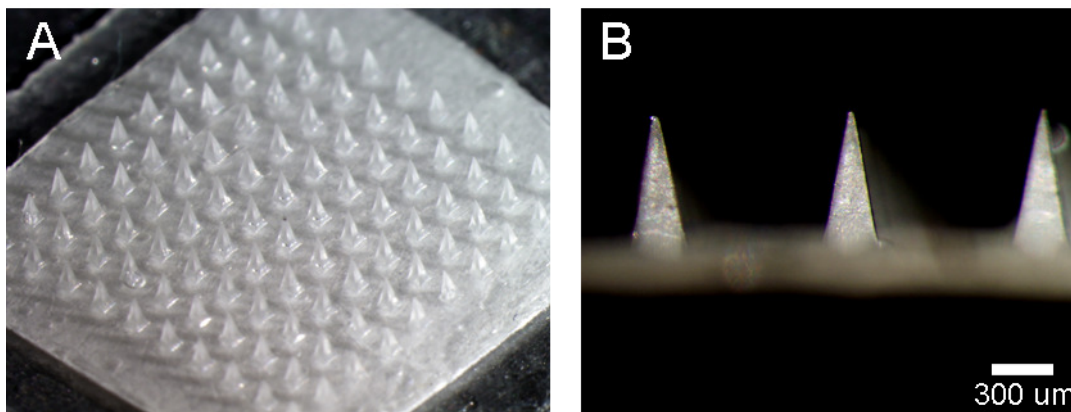
Fig. 5.1. Dissolving microneedles encapsulating inactivated influenza virus. (A) A 10 x 10 microneedle array. (B) Side view of microneedles.

5.4.2 Effect of Microneedle's Drying Methods on HA Potency

We sought to select a drying method that maintains the most HA potency after microneedle processing. Microneedles containing influenza vaccine were subject to three different drying methods including lyophilization, thermal dry at 25°C and at 45°C. According to Fig. 5.2, microneedles dried by lyophilization maintained an average of 80% HA potency relative to the unprocessed vaccine at 4°C. The drying processes involving evaporation of water from the microneedles by heat at 25°C and 45°C caused approximately 50% and 55% loss of HA potency respectively. Lyophilization was able to maintain the highest HA potency compared to thermal drying method at 25°C and 45°C (Student's t-test, $p<0.05$). Due to the difference between each drying method's water removal rate and drying mechanisms, the resulting residual moisture in the microneedles might vary. To investigate if the residual moisture in the microneedles would have further effect on the HA potency, we stored all of the microneedles dried by different methods in separate sealed glass vials containing desiccants for five days at room temperature. The moisture content of all the microneedles should have reached equilibrium with the desiccant-controlled environment. The result showed that there was no significant difference of HA potency between microneedles that were immediately fabricated and microneedles that were stored over 5 days under the same condition (Student's t-test, $p>0.05$) (Fig. 5.2).
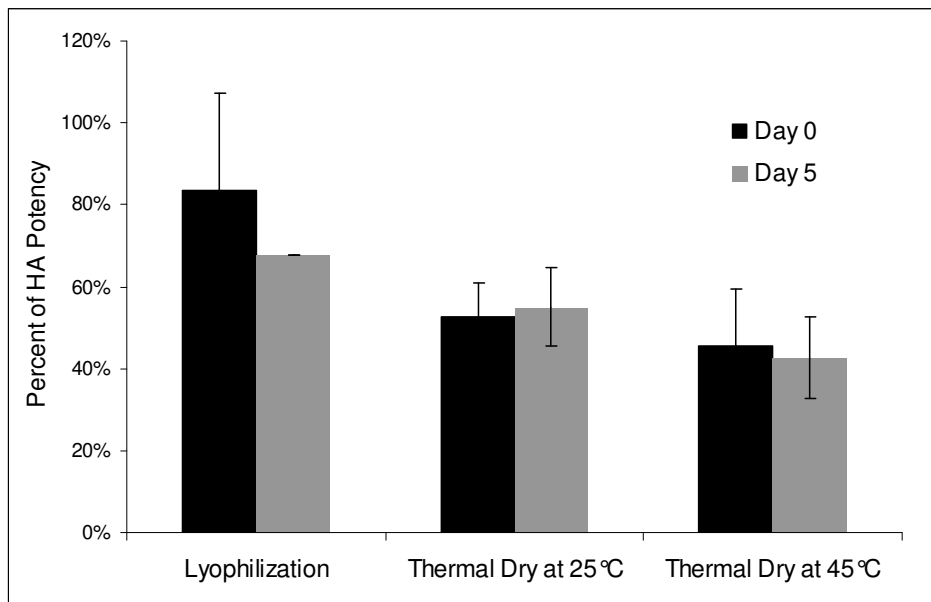
Fig. 5.2. Effect of microneedle fabrication drying process on HA activity. Day 0 indicates the dried microneedles immediately after fabrication. Day 5 indicates the microneedles stored in sealed containers with desiccants at 25°C over five days. (N = 4)

5.4.3 Effect of Formulation on HA potency

The goal was to determine the most appropriate formulation composition for stable vaccine encapsulation and microneedle fabrication. The formulation used in this study primarily consisted of PVA and sucrose. By varying the ratio of these two excipients, we aim to determine the effect of formulation composition on HA potency. The formulation containing only PVA led to 80% loss of HA potency when lyophilized with the encapsulated vaccine (Fig. 5.3). Inclusion of 33% sucrose in the formulation resulted in a significant recovery of the HA potency up to approximately 70%. Further increment of sucrose in the formulation did not significantly increase the HA potency (ANOVA, $p > 0.05$). Hence, the presence of sucrose was critical but the amount of sucrose need not be abundant for proper maintenance of HA potency.
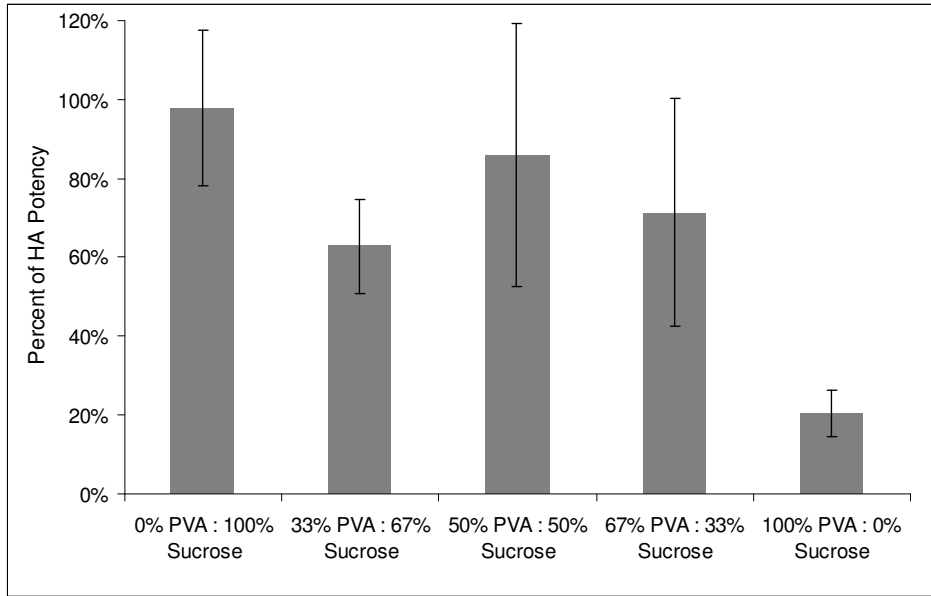
Fig. 5.3. Effect of formulation on HA activity. Each bar shows a different formulation composition consisting PVA and/or sucrose dissolved in DI water. (N = 4)

5.4.4 Stability of Encapsulated Vaccine in Dry State versus Unprocessed Vaccine in Wet State at Various Temperatures

We hypothesized that vaccine formulated into dry state is more stable than unprocessed vaccine in wet state. To test this hypothesis, we reformulated and processed vaccine into solid dissolving microneedles and stored at 4°C, 25°C, 37°C and 45°C over extended periods of time. A set of unprocessed vaccine solutions was allotted and stored in parallel with the processed vaccine samples at those four temperatures. The unprocessed vaccine stored at 4°C (control) remained stable throughout the entire study. The processed encapsulated vaccine maintained approximately 60% HA potency over 4 weeks, even with those samples subject to elevated temperatures. There was no significant HA potency difference among the encapsulated vaccine groups stored at different temperatures within 4 weeks (One-way ANOVA, p>0.05). On the other hand, the unprocessed vaccine stored outside of refrigeration showed a dramatic HA potency drop within a few days. Based

92

on the long-term stability study shown in Fig. 5.4, the encapsulated vaccine processed into dried microneedles was significantly more stable than the unprocessed vaccine in wet solution state (Student's t-test, $p < 0.05$).
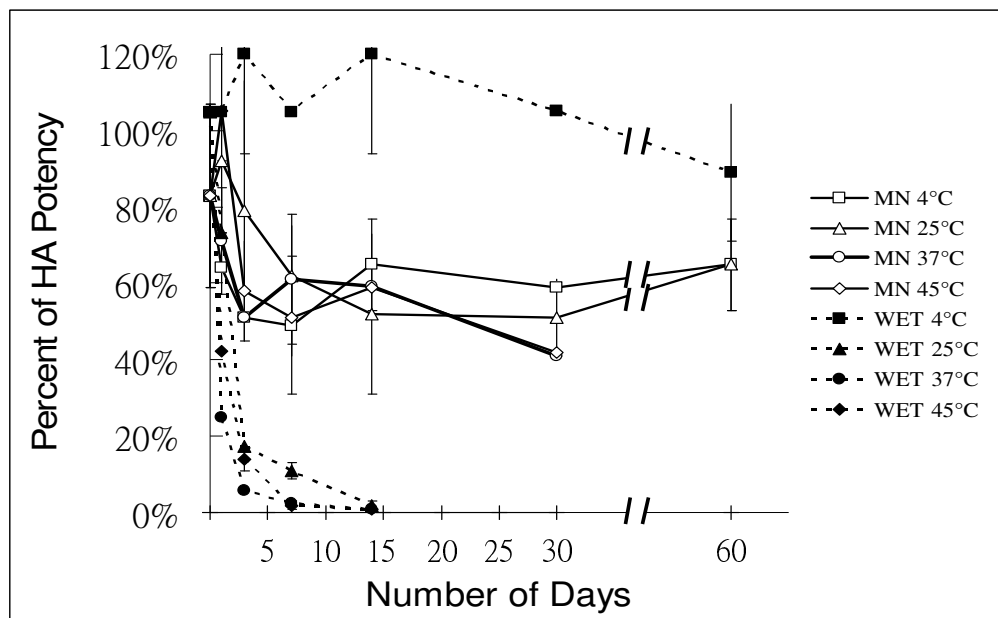
Fig. 5.4. Comparison of the long-term stability of unprocessed vaccine solutions versus dried microneedle vaccine samples based on HA potency under different temperatures. MN indicates the processed vaccine encapsulated within microneedles. WET indicates the unprocessed vaccine in solution. (N≥3)

5.4.5   Effect of Different Packaging Conditions on Encapsulated Vaccine Stability

To answer the question of whether the stability of encapsulated vaccine was influenced by different packaging condition over the long term, we stored the microneedle samples encapsulating the vaccine under three packaging conditions. Microneedles were placed in open containers without any control of humidity (N), or in sealed containers with controlled humidity by desiccants (D), or in sealed containers filled with nitrogen gas and with controlled humidity by desiccants (DV).

93

Fig. 5.5 showed that the HA potencies of all encapsulated vaccine stored in three packaging conditions were equivalent and remained unchanged relative to the freshly fabricated microneedles on Day 0 throughout 8 weeks at 25°C (One-way ANOVA, p>0.05).
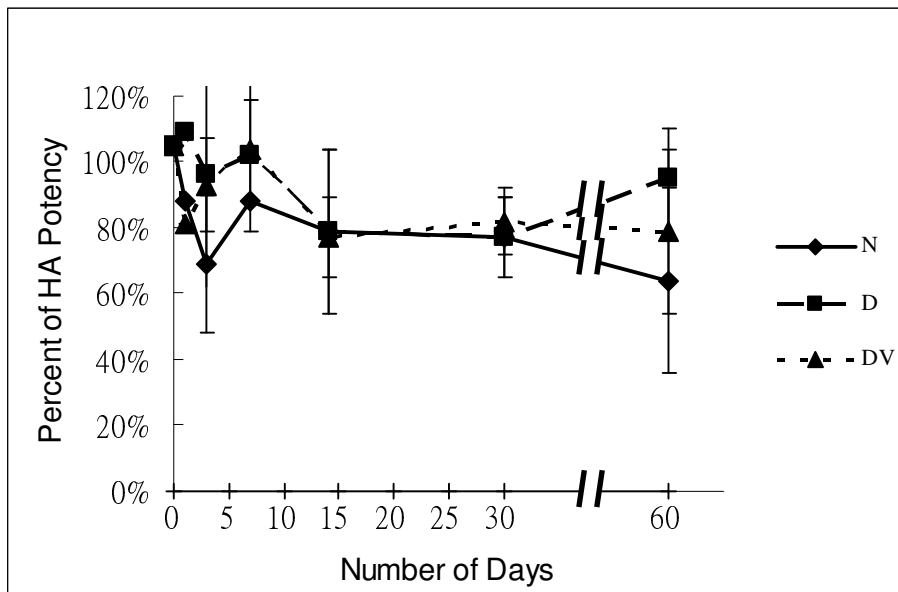
Fig. 5.5. Comparison of the long-term stability of dried microneedle vaccine samples stored under different packaging condition. **N**: Open containers without any control of humidity. **D**: Sealed containers with controlled humidity by desiccants. **DV**: Sealed containers filled with nitrogen gas and with controlled humidity by desiccants. (N≥3)

5.4.6   Antigenic Properties of Encapsulated Vaccine and Unprocessed Vaccine under Different Thermal Stresses

We used a different approach, the capture ELISA, to validate the stability of encapsulated vaccine and unprocessed vaccine at different temperatures based on the HA's antigenic property. Vaccine encapsulated in microneedles and unprocessed vaccine solutions were stored in parallel at 4°C, 25°C, 37°C and 45°C over a period of 2 weeks. We found that the unprocessed vaccine stored over 2 weeks outside of

refrigeration (25°C, 37°C and 45°C) resulted in a four-fold loss in HA binding activity against Goat-anti Flu H1N1 antibody. On the contrary, the encapsulated vaccine, even with the ones exposed to elevated temperatures for 2 weeks, showed equivalent binding activities to the control (unprocessed vaccine at 4°C) (Fig. 5.6).
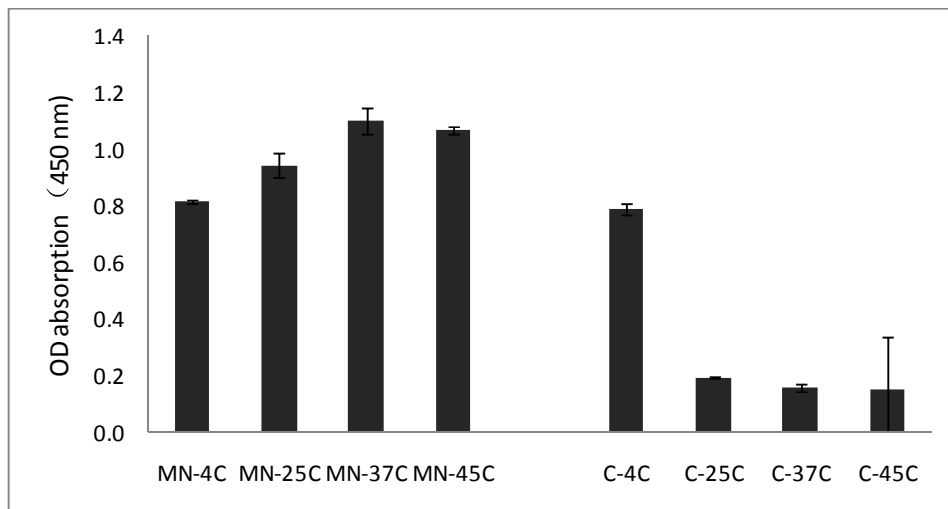
Fig. 5.6. Evaluation of vaccine stability over 2 weeks using capture ELISA. Left: Microneedle samples (MN) containing encapsulated vaccine stored at 4°C, 25°C, 37°C and 45°C. Right: unprocessed vaccine solution (C) stored at 4°C (control), 25°C, 37°C and 45°C. (N≥3)

5.4.7   Morphology of Inactivated Influenza Viruses under Different Temperatures

We further examined the stability of encapsulated vaccine and unprocessed vaccine at different temperatures based on the morphological integrity of virus particles. The virus particles collected from dissolved microneedle solution and unprocessed vaccine solution were negatively stained with 2% phosphotungstic acid and examined under electron microscope. As shown in Fig. 5.7, the encapsulated vaccine stored at 4°C, 25°C, 37°C and 45°C (Fig 5.7A) as well as the unprocessed vaccine stored at 4°C vividly showed intact virus particle structure with a circular

contour of lipid bilayer. The integrity of the encapsulated virus particles was maintained even under elevated temperatures for 2 weeks. On the other hand, the unprocessed vaccine stored at 25°C, 37°C and 45°C showed ruptured or swollen particle structures (Fig 5.7B). The lipid bilayer of those unprocessed virus particles subject to elevated temperatures was not distinctively visible compared to that of the encapsulated virus particles.
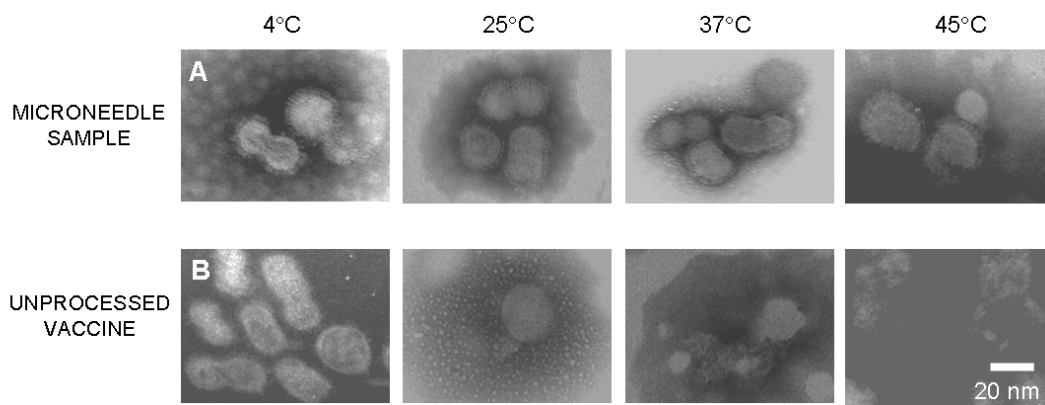
Fig. 5.7. Images of electron microscopy of negatively stained inactivated influenza virus particles stored at different temperatures. (A) The encapsulated virus particles dissolved off the microneedles stored at 4°C, 25°C, 37°C and 45°C maintained intact particle morphology with visible lipid bilayer structures. (B) The unprocessed virus particles stored at 4°C kept an intact morphology while all other unprocessed virus particles stored at elevated temperatures showed ruptured structures or absent lipid bilayers.

5.5　Discussion

While most lyophilized vaccine powder requires reconstitution for injection, some delivery systems have taken the advantage of dried vaccine for immunization. One example is the use of solid microneedles to deliver dried vaccine into the skin [117, 118]. Differ from other microneedle systems, dissolving microneedles encapsulate drugs and biomolecules within the needle matrix [22, 23, 76]. In most cases, fabrication of dissolving microneedles requires water removal, a step that exposes the molecules to drying stress. Therefore, we evaluated three drying approaches: lyophilization, thermal dry at 25°C and at 45°C. The results showed that the lyophilization maintained the most HA potency compared to all other methods attempted. Although lyophilization may associate with higher cost as it requires more sophisticated equipment and drying time from hours to days, the overall cost may be lower if vaccine is batch processed and if the process results less vaccine wastage due to damage from the drying stress.

Formulation played a critical role in vaccine stability. Adoption of sugar glass technology has been described in literatures for protecting proteins, liposomes and viruses from drying stresses [106-108, 110, 111]. Similarly, our formulation containing PVA and sucrose also protected the vaccine from freezing stress during lyophilization. The formulation was able to maintain a long-term stability of the vaccine at various temperatures. Although inclusion of sugars have shown to enhance the stability of biomolecules, crystallization of sugars can cause damage to the vaccine antigens if the sample is not properly dried [88]. According to Fig. 5.3, addition of merely 33% sugar recovered almost all HA potency. Based on this finding, we did not use formulations that have a dominant presence of sugars for the long-term

stability studies to avoid crystallization of sugars.

One of the obstacles of performing HA assay with the dissolved microneedle solution was the presence of PVA. PVA interfered with the HA assay by promoting RBC precipitation. To overcome this problem, we separated the vaccine from the polymer in the dissolved microneedle solution by centrifugation. The virus particles were heavier enough to be spun down while PVA and other excipients remained suspended in solution. We collected the pellets and re-suspended into aqueous samples for the assays. In this way, the reduced presence of PVA in the re-suspended vaccine samples greatly minimized the assay interference. But another issue arose as we applied high centrifugal force to the vaccine. We found that unprocessed vaccine under high speed centrifugation lost as much as eight-fold HA potency (data not shown). However, addition of the microneedle excipients (i.e. PVA and sucrose) to unprocessed vaccine rescued the HA potency loss from the centrifugal damage. We hypothesize that these excipients might form a coating on the virus particles; these coatings prevented the virus particles from aggregating and reduced non-specific interaction with the container surface promoted by the centrifugal force.

According to Fig. 5.4, HA potency of all the encapsulated vaccine samples remained unchanged for at least four weeks under all storage temperatures (4°C, 25°C, 37°C and 45°C), whereas unprocessed vaccine solutions subject to elevated temperatures lost all HA potency within a few days. It was clear that the encapsulated vaccine in dry state was more resistant to thermal variation than the unprocessed vaccine. One question that may arise is the discrepancy of HA potency between the encapsulated vaccine immediately after microneedle processing and the unprocessed vaccine at 4°C on Day 0 (the control). We proposed several explanations to address this question. We believe that the drying process might cause some damage to the vaccine due to freezing and drying stresses. As mentioned earlier, centrifugation led to

a dramatic HA potency loss of the unprocessed vaccine. Even though adding PVA and other excipients secured the vaccine from significant damage, some loss (0~50%) was still seen (data not shown). We might also lose some vaccine as we isolated the vaccine pellet by removing the supernatant. Moreover, throughout the whole microneedle dissolution and solution transfer processes, the chance of non-specific interaction of the vaccine with the container surfaces was also increased.

We did not observe any difference in the encapsulated vaccine stability stored under different packaging conditions. Insensitivity of vaccine stability to packaging condition is advantageous because accidental damage to the package containing microneedles, or opened package prior to use would not raise concerns for instant loss of stability. However, proper packaging is still important to keep moisture and physical damage away from the microneedles.

Potent stability of encapsulated vaccine in dissolving microneedles offers many benefits to modern vaccination. Reduced sensitivity of encapsulated vaccine to thermal variation decreases the reliance on cold chain, which in turn could save cost associated with refrigerated equipment, facilities and personnel. By drying vaccine into solid microneedles, warehouse storage space and weight associated with transport cost are greatly minimized. Transport vaccines to developing countries where hot climate is common would benefit from this potent stability by encapsulating vaccines within microneedles.

5.6   Conclusions

We have evaluated the stability of encapsulated vaccine during microneedle fabrication and post-microneedle processing. Drying by lyophilization maintained the most vaccine stability. Inclusion of sucrose in the formulation also minimized the HA potency loss during microneedle processing. Three techniques including HA assay, capture ELISA and TEM have validated the potent stability of encapsulated vaccine over their unprocessed vaccine counterparts outside of refrigeration for extended periods of time. Furthermore, the encapsulated vaccine stability was independent of the packaging conditions we studied. The potent stability of encapsulated vaccine offered by solid microneedle dosage form could potentially reduce the dependency of cold chain, eliminate the need of reconstitution, require less storage space and allow higher portability.

5.7   Acknowledgements

CHAPTER 6

Immunization of Mice using Arrowhead Microneedles Encapsulating Inactivated Influenza Virus

Leonard Y. Chu[1], Ling Ye[2], Ke Dong[2], Richard W. Compans[2], Chinglai Yang[2], Mark R. Prausnitz[1,3]

1. Wallace H. Coulter Department of Biomedical Engineering**,**
Georgia Institute of Technology, Atlanta, GA 30332, USA
2. Department of Microbiology and Immunology and Emory Vaccine Center,
Emory University School of Medicine, Atlanta, GA 30329 USA
3. School of Chemical & Biomolecular Engineering,
Georgia Institute of Technology, Atlanta, GA 30332, USA

6.1 Abstract

Current vaccination largely relies on injection using hypodermic needles. This method of administration has low patient compliance, produces sharp biohazardous waste after use and requires highly trained personnel. In this study, arrowhead microneedles were used to administer inactivated influenza vaccine (IIV) (A/Puerto Rico/R/8/34) (H1N1) rapidly into the skin. We aimed to find out if cutaneous delivery of IIV using arrowhead microneedles elicits comparable immune response to the intramuscular injection using hypodermic needles. We delivered a dose of 10 µg IIV to Balb/C mice. The results showed that cutaneous delivery using arrowhead microneedles induced statistically comparable levels of antibody responses against influenza virus to intramuscular injection after a single immunization. Microneedle immunization protected all the mice from lethal challenge with homologous influenza virus (PR8), while 67% mice were protected from challenge with heterologous influenza virus (WSN). In sum, arrowhead microneedles could administer IIV into the skin rapidly within one minute and induced potent immune responses that protected the mice from lethal challenges. Unlike hypodermic needles, arrowhead microneedles do not generate sharp biohazardous waste and can potentially be self-administered.

6.2 Introduction

Skin offers an attractive route for drug and biopharmaceutical delivery due to the avoidance of first-pass effect. Abundant presence of antigen presenting cells in the epidermis and dermis layer of the skin also serve as excellent vaccine delivery targets for triggering immune responses [158]. However, challenges for transdermal delivery lie upon the skin's outermost layer, stratum corneum, which prevents highly hydrophilic drugs and macromolecules from entering into the body [3]. To circumvent this skin barrier, hypodermic needles administer vaccines by penetrating deeply into tissues or muscles. More targeted delivery of vaccines to the skin is feasible by using the Mantoux technique, but this method requires highly trained personal [159]. Another approach for targeted vaccine delivery to the skin is to use miniaturized hypodermic needles with limited exposed length that only penetrate a certain depth into the skin [116, 134]. Apart from the most widely used hypodermic needles, bifurcated needles, the fork-like metal needles, have also been used to deliver smallpox vaccine by repeatedly jabbing the skin [160-162]. Either use of hypodermic or bifurcated needles cause pain and produce sharp biohazardous waste after use. Moreover, re-using and sharing of these needles pose the risk of blood-borne pathogen disease transmission.

Many alternative delivery methods aim to administer vaccines across the skin in a less invasive way. Immunization by physical perturbation of stratum corneum using tape stripping technique has shown to enhance antibody response compared to hydration of the skin alone [130]. Immunization by electrical means has been demonstrated using electroporation to enhance DNA vaccine delivery across the skin [163, 164]. Miniaturized needle structure measured in micron-size, also known as microneedles, have also induced potent immune responses in mice by delivering

coated vaccines into the skin [117, 118]. Building upon many years of technological advancement of microneedles [15, 16, 19, 20, 23, 63], we have designed a new type of microneedles called arrowhead microneedles for drug and vaccine delivery. Arrowhead microneedle's sharp tips dissolve upon insertion into skin while the remaining dull shafts and backing can be removed from the skin quickly without producing sharp waste.

The goal of this study was to compare the immune responses of cutaneous delivery using arrowhead microneedle with intramuscular administration of IIV using hypodermic needles in Balb/C mice. We hypothesized that cutaneous immunization using microneedles would generate comparable immune responses to intramuscular immunization. We also hypothesized that single immunization using microneedles at a dose of 10 µg IIV could protect mice from lethal challenge by the homologous virus and possibly the heterologous strain.

6.3 Materials and Methods

6.3.1 Inactivated Influenza Virus Preparation

Influenza virus (A/Puerto Rico/R/8/34) (H1N1) were inoculated and grown in embryonated chicken eggs. Three days post-inoculation, the allantoic fluid was harvested from the infected eggs. Harvested allantoic fluid was then concentrated with Quick-stand filtration system and purified with ultracentrifugation through discontinuous sucrose gradient. The virus used for immunization was inactivated with 0.1% formalin for 3 days at 4°C. After inactivation, the purified virus was characterized by SDS-PAGE and western blot to examine the presence of specific proteins. Hemagglutination (HA) assay was performed to evaluate the function and integrity of hemagglutinin proteins. The virus was also negatively stained with 2% phosphotungstic acid to check the virus morphology under an electron microscope (Hitachi 7500, Japan).

6.3.2 Microneedle Fabrication and Inactivated Influenza Virus Encapsulation

Arrowhead microneedles were fabricated as described previously in Chapter 4: "Rapid cutaneous delivery using arrowhead microneedles". For immunization study, 10 µg IIV containing a trace amount of trehalose was loaded into a polydimethylsiloxane (PDMS) mold. For in vivo insertion test, sulforhodamine B was used for visual inspection of the insertion spots on mouse skin. An excipient blend consisting polyvinyl alcohol (PVA) and sucrose (1:1 ratio by weight) dissolved in DI water was cast onto the mold by vacuum and centrifuge. Arrays of fifty 700 µm tall stainless steel shafts (5 x 10) was aligned to the PDMS mold cast with excipient blend, and then freeze-dried overnight. After drying, the dried excipient blend connected to

the metal shafts was removed from the PDMS mold, forming arrowhead microneedles.

6.3.3 In Vivo Insertion Test

Prior to the immunization study, in vivo assessment of microneedle insertion on mouse skin was performed following the Institute for Animal Care and Use Committee (IACUC) guidelines. Female Balb/c mice were purchased from Charles River Laboratory and housed at the Georgia Tech Physiological Research Laboratory. The mice were anesthetized in a chamber filled with 5% isofluorance with an oxygen feed rate at 1000 ml/min. The mice were transferred from the chamber to a warm procedure stage immediately when they lost consciousness. The mice's noses were covered with rubber masks flowing 2% isofluorane with an oxygen feed rate at 400 ml/min. The hair on the backside of the mice was fist removed gently by a clipper. Then, the depilatory cream (Nair) was applied onto the shaved region for 3 min and excess Nair was wiped away with wet gauzes. The step of applying and removing Nair on the skin was repeated two to three times for complete removal of the hair at the desired insertion site. After the hair was removed, approximately 1.5 cm x 1.5 cm nude skin was pinched onto a flat surface. Microneedles were inserted perpendicularly to the nude skin for specified time durations. Images of the inserted skin were taken using a stereoscope (Olympus SZX16, Pittsburgh, PA). While the mice were still unconscious under anesthesia, they were euthanized in a CO_2 chamber in accordance to the IACUC.

6.3.4 Immunization Study Design

Week 0	Week 2	Week 3	Week 4	Week 6

Immunization (dose: 10 µg)

Blood sample collection

Challenge by mouse-adapted PR8 and WSN (100 LD50)

Sacrifice mice, Blood sample collection
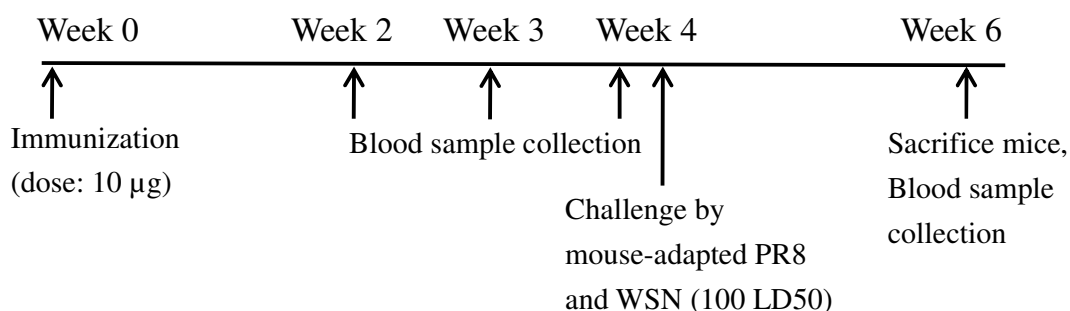
Fig. 6.1. Single immunization timeline. **Week 0**: Mice (six per group) were immunized by intramuscular injection and cutaneous microneedle insertion. **Week 2, 3 and 4**:   Blood samples were collected retro-orbitally for antibody serum and HAI analyses. **Week 4**: After collecting the blood samples, the mice were challenged by mouse-adapted PR8 and WSN viruses. **Week 6**: The mice were sacrificed and blood samples were collected.

For the immunization study, mice were divided into four groups: (i) Intramuscular injection of PBS using hypodermic needles (control); (ii) Intramuscular injection of IIV; (iii) Intramuscular injection of IIV dissolved off the microneedles; And (iv) cutaneous insertion using microneedles. Each mouse was given a dose of 10 µg IIV.

6.3.5 Immunization of Mice

Female Balb/C mice (6-8 weeks old) were purchased from Charles River Laboratories and housed at the Emory University animal facility in micro-isolator cages. For intramuscular immunization, 10 µg IIV suspended in 100 µl PBS was injected into mouse quadriceps. For cutaneous immunization by arrowhead microneedles, the hair on the back of the mouse was removed by depilatory cream

(Nair) and washed with 70% ethanol one day before the immunization. Prior to microneedle insertion, the mice were anesthetized by Ketamine and Xylazine. Approximately 1.5 cm x 1.5 cm skin was pinched onto a flat surface and the microneedle array was pressed perpendicularly to the skin for 1 min.

6.3.6   ELISA and Hemagglutination Inhibition Assay

Blood samples were drawn retro-orbitally from mice on day 14, day 21 and day 28 post-immunization and 2 weeks after the lethal challenge.

ELISA assay was performed following the established protocol to measure the presence of influenza hemagglutinin (HA) specific antibodies in individual mouse sera [165]. Briefly, purified His-tagged HA proteins were used as the coating antigens. Standard curve was generated by coating each ELISA plate with serial two-fold dilutions of purified mouse antibodies with known concentration. The concentrations of influenza HA specific antibodies in serum samples were calculated by using the established standard curves.

The paired samples were tested together by hemagglutination inhibition (HAI) assay following established protocols [166]. The sera were treated with receptor-destroying enzyme (RDE) (Kenka Seiken, Tokyo, Japan) (I:3) at 37°C overnight to remove nonspecific inhibitors. The residual RDE was destroyed by heat inactivation at 56°C for 30 min. Serial two-fold dilutions of RDE-treated serum (1 in 10) were titrated in a 96-well microtiter plate (Corning Costar Corp, Cambridge MA) against 4 hemagglutinin units of reference antigens (H1N1) using 0.25% chicken erythrocytes (Lampire, Pipersville, PA). After 45 min of waiting, the HAI titer was recorded based on the highest serum dilution that inhibited hemagglutination.

6.3.7 Lethal Virus Challenge

Live influenza virus challenge was conducted in a BSL+ animal facility. Four weeks after immunization, mice were challenged under light anesthesia by intranasal instillation with 100 x LD50 of mouse-adapted influenza virus A/PR/8/34 diluted in 50 µl PBS. After the challenge, mice were monitored for weight change and signs of illness on a daily basis. Mice that exhibited severe sighs of illness and significant weight loss (>25%) were euthanized in accordance with IACUC. At the end of the challenge study, mice that survived the challenge were sacrificed and blood samples were collected for post-immunization analyses.

6.4 Results

6.4.1 In Vivo Arrowhead Microneedle Insertion Test

Prior to immunizing the mice, we wanted to demonstrate the capability of encapsulating IIV into arrowhead microneedles and successfully inserting the needles in vivo. Arrowhead microneedles were fabricated by capping sharp dissolvable tips onto mechanically robust metal shafts (Fig. 6.2A). The tips of the arrowhead microneedles were made of PVA/sucrose blend. These needles dissolved upon insertion into skin,and produced no sharp biohazardous waste. Each microneedle had an overall length of 1.3 mm, consisting of a 600 µm tall pyramidal tip supported by an 800 µm shaft with 100 µm overlap (Fig. 6.2B). The microneedles encapsulating IIV appeared colorless and opaque. For visual inspection, we incorporated sulforhodamine B into the needles to show the encapsulation of molecules within the microneedles and the insertion on the skin (Fig. 6.2C, 6.2D). The microneedles encapsulating sulforhodamine B were inserted into the skin of an anesthesized mouse for 1 min. The microneedle tips dissolved and released sulforhodamine B into the mouse skin, creating 5 x 10 array of pink dots (Fig. 6.2D).
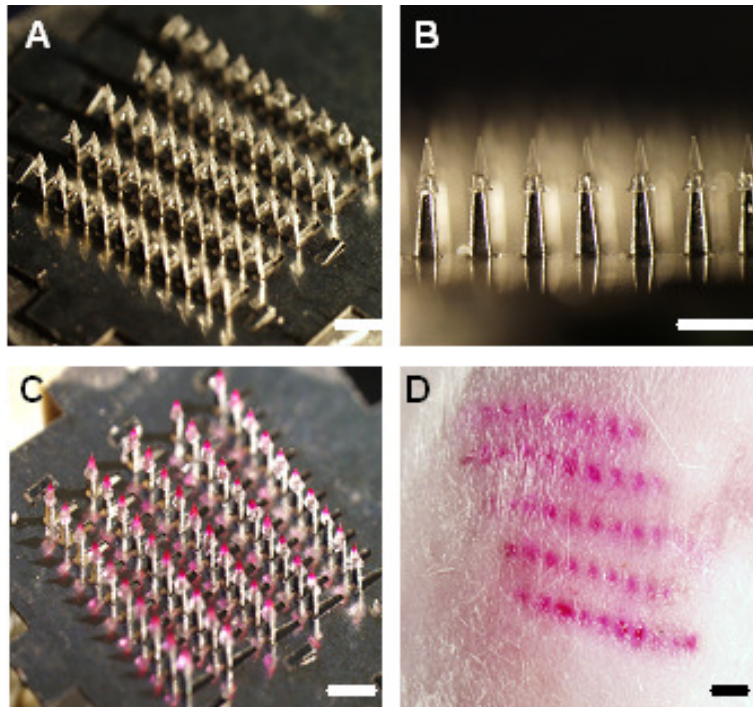
Fig. 6.2. An array of 10 x 5 arrowhead microneedles: (A) Encapsulating IIV; (B) Side view; (C) Encapsulating sulforhodamine B; And (D) insertion into mouse skin in vivo. Bar = 1 mm

6.4.2　Induction of Antibody Responses by Cutaneous Delivery of IIV Vaccine using Microneedles

The goal was to compare the immune responses induced by cutaneous delivery of IIV vaccine using arrowhead microneedle (MN) with those induced by intramuscular (IM) injection. Blood samples were collected at 2 weeks, 3 weeks and 4 weeks post immunization and analyzed for antibody responses against the HA protein and the HAI titers against the inactivated influenza virus. As shown in Fig. 6.3A, cutaneous delivery of IIV vaccine using MN induced comparable levels of antibody responses against homologous influenza virus to IM injection 4 weeks after a single immunization. While the average antibody responses induced by microneedles appeared lower than that obtained by intramuscular injection, the difference was statistically insignificant (student's t-test, $p > 0.05$). High antibody responses were

111

elicited in all immunized groups against PR8 antigens. Intramuscular injection of IIV dissolved off the microneedles induced similar levels of antibody responses compared to other groups (student's t-test, p<0.05), indicating that the immunogenicity of IIV remained unchanged during microneedle encapsulation and drying process. We further analyzed the HAI titers induced by different immunization approaches. As shown in Fig. 6.3B, HAI activity was detected in all vaccinated groups and the HAI levels were in direct correlation with the level of antibody responses against HA measured by ELISA (Fig. 6.3A).
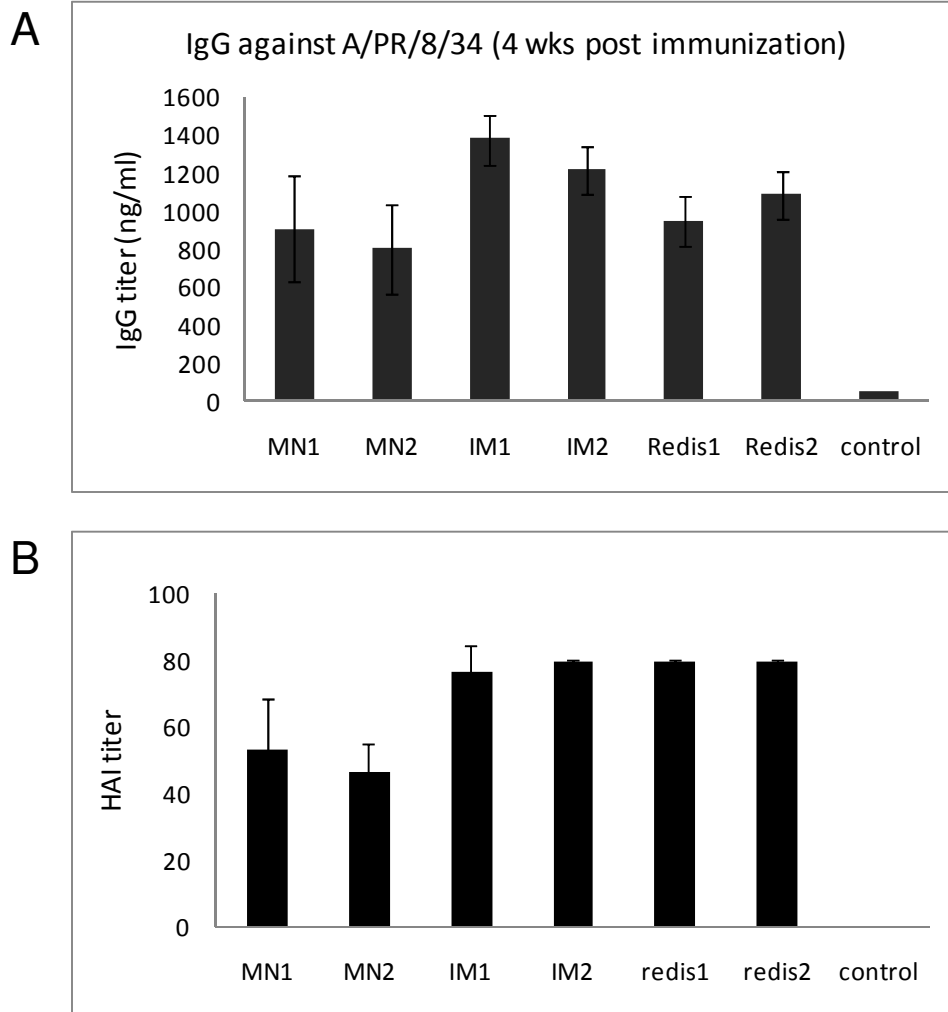
Fig. 6.3. Comparison of induced antibody responses 4 weeks after immunization. Eight groups of mice were immunized, six mice per group. Mice were immunized by microneedles (MN), intramuscular injection (IM), intramuscular injection of IIV dissolved off the microneedles (Redis) and intramuscular injection of PBS (control). (A) The serum antibody levels against HA proteins were measured by ELISA. (B) The HAI activity was determined by the maximum dilution of serum samples that inhibited hemagglutination.

6.4.3   Protection of Mice against Lethal Influenza Virus Challenge with a Single Immunization of IIV Vaccine

Based on the strong antibody responses induced by cutaneous delivery of IIV using microneedles after a single immunization, we aimed to test whether single immunization could protect mice against lethal virus challenge. At week 4 post-immunization, mice were challenged with 100 LD50 of mouse-adapted homologous influenza virus (PR8) and heterologous virus (WSN). As shown in Fig. 6.4, while all of the mice in the control groups succumbed to challenge and were sacrificed between days 5 and 8 post-challenge, all mice immunized by microneedles encapsulating the IIV or intramuscular injections protected the mice from the lethal challenge with PR8. Although all of the experimental groups showed as much as 20% weight loss when infected with the heterologous virus WSN, intramuscular injection of IIV and IIV dissolved off the microneedles gave full protection to all the mice. Immunization using microneedles protected 4 out of 6 mice, or 67% survival rate of the mice challenged with WSN.
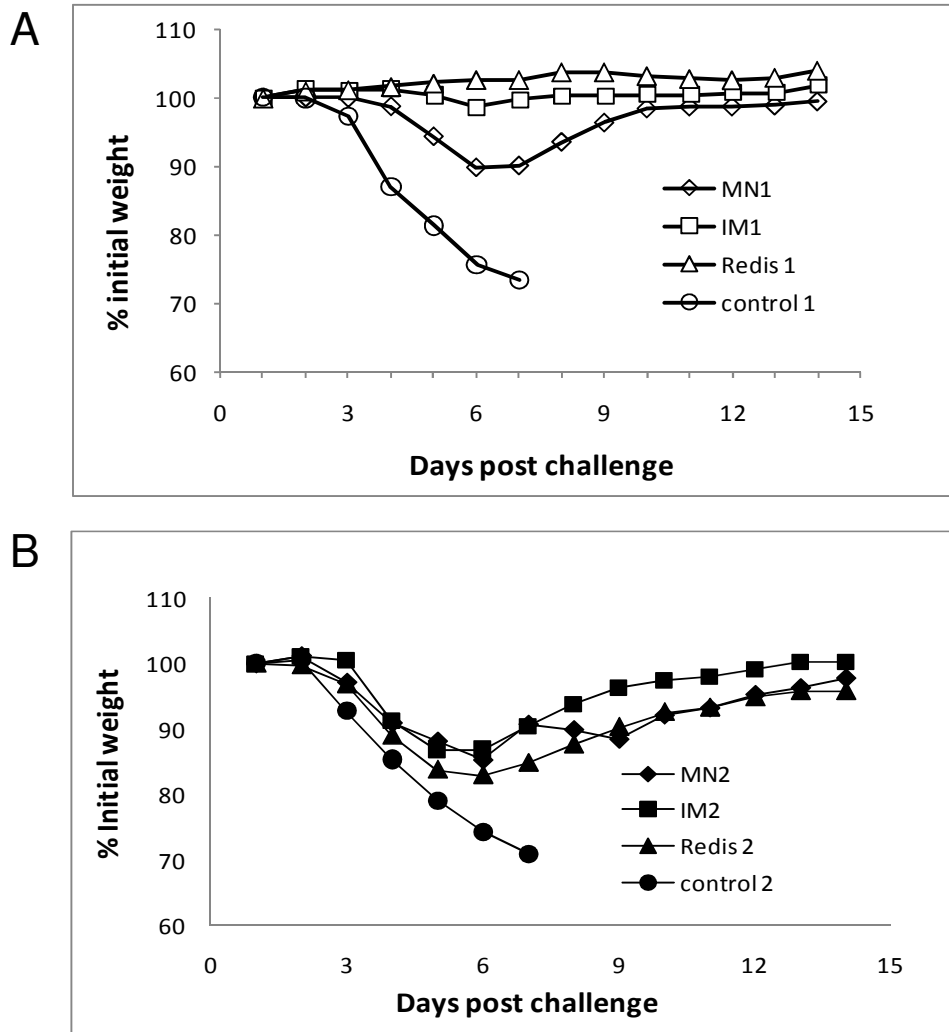
Fig. 6.4. Change of mouse weight over two weeks after lethal challenges. (A) Four groups were challenged by homologous virus strain (PR8); (B) Another four groups were challenged by heterologous virus strain (WSN). Each group consisted of 6 mice. A dose of 10 µg IIV was given to each mouse. Mice were immunized by microneedles (MN), intramuscular injection of IIV (IM), intramuscular injection of IIV dissolved off the microneedles (Redis) and intramuscular injection of PBS (control). Mice were sacrificed when the body weight lost more than 30 %.
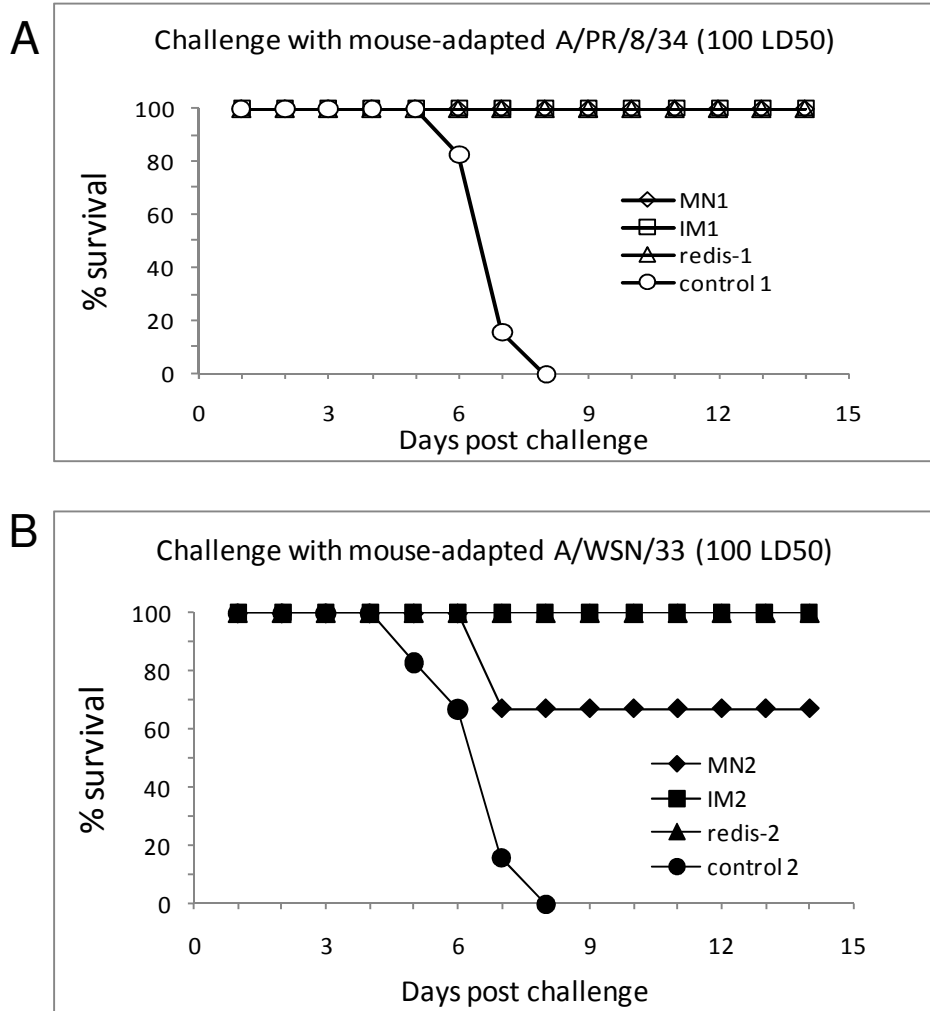
Fig. 6.5. Survival rate of mice after lethal challenges. Mice were monitored for additional two weeks of their protection against infection of (A) homologous strain (PR8), (B) heterologous strain (WSN). Mice were immunized with a dose of 10 µg IIV by microneedles (MN), intramuscular injection (IM), intramuscular injection of IIV dissolved off the microneedles (Redis), and intramuscular injection of PBS (control). Percent of survival was calculated based on a total of six mice in each group.

6.5   Discussion

It is advantageous to administer drug or vaccine rapidly and effectively, especially in the situation where time is limited and traffic of patients is severe. To achieve a rapid, effective and safe delivery, we introduced a new type of dissolving microneedles called arrowhead microneedles. The key advantage of dissolving microneedles is the disappearance of the sharp needle tips after administration. For the first time, in vivo delivery using dissolving microneedles could be completed within one minute. The enhanced delivery rate was achieved by adopting two strategies. The first strategy involved the enhancement of dissolution rate of the microneedle tips. We incorporated a highly water-soluble excipient, sucrose, into the formulation while reducing the presence of less soluble polyvinyl alcohol. Even though microneedles made solely of sucrose could dissolve even more readily, poor mechanical property of sucrose prevented the needles from inserting reliably into the skin. The second strategy was to insert the needles fully into the skin. Differ from other existing dissolving microneedles in which the needle tips are connected to the backing, arrowhead microneedle tips are spaced apart from the backing by elongated shafts. This extension of needles by the shafts allowed complete insertion of the needle tips into the mushy mouse skin. Complete embedment of the needle tips maximized the area of contact with the moisture in the skin tissue, thereby allowed a faster dissolution.

The antibody level against homologous influenza virus induced by cutaneous immunization using arrowhead microneedles was statistically commensurate with the intramuscular injection using hypodermic needles. However, the average antibody level appeared lower for the microneedle immunization. Similar trend was also

observed from the HAI titer. We believe the lower averages were due to lower delivery efficiency. We have observed that more consistent delivery around 90% was achieved in pig cadaver skin, whereas in vivo delivery in mice resulted more variable delivery ranged from 60% to 90% (data not shown). Due to improper insertions of the needle arrays into the mice, two mice had shown extraordinary low antibody titers, which were reflected in the challenge study by the heterologous strain (WSN). Two mice died in the challenge, while other mice with comparable antibody titers to the intramuscular injection groups stayed alive.

Due to the difficulty of inserting a microneedle array measured approximately 1 cm x 1 cm into a limited surface area of a mouse skin, we offer some recommendations for improvements on in vivo insertion of microneedle array into mice.

1. Identify regions where the skin is easy to stretch without over jamming the mouse body.

2. Fully anesthetized the mice during the entire course of administration. Any animal movement can disrupt the insertion, especially for small animals like mice whose skin has to be stretched intensively for delivery.

3. The mouse hair on the site of microneedle insertion must be removed thoroughly. Residual hair can impede the microneedles from penetrating into the skin. The area of depilation also has to be large enough to accommodate the entire microneedle array. Additional depilated area is preferred because pinching a piece of nude skin for microneedle insertion can not always be right on the target; larger depilated area eases the effort to aim the microneedles to the depilated skin site.

4. Prior to microneedle insertion, the microneedles must be stored and packaged properly. Since dissolving microneedles are made of water-soluble excipients,

many excipients are hygroscopic by nature. Prolonged exposure to high moisture environment such as inside refrigerator or in the basement with high humidity can weaken the mechanical properties of the microneedle's dissolvable tips. The surface of the animal skin also has to be dried completely to prevent premature dissolution of microneedles before insertion.

6.6   Conclusions

We encapsulated inactivated influenza virus within arrowhead microneedles for cutaneous immunization in mice. The results showed that cutaneous delivery using arrowhead microneedles induced statistically comparable levels of antibody responses against influenza virus to intramuscular injection after a single immunization. Microneedle immunization protected all the mice from lethal challenge by homologous influenza virus (PR8), while 4 out of 6 mice were protected from challenge by heterologous influenza virus WSN. Based on the results, arrowhead microneedles were able to administer vaccine rapidly and induced immune response effectively. The microneedles can serve as a patient compliant and potentially self-administered tool for future vaccine delivery.

6.7   Acknowledgements

CHAPTER 7

DISCUSSION

Dissolving microneedles offer great promise to the next generation of drug and vaccine delivery across the skin as an alternative to hypodermic needles. The following discussion is devoted to the technical details regarding dissolving microneedle fabrication, delivery to skin, formulation, stability of encapsulated vaccine, in vivo immunization, and future directions of dissolving microneedles.

7.1   Mass Fabrication of Microneedles

Three basic steps of dissolving microneedle fabrication developed in this project include drug loading into a mold, casting water-soluble excipients and drying the microneedles.

Drug loading is critical from the manufacturing cost point of view. Many drugs or vaccines are expensive and time consuming to produce. Therefore, the drug loading process has to be efficient with minimal wastage. Ideally, all drug intended for delivery has to be completely loaded into the tips of the microneedle mold. Any residual drug remaining on the mold surface during fabrication would end up in the microneedle backing and is therefore considered wasted. When mass producing the needles, if drug wastage is not carefully controlled, the amount of wastage can add up to a significant loss. Drug encapsulated in the backing has very limited access into the skin due to the following reasons: First, the size of the molecules might be too large to passively diffuse across the non-inserted portion of the skin where the stratum corneum is intact. Second, the interstitial fluid from the skin might not provide

121

enough moisture to wet the backing. As a result, the backing may not be permeable enough for the drug to diffuse into the skin. Last, the skin might reseal itself before all the drug gets into the skin.

To fabricate dissolving microneedles, it takes some time for the microneedle matrix materials (i.e. polymer solution) to dry. During the process of drying, the encapsulated drug in theory can freely diffuse within the microneedle matrix made of polymer solution. We found that concentrated polymer solution with less water content, higher viscosity and thereby lower diffusivity prevented excessive diffusion of drug, thereby kept the drug localized in the microneedles. However, when mass producing the needles, transfer of such viscous solution needs to be considered. Not only the viscous solution is harder to transfer, the solution tends to dry out quicker. Biologics in particular, are prone to damage by uncontrolled drying process. Based on these constraints, it is important to make the fabrication process flow efficiently and keep the polymer solution wet before the formal drying step. Drying is also crucial for determining the mechanical properties and structure of the microneedle matrix. Improper drying can cause the microneedle matrix to deform due to non-uniform polymeric tension when dried or degradation of the materials if exposed to improper temperature.

Drying of microneedles can often be done on a batch scale. There are many different ways to dry microneedles. Miyano et al's maltose dissolving microneedles used a melting technique at elevated temperature. In such case, no water was involved during their dissolving microneedle fabrication process [20]. Lee et al used centrifugal force to compressing carboxymethyl cellulose (CMC) microneedles while drying at 37°C over hours [23]. The spinning provided air ventilation as well as compression force to prevent deformation of the polymer needles upon drying. The more concentrated the polymer solution, the less time is required to dry. However, the

drying time and drying condition can be formulation dependent. For example, many sugars such as trehalose and sucrose have good water retention properties. Formulations containing those excipients will require a longer time to dry, possibly requiring an elevated temperature. In this study, the polymer blend PVA/PVP could be dried at room temperature over night, or with the assistance of vacuum to shorten the drying time. In the case of the PVA/sucrose blend used for encapsulating vaccine, freeze-dry (lyophilization) is recommended to avoid thermal damage to the vaccine. Although freeze-dry is a time-consuming process, batch drying can be done to achieve higher yield.

7.2   Parameters for Uniform and Consistent Microneedle Insertion and Delivery to Skin

Microneedle insertion determines the consistency of delivery and total delivered dose. The parameters involved in microneedle insertion include the aspect ratio of the needle, the spacing from needle-to-needle, the geometry of the needles, and the overall size of the needle array. If microneedle's aspect ratio is too low, meaning the needle has a wide base relative to its height, the needle will not be able to penetrate the skin fully due to skin deflection. In contrast, if the aspect ratio is too high, the needle, especially dissolving microneedle, may break before inserting into the skin. The extreme case of these two situations can cause all-or-none inconsistent delivery. The needle-to-needle spacing would determine how much force is pushing against a given area. If the needles are packed too close to each other, the skin would see the needles as a single entity and deflect accordingly (i.e. like the "bed of nails" effect). Needles located far apart from each other can help overcome the skin deflection, but the number of needles may be limited for a given array size. Geometry of needles also

123

plays a critical role in insertion. Pyramidal needles have shown stronger mechanical strength than conical needles with comparable dimensions [23]. It is clear that stronger needles would produce more consistent delivery with less mechanical failures. Finally, the overall size of needle array is important to the uniformity of insertion on the skin. Even though a human has a relatively large skin surface area, skin curvature still exists in many regions. An array that is too large can result in partial insertion of the needle array into the skin. Even if the backing is flexible and is able to conform against the skin curvature, most insertion requires the needles to penetrate perpendicularly to the skin surface.

7.3 Formulations for Desired Delivery Profile and Stability of Biopharmaceuticals

Dissolving microneedles typically consists of excipients including binders, fillers or a mix of both. In general, binders are long chain polymers that provide viscosity, binding property to other excipients and mechanical strength to the microneedles. The binders are relatively less water-soluble, become swollen when in contact with water, or sometimes form into a gel. Thus, they are often used for slow or controlled drug release. Dissolvable fillers typically are very water soluble. They can be prepared into a highly concentrated solution or even over-saturate the solution. They are useful in filling the space and forming the shape of microneedles to offset the constraints of binder's high viscosity. Since they readily dissolve in water or other organic solvent, they expedite the release of drug. Examples of fillers include trehalose, maltose, sucrose, dextran and dextrin, and so on. Therefore, we can achieve a desirable dissolution rate and release profile by adjusting the ratio of binders and fillers in a given formulation.

Fillers such as the sugar family have proven roles in stabilizing biological molecules. An extensive literature has shown that these fillers (stabilizers) protect the proteins from freezing stress and other thermal damage [112-114]. Although the exact mechanisms of stabilizing biological molecules by the stabilizers are not fully validated at this point, we found the sugars are useful in serving dual functions for microneedles as fillers and stabilizers.

7.4 Immunization of Animal Models using Microneedles

To choose an animal model for assessing microneedle delivery, we need to consider two main factors: skin property of the animal and measurable physiological or immune responses. To mimic human skin, animal skin should be anatomically similar. Ideally, the skin should have similar thickness of stratum corneum, epidermis, dermis and even the subcutaneous fatty tissue. The skin should also have similar elasticity and cellular composition. When performing a microneedle insertion, the insertion site on the skin should be hairless, or thoroughly depilated without causing any damage to the skin.

In this project, we used mice as our primary animal model for immunization. The advantages of using mice are: (i) Plenty of experience and data already exist. (ii) Relatively cheap in terms of the animal cost, caging and living expense. (iii) Mice can be challenged by mouse-adapted influenza virus. The main disadvantages of using mice are: (i) Mice are too small with limited available skin surface. As a result, it is difficult to apply a microneedle array onto the skin properly. (ii) Mouse skin is too deformable. Lack of skin tension can lead to excessive skin deflection upon insertion.

Other animal models such as pigs, ferrets and guinea pigs have their own pros and cons. High cost, and lack of facility and prior experience dealing with the animals

are the major obstacles for choosing those animal models. There is no single ideal animal model for preclinical studies, but to this point we have collected some important data and tested our hypotheses based on our animal model, mice.

7.5   Future Directions of Dissolving Microneedles

The key advantage of dissolving microneedles is the ability of the needle tips to dissolve and become non-sharp after use. In this project, the newly introduced arrowhead microneedles has added features to the conventional dissolving polymer microneedles enabling full needle insertion into the skin and rapid delivery. However, the current arrowhead microneedles fabricated in this project still rely on non-degradable components – the metal shafts and backing. Although the dull shafts may not be considered as biohazardous sharps, the accumulation of the waste is still an environmental burden that needs to be addressed. In addition, the bending of the metal shafts out-of-plane is an extremely tedious step to the fabrication process if done manually. The imprecision of bending the shafts can also lead to misalignment of the shafts to the polymer tips. To take a step closer to mass manufacturing and to benefit the environment, the shafts can be made by molding technique using degradable materials such as resins or ceramics. Although the use of degradable materials can be environmental friendly, the mechanical properties of those materials have to be carefully evaluated.

Another topic to be addressed regarding dissolving microneedles is the size and the number of needles required for delivery. Larger needle size can encapsulate more drugs and thus require fewer needles and smaller skin area. However, bulkier needles can be difficult to insert and may require additional length to overcome the skin deflection. Such enhancement of needle size may also be associated with greater pain

[145]. Although smaller needles encapsulate less drug per needle, they are easier to insert. Larger dose can be achieved if we increase the number of needles, but the overall array size may increase. If the array gets too large, human skin curvature may pose a challenge for achieving a uniform insertion of the microneedle array. Since microneedle array does not have to be a square or polygon as seen in many existing prototypes, the shape and size of the array can be tailored to fit the chosen skin area for an optimal microneedle application.

CHAPTER 8

CONCLUSIONS

As an alternative tool to hypodermic needles, dissolving microneedles have been shown to deliver drug and vaccine effectively into the skin. This project covers abroad scope of dissolving microneedles from fabrication to preclinical study. Conclusions from each study are summarized below:

8.1 Controlled Drug Loading and Encapsulation in Dissolving Microneedles

The goal was to develop dissolving microneedle fabrication process and design for improved drug delivery into skin. We have shown that higher skin bioavailability can be achieved by (i) localizing drug in the microneedle tip, (ii) increasing the amount of drug loaded in microneedles while minimizing wastage, and (iii) inserting microneedles more fully into the skin. Specific findings are listed below:

- Highly concentrated polymer solution used as the microneedle matrix allowed better drug localization in the microneedle tips during casting and drying steps.
- When only dilute polymer solution could be prepared due to viscosity constraints, a novel technique that involves creating bubbles in the base of microneedles could keep the drug localized in the needle tips.
- Localization of drug in microneedle tip was one of the key factors that determined delivery efficiency to the skin. The more localized the drug was in the tip, the higher the delivery efficiency. Diffusion of drug into the backing resulted in poor delivery efficiency.

- By loading the drug only into the microneedles but not in the backing, the amount of loaded drug (the dose) could be accurately estimated. This method of drug loading maximized the delivery efficiency while minimizing drug wastage. The additional volume offered by the pedestal allowed greater drug loading into the microneedles.

- The incorporation of a pedestal onto the base of the microneedle allowed the needle to insert more fully into the skin. As a result of more complete insertion, the needles dissolved faster within the skin and more drug was delivered.

8.2 Development of Arrowhead Microneedles for Rapid Cutaneous Delivery

To deliver drugs more efficiently and insert needle tips more completely into skin, we modified the pyramidal dissolving microneedle design into arrowhead microneedles. Arrowhead microneedles could fully embed the needle tips within the skin. Upon insertion, the needle tips either dissolved or mechanically separated from the shafts and backing. Similar to the pyramidal dissolving microneedles, the sharp arrowhead microneedle tips could also dissolve and leave no biohazardous sharp waste after use. Specific findings are listed below:

- Arrowhead microneedles increased the aspect ratio of dissolving microneedles without compromising the mechanical properties.

- To overcome variable skin thickness or target different regions within the skin, arrowhead microneedles could penetrate to various insertion depths by varying the shaft length.

- Arrowhead microneedles allowed complete insertion of the needle tips into skin and then released the drug within. The drug could be delivered by dissolving the

129

tips within the skin or by mechanical separation of the tips from the shafts. Both mechanisms of delivery resulted in high delivery efficiency on a scale of seconds in porcine cadaver skin.

- Drug delivery using arrowhead microneedles carrying biodegradable (i.e. non-dissolving) tips could achieve controlled release. The mechanical separation of the tips from the shafts allowed implantation of the biodegradable tips within the skin in seconds while the backing was removed soon after administration.

- Arrowhead microneedles produced no sharp waste after use. Upon insertion, the needle's sharp tips were dissolved or embedded within the skin, leaving behind the dull shafts.   Reapplying the dull shafts caused no apparent damage to the skin.

8.3   Stability of Influenza Vaccine Encapsulated in Dissolving Microneedles

The goal of this study was to encapsulate influenza vaccine in dissolving microneedles for transcutaneous delivery while maintaining the vaccine stability during and post microneedle processing. We evaluated the stability of the encapsulated vaccine based on hemagglutination (HA) potency, antigenicity of hemagglutinin and virus morphology. We found that vaccine processed into microneedles was more stable compared to unprocessed vaccine in solution. Specific findings are listed below:

- Among the three microneedle drying methods: lyophilization, thermal dry at 25°C and thermal dry at 45°C over night, lyophilization was the best method in maintaining the HA potency.

- The presence of sucrose in the formulation (i.e. polymer solution used for

microneedle matrix) helped maintained the HA potency dramatically. Without sucrose, polyvinyl alcohol in the formulation alone led to a significant HA potency loss.

- Encapsulated influenza vaccine processed into solid microneedles maintained HA potency for at least one month independent of storage temperature.

- Unprocessed influenza vaccine in solution was stable at 4°C but lost the HA activity dramatically within days at 25°C, 37°C, and 45°C.

- The HA potency of vaccine encapsulated in microneedles was independent of packaging condition used in this study for at least two months at 25°C.

- For two-week storage, the vaccine encapsulated in microneedles was able to maintain the HA's antigenic property at 4°C, 25°C, 37°C and 45°C while the unprocessed vaccine stored at 25°C, 37°C and 45°C lost nearly all HA's antigenic property.

- For two-week storage, the vaccine encapsulated in microneedles maintained its virus particle morphology at 4°C, 25°C, 37°C and 45°C while the unprocessed vaccine stored at 25°C, 37°C and 45°C showed ruptured particles or virus debris under electron microscopy.

8.4 Protection against Lethal Virus Challenge in Immunized Mice using Arrowhead Microneedles

After optimizing drug loading and encapsulation, delivery to the skin, and stability of the vaccine, we aimed to evaluate in vivo immunization of mice using arrowhead microneedles encapsulating influenza vaccine. The immunized mice were challenged by homologous influenza virus PR8 and heterologous virus WSN. The results showed that cutaneous immunization by arrowhead microneedles protected the

mice against lethal influenza virus challenge. Specific findings are listed below:

- Antibody responses induced by arrowhead microneedle encapsulating PR8 were statistically indistinguishable from the intramuscular injection (Student's t-test, $p > 0.05$).
- Hemagglutination inhibition titer levels were directly correlated with the levels of the antibody responses.
- Intramuscular injection of reconstituted solution of arrowhead microneedles produced equivalent antibody responses and hemagglutination inhibition titer levels to intramuscular injection of unprocessed vaccine. This finding showed that the microneedle processing did not cause significant damage to the vaccine.
- All mice immunized by microneedles showed similar weight loss to mice immunized by intramuscular injection.
- All mice immunized by microneedles and intramuscular injection were protected from the homologous lethal virus challenge.
- Four out of six mice immunized by microneedles were protected while all mice immunized by intramuscular injection were protected from the heterologous lethal virus challenge.

CHAPTER 9

FUTURE DIRECTIONS

This project covers many fundamental aspects of drug and vaccine delivery using microneedles, including dissolving microneedle fabrication processes, in vitro evaluation of needle insertion, stability of encapsulated vaccine and in vivo immunization. To bring this technology closer to human clinical trial and the market, additional plans are recommended as follows.

9.1 Optimization of Microneedle Geometry and Design for Clinical Application

This project involves several modifications of microneedle geometry. Examples of microneedle structural change include the addition of pedestal, incorporation of a bubble in the needle base and mounting of shafts to form arrowheads. These geometrical changes led to improvement to drug delivery. For instance, pedestal needles allowed greater loading of drug while keeping the drug wastage low. Elongation of microneedles by adding pedestals also generated deeper insertions into the skin, which in turn led to higher delivery efficiency. Although conical and pyramidal microneedles have been fabricated and evaluated in some literature [18, 19, 22, 23, 63, 140, 144], more studies are needed to address the correlation between geometry and aspect-ratio on needle mechanical property and insertion into the skin. Optimization of microneedle geometry is important because appropriate geometry and needle size could facilitate insertion with minimal pain, cause minimal skin deflection, avoid mechanical failure of needles, and possess extensive drug loading capacity. All of these parameters are critical for feasible self-administration and reproducible clinical practice

9.2 In Vivo Stability Assessment of Vaccine Encapsulated in Microneedles

The stability of influenza vaccine has been evaluated using in vitro assays including HA assay, capture ELISA and TEM. The encapsulated vaccine microneedle samples and unprocessed vaccine solutions have been stored at different temperatures under different packaging conditions. We found that the encapsulated vaccine maintained its morphology, hemagglutination activity and HA antigenic property over extend periods of time while unprocessed vaccine was very vulnerable to temperature variation. The next step would be to evaluate both encapsulated vaccine samples and unprocessed vaccine in vivo. The animal models used for this study should be able to generate assessable immune responses and be susceptible to lethal virus challenge.

9.3 In Vivo Vaccination of Different Animal Models

While all studies conducted here used mice as the animal model, future studies should expand to other animal models. Although using mice has the advantages of leveraging the established data and experience, the size and the skin properties of mice made needle array insertion very difficult. Therefore, animals that have appropriate size and similar skin property to human skin like guinea pigs, ferrets or pigs are worth evaluating.

From the delivery perspective, one-minute dissolution-based immunization using arrowhead microneedles had now been done in mice. The other delivery mechanism based on mechanical separation (i.e. shearing) should also be evaluated in vivo. This one-second delivery aided by shear force can be very beneficial to mass vaccination campaign in which time is an important concern. In sum, a careful plan for establishing new animal models for immunization will bring the technology closer to human clinical trial and actual medical practice.

CHAPTER 10

REFERENCES

1.   Langer, R., *Drug delivery and targeting.* Nature, 1998. **392**: p. 5-10.

2.   Cleland, J.L., Daugherty, A., and Mrsny, R., *Emerging protein delivery methods.* Curr. Opin. Biotechnol., 2001. **12**(2): p. 212-219.

3.   Prausnitz, M.R., and Langer, R., *Transdermal drug delivery.* Nature Biotech., 2008. **26**(11): p. 1261-1268.

4.   Hamilton, J.G., *Needle phobia: A neglected diagnosis.* J. Fam Prac. , 1995. **41**(2): p. 169-175.

5.   Nir, Y., Paz. A., Sabo, E., and Potasman, I., *Fear of injections in young adults: Prevalence and associations.* Am. J. Trop. Med. Hyg., 2003. **68**(3): p. 341-344.

6.   Deacon, B., Abramowitz, J., *Fear of needles and vasovagal reactions among phlebotomy patients.* J. Anxiety Disord., 2006. **20**(7): p. 946-960.

7.   Simonsen, L., Kane, A., Lloyd, J., Zaffran, M., and Kane, M., *Unsafe injections in the developing world and transmission of blood-borne pathogens.* Bulletin of the World Health Organization, 1999. **77**(10): p. 789-800.

8.   Prausnitz, M.R., *Microneedles for transdermal drug delivery.* Adv. Drug Deliv. Rev., 2004. **56**(5): p. 581-587.

9.   Arora, A., Prausnitz, M.R., and Mitragotri, S., *Micro-scale devices for transdermal drug delivery.* Inter. J. Pharm., 2008. **364**(2): p. 227-236.

10.   Chabri, F., Bouris, K., Jones, T., Barrow, D., Hann, A., Allender, C., Brain, K., and Birchall, J., *Microfabricated silicon microneedles for nonviral cutaneous gene delivery.* Br. J. Dermatol., 2004. **150**(5): p. 869-877.

11.   Oh, J.H., Park, H.H., Do, K.Y., Han, M., Hyun, D.H., Kim, C.G., Kim, C.H.,

Lee, S.S., Hwang, S.J., Shin, S.C., and Cho, C.W., *Influence of the delivery systems using a microneedle array on the permeation of a hydrophilic molecule, calcein.* Eur. J. Pharm. Biopharm., 2008. **69**: p. 1040-1045.

12. Qiu, Y., Gao, Y., Hu, K., and Li, F., *Enhancement of skin permeation of docetaxel: A novel approach combining microneedle and elastic liposomes.* J. Control. Release, 2008. **129**: p. 144-150.

13. Banks, S.L., Pinninti, R.R., Gill, H.S., Crooks, P.A., Prausnitz, M.R., and Stinchcomb, A.L., *Flux across microneedle-treated skin is increased by increasing charge of naltrexone and naltrexol in vitro.* Pharm. Res., 2008. **25**(7): p. 1677-1684.

14. Wermeling, D.P., Banks, S.L., Hudson, D.A., Gill, H.S., Gupta, J., Prausnitz, M.R., and Stinchcomb, A.L., *Microneedles permit transdermal delivery of a skin-impermeant medication to humans.* Proc. Natl. Acad. Sci., 2007. **105**(6): p. 2058-2063.

15. Gill, H., and Prausnitz, M.R., *Coated microneedles for transdermal delivery.* J. Control. Release, 2007. **117**(2): p. 227-237.

16. Cormier, M., Johnson, B., Ameri, M., Nyam, K., Libiran, L., Zhang, D.D., and Daddona, P., *Transdermal delivery of desmopressin using a coated microneedle array patch system.* J. Control. Release, 2004. **97**(3): p. 503-511.

17. Han, M., Kim, D.K., Kang, S.H., Yoon, H.R., Kim, B.Y., Lee, S.S., Kim, K.D., and Lee, H.G., *Improvement in antigen-delivery using fabrication of a grooves-embedded microneedle array.* Sens. Actuators B: Chem., 2009. **137**(1): p. 274-28-.

18. Park, J.H., Allen, M.G., and Prausnitz, M.R., *Biodegradable polymer microneedles: Fabrication, mechanics and transdermal drug delivery.* J. Control. Release, 2005. **104**(1): p. 51-66.

19. Park, J.H., Allen, M.G., and Prausnitz, M.R., *Polymer microneedles for controlled-release drug delivery.* Pharm. Res., 2006. **23**(5): p. 1008-1019.

20. Miyano, T., Tobinga, Y., Kanno, T., Matsuzaki, Y., Takeda, H., Wakui, M., and

Hanada, K., *Sugar micro needles as transdermic drug delivery system.* Biomed. Microdevices, 2005. **7**(3): p. 185-188.

21. Ito, Y., Yoshimitsu, J.I., Shiroyama, K., Sugioka, N., and Takada, K., *Self-dissolving microneedles for the percutaneous absorption of EPO in mice.* J. Drug Target., 2006. **14**(5): p. 255-261.

22. Sullivan, S.P., Murthy, N., and Prausnitz, M.R., *Minimally invasive protein delivery with rapidly dissolving polymer microneedles.* Adv. Mater., 2008. **20**(5): p. 933-938.

23. Lee, J.W., Park, J.H., and Prausnitz, M.R., *Dissolving microneedles for transdermal drug delivery.* Biomaterials, 2007. **29**(13): p. 2113-2124.

24. Langer, R., Peppas, N.A., *Advances in biomaterials, drug delivery, and bionanotechnology.* AIChE J., 2003. **49**: p. 2990-3006.

25. Gonzalezrothi, R.J., and Schreier, H., *Pulmonary delivery of liposome-encapsulated drugs in asthma therapy.* Clin. Immunother., 1995. **4**(5): p. 331-337.

26. Onoue, S., Misaka, S., Kawabata, Y., and Yamada, S., *New treatments for chronic obstructive pulmonary disease and viable formulation/device options for inhalation therapy.* Expert Opin. Drug Deliv., 2009. **6**(8): p. 793-811.

27. Dubus, J.C., and Ravilly, S., *Inhaled therapies in cystic fibrosis.* Rev. Mal. Respir., 2008. **25**(8): p. 989-998.

28. Niven, R.W., *Delivery of biotherapeutics by inhalation aerosol.* Crit. Rev. Therap. Drug Carrier Syst., 1995. **12**: p. 151-231.

29. Patton, J.S., *Mechanisms of macromolecule absorption by the lungs.* Adv. Drug Deliv. Rev., 1996. **19**: p. 3-36.

30. Service, R.F., *Drug delivery takes a deep breath.* Science, 1997. **277**: p. 1199-1120.

31. Prausnitz, M.R., Mitragotri, S., and Langer, R., *Current status and future*

potential of transdermal drug delivery. Nat. Rev. Drug Discov., 2004. **3**: p. 115-124.

32.   Elias, P.M., *Epidermal lipids, barrier function, and desquamation.* J. Invest. Dematol., 1983. **80**: p. 44-49.

33.   Cheng, X., Koch, P.J., *In vivo function of desmosomes.* J. Dermatol., 2004. **31**: p. 171-187.

34.   Huber, O., *Structure and function of desmosomal proteins and their role in development and disease.* Cell mol. life Sci., 2003. **60**: p. 1872-1890.

35.   Weniger, B.G., and Papania, M.J., *Alternative vaccine delivery methods.* Vaccines (section 3:Vaccines in development and new vaccine strategies), 2008: p. 1357-1392.

36.   Banchereau, J., and Steinman, R.M., *Dendritic cells and the control of immunity.* Nature Reviews: Drug Discovery, 1998. **392**(19): p. 245-252.

37.   Romani, N., Holzmann, S., Tripp, C.H., Kock, F., and Stoitzner, P., *Langerhans cells - dendritic cells of the epidermis.* APMIS, 2003. **111**(7-8): p. 725-740.

38.   Sallusto, F., *Origin and migratory properties of dendritic cells in the skin.* Curr. Opin. Allerg. Clin. Immunol., 2001. **1**(5): p. 411-418.

39.   Goldsby, R.A., Kindt, T.J., Kuby, J., and Osborne, B.A., *Immunology: Fifth Edition.* Freeman & Company, 2003: p. 603.

40.   Yu, R.C., Abrams, D.C., Alaibac, M., and Chu, A.C., *Morphological and quantitative analyses of normal epidermal Langerhans cells using confocal scanning laser microscopy.* Br. J. Dermatol., 1994. **131**(6): p. 843-848.

41.   Naik, A., Kalia, Y.N., and Guy, R.H., *Transdermal drug delivery: overcoming the skin's barrier function.* Pharm. Sci. Technol. To., 2000. **3**(9): p. 318-326.

42.   William, A.C., and Barry, B.W., *Penetration enhancers.* Adv. Drug Deliv. Rev., 2004. **56**(5): p. 603-618.

43. Smith, E.W., and Maibach, H.I., *Percutaneous Penetration Enhancers.* Taylor and Francis Group, Boca Raton, FL, 2006.

44. Chen, Y., Shen, Y., Guo, X., Zhang, C., Yang, W., Ma, Minglu, Liu, S., Zhang, M., and Wen, L.P., *Transdermal protein delivery by a coadministered peptide identified via phage display.* Nat. Biotech., 2006. **24**(4): p. 455-460.

45. Kim, Y.C., Ludovice, P.J. and Prausnitz, M.R., *Transdermal delivery enhanced by magainin pore-forming peptide.* J. Control. Release, 2007. **122**(3): p. 375-383.

46. Banga, A.K., *Electrically-assisted transdermal and topical drug delivery.* Taylor & Francis, London;1998.

47. Kalia, Y.N., Naik, A., Garrison, J. and Guy, R.H., *Iontophoretic drug delivery.* Adv. Drug Deliv. Rev., 2004. **56**(5): p. 619-658.

48. Subramony, J.A., Sharma, A. and Phipps, J.B., *Microprocessor controlled transdermal drug delivery.* Int. J. Pharm., 2006. **317**(1): p. 1-6.

49. Zempsky, W.T., Sullivan, J., Paulson, D.M. and Hoath, S.B., *Evaluation of a low-dose lidocaine iontophoresis system for topical anesthesia in adults and children: a randomized, controlled trial.* Clin. Ther., 2004. **26**(7): p. 1110-1119.

50. Ashburn, M.A., Streisand, J., Zhang, J., Love, G., Rowin, M., Niu, S., Kievit, J.K., Kroep, J.R., and Mertens, M.J., *The iontophoresis of fentanyl citrate in humans.* Anesthesiology, 1995. **82**(5): p. 1146-1153.

51. Carter, E.P., Barrett, A.D., Heeley, A.F., and Kuzemko, J.A., *Improved sweat test method for the diagnosis of cystic fibrosis.* Arch. Dis. Child., 1984. **59**: p. 919-922.

52. Beauchamp, M., and Lands, L.C., *Sweat-testing: a review of current technical requirements.* Pediatr. Pulmonol., 2005. **39**(6): p. 507-511.

53. Becker, B.M., Helfrich, S., Baker, E., Lovgren, K., Minugh, A., and Machan,

J.T., *Ultrasound with topical anesthetic rapidly decreases pain of intravenous cannulation.* Acd. Emerg. Med., 2005. **12**(4): p. 289-295.

54.   Mitragotri, S., Blankschtein, D., and Langer, R., *Ultrasound-mediated transdermal protein delivery.* Science, 1995. **269**(5225): p. 850-853.

55.   Ogura, M., Paliwal, S., and Mitragotri, S., *Low-frequency sonophoresis: Current status and future prospects.* Adv. Drug Deliv. Rev., 2008. **60**(10): p. 1218-1223.

56.   Banga, A.K., *Microporation applications for enhancing drug delivery.* Expert Opin. Drug Deliv., 2009. **6**(4): p. 343-354.

57.   Levin, G., Gershonowitz, A., Sacks, H., Stern, M., Sherman, A., Rudaev, S., Zivin, I., and Phillip, M., *Transdermal delivery of human growth hormone through RF-microchannels.* Pharm. Res., 2005. **22**(4): p. 550-555.

58.   Badkar, A.V., Smith, A.M., Eppstein, J.A., and Banga, A.K., *Transdermal delivery of interferon alpha-2B using microporation and iontophoresis in hairless rats.* Pharm. Res., 2007. **24**(7): p. 1389-1395.

59.   Lanke, S.S.S., Kolli, C.S., Strom, J.G., and Banga, A.K., *Enhanced transdermal delivery of low molecular weight heparin by barrier perturbation.* Int. J. Pharm., 2009. **365**(1-2): p. 26-33.

60.   Wu, X.M., Todo, H., and Sugibayashi, K., *Effects of pretreatment of needle puncture and sandpaper abrasion on the in vitro skin permeation of fluorescein isothiocyanate (FITC)-dextran.* Int. J. Pharm., 2006. **316**(1-2): p. 102-108.

61.   Glenn, G.M., Flyer, D.C., Ellingsworth, L.R., Frech, S.A., Frerichs, D.M., Seid, R.C., and Yu, J., *Transcutaneous immunization with heat-labile enterotoxin: development of a needle-free vaccine patch.* Expert Rev. Vaccines, 2007. **6**(5): p. 809-819.

62.   Gill, H.S., Andrews, S.N., Sakthivel, S.K., Fedanov, A., Williams, L.R., Garber, D.A, Priddy, F.H., Yellin, S., Feinberg, M.B., Staprans, S.I., and Prausnitz, M.R., *Selective removal of stratum corneum by microdermabrasion*

to increase skin permeability. Euro. J. Pharm. Sci., 2009. **38**(2): p. 95-103.

63. McAllister, D.V., Wang P.M., Davis, S.P., Park J.H., Canatella, P.J., Allen, M.G., and Prausnitz, M.R., *Microfabricated needles for transdermal delivery of macromolecules and nanoparticles: fabrication methods and transport studies.* Proc. Natl. Acd. Sci., 2003. **100**(24): p. 13755-13760.

64. Kaushik, S., Hord, A.H., Denson, D.D., McAllister, D.V., Smitra, S., Allen, M.G., and Prausnitz, M.R., *Lack of pain associated with microfabricated microneedles.* Anesth. Analg., 2001. **92**: p. 502-504.

65. Haq, M.I., Smith, D.N., Kalavala, M., Edwards, C., Anstey, A., Morrissey, A., and Birchall, J.C., *Clinical administration of microneedles: skin puncture, pain and sensation.* Biomed. Microdevices, 2009. **11**: p. 35-47.

66. Martanto, W., Davis, S., Holiday, N., Wang, J., Gill, H., and Prausnitz, M.R., *Transdermal delivery of insulin using microneedles in vivo.* Proceedings of international symposium on controlled release bioactive material, 2003. **666**.

67. Henry, S., McAllister, D.V., Allen, M.G., and Prausnitz M.R., *Microfabricated microneedles: A novel approach to transdermal drug delivery.* J. Pharm. Sci., 1998. **87**(8): p. 922-925.

68. Runyan, W.R., and Bean, K.E., *Semiconductor Integrated Circuit Processing Technology*, ed. Addison-Wesley. 1990, New York.

69. Kim, K., Park, D.S., Lu, H.M., Che, W., Kim, K., Lee, J.B., and Ahn, C.H., *A tapered hollow metallic microneedle array using backside exposure of SU-8.* J. Micromechanics Microengineering, 2004. **14**: p. 597-603.

70. Chandrasekaran, S., Brazzle, J.D., and Frazier, A.B., *Surface micromachined metallic microneedles.* J. Microelectromech. Syst., 2003. **12**(3): p. 281-288.

71. Griss, P., Enoksson, P., and Stemme, G., *Micromachined barbed spikes for mechanical chip attachment.* Sens. Actuators A. Phys., 2002. **95**: p. 94-99.

72. Braybrook, J.H., *Biocompatibility: Assessment of Medical Devices and Materials*, ed. Wiley. 1997, New York.

73.   Gill, H.S., and Prausnitz, M.R., *Coating formulations for microneedles.* Pharm. Res., 2007. **24**(7): p. 1369-1380.

74.   Park, J.H., Choi, S.O., Kamath, R., Yoon, Y.K., Allen, M.G., and Prausnitz, M.R., *Polymer particle-based micromolding to fabricate novel microstructures.* Biomed. Microdevices, 2007. **9**(2): p. 223-234.

75.   Kolli, C.S., and Banga, A.K., *Characterization of solid maltose microneedles and their use for transdermal delivery.* Pharm. Res., 2007. **25**(1): p. 104-113.

76.   Ito, Y., Hagiwara, E., Saeki, A., Sugioka, N., and Takada, K., *Feasibility of microneedles for percutaneous absorption of insulin.* Eur. J. Pharm. Sci., 2006. **29**(1): p. 82-88.

77.   U.S. Food and Drug Administration, *Inactive Ingredient Search for Approved Drug Products <http://www.accessdata.fda.gov/scripts/cder/iig/index.cfm>.*

78.   Isolyser Company, I.C., Inc. 4320 International Boulevard, N.W., Norcross, GA. JSCI, Bulletin of Osaka Medical, 1968.

79.   Sanders, J.M., and Matthews, H.B., *Vaginal absorption of polyvinyl alcohol in Fischer 344 rats.* Hum. Exp. Toxicol., 1990. **9**(2): p. 71-77.

80.   Hueper, W.C., *Organic lesions produced by polyvinyl alcohol in rats and rabbits.* Arch. Pathol, 1939. **28**: p. 510-531.

81.   Shibuya, T., Tanaka, N., Katoh, M., Matsuda, Y.T., and Morita, K., *Mutagenicity testing of ST-film with the Ames test, chromosome test in vitro and micronucleus test in female mice.* J. Toxicol. Sci., 1985. **10**(2): p. 135-141.

82.   Schweikl, H., Schmalz, G., and Gottke, C., *Mutagenic activity of various dentine bonding agents.* Biomaterials, 1996. **17**(14): p. 1451-1456.

83.   Colorcon, *Polyvinyl Alcohol (PVA): Study of the effects of PVA on fertility, early embryonic development to weaning, and the growth and development when administered in the diet to rats.* 2001.

84.   Hort, E., and Gasman, R., *N-Vinyl monomers and polymers, in Encyclopedia of Chemical Technology*. John Willey & Sons, ed. E. K. Othmer. 1983, New York, NY. 960-979.

85.   Nair, B., *Final report on the safety assessment of polyvinylpyrrolidone (PVP)*. Int. J. Toxicol., 1998. **17**(4): p. 95-130.

86.   Morgan, A.M., *Localized reactions to injected therapeutic materials.* J. Cutan. Pathol., 1995. **22**(3): p. 193-214.

87.   Robinson, B.V., Sullivan, F.M., Borzelleca, J.F., and Schwartz, S.L. , *PVP: A critical review of the kinetics and toxicology of polyvinylpyrrolidone*. 1990, Chelsea, MI: Lewis Publishers, Inc.

88.   Amorij, J.P., Huckriede, A., Wilschut, J., Frijlink, .H.W., and Hinrichs, W.L.J., *Development of stable influenza vaccine powder formulations: Challenges and possibilities.* Pharm. Res., 2008. **25**(6): p. 1256-1273.

89.   WHO media center, *Influenza.* Fact Sheet, 2003. **211**.

90.   Couch, R.B., and Kasel, J.A., *Immunity to influenza in man.* Annu. Rev. Microbiol. , 1983. **37**: p. 529-549.

91.   Smith, N.M., Bresee, J.S., Shay D.K., Uyeki, T.M., Cox, N.J., and Strikas, R.A., *Prevention and control of influenza: Recommendations of the advisory committee on immunization practices (ACIP).* MMWR, 2006. **55**(RR10): p. 1.

92.   Recommendations of the Immunization Practices Advisory Committee, C.D.C., *Monovalent influenza A (H1N1) vaccine, 1986-1987.* Ann. Inter. Med., 1986. **105**(5): p. 737-739.

93.   Amorij, J.P., Meulenaar, J., Hinrichs, W.L., Stegmann, T., Huckriede, A., Coenen, F., and Frijlink, H.W., *Rational design of an influenza subunit vaccine powder with sugar glass technology: Preventing conformational changes of haemagglutinin during freezing and freeze-drying.* Vaccine, 2007. **25**(35): p. 6447-6457.

94.   *WHO Department of Immunization, Vaccines and Biologicals. Temperature*

sensitivity of vaccines. 2006.

95.   ICH, Q1A (R2). Stability testing guidelines: Stability testing of new drug
        substances and products. ICH step 5. CPMP/ICH/2736/99.

96.   ICH, Q5C. Stability testing of biotechnological/biological products. ICH step
        4. CPMP/ICH/138/95.

97.   Coenen, F., Tolboom, J.T., and Frijlink, H.W., *Stability of influenza sub-unit
        vaccine. Does a couple of days outside of the refrigerator matter?* Vaccine,
        2006. **24**(4): p. 525-531.

98.   Luykx, D.M., Casteleijn, M.G., Jiskoot, W., Westdijk, J., and Jongen, P.M.,
        *Physicochemical studies on the stability of influenza haemagglutinin in
        vaccine bulk material.* Eur. J. Pharm. Sci., 2004. **23**(1): p. 65-75.

99.   Killeen, R.M., *Practical management of vaccines.* CPI/RPC, 2007. **140**(S2): p.
        S1-S22.

100.   Setia, S., Mainzer, H., Washington, M.L., Coil, G., Snyder, R., and Weniger,
        B.G., *Frequency and causes of vaccine wastage.* Vaccine, 2002. **20**(7-8): p.
        1148-1156.

101.   Giudice, E.L., and Campbell, J.D., *Needle-free vaccine delivery.* Adv. Drug
        Deliv. Rev., 2006. **58**(1): p. 68-89.

102.   O'Hagan, D.T., and Rappuoli, R., *Novel approaches to vaccine delivery.*
        Pharm. Res., 2004. **21**(9): p. 1519-1530.

103.   Wang, W., *Lyophilization and development of solid protein pharmaceuticals.*
        Int. J. Pharm., 2000. **203**(1-2): p. 1-60.

104.   Tang, X., and Pikal, M.J., *Design of freeze-drying processes for
        pharmaceuticals: practical advice.* Pharm. Res., 2007. **21**(2): p. 191-200.

105.   Heller, M.C., Carpenter, J.F., and Randolph, T.W., *Protein formulation and
        lyophilization cycle design: prevention of damage due to freeze-concentration
        induced phase separation.* Biotechnol. Bioeng., 1999. **63**(2): p. 166-174.

106.   Randolph, T.W., *Phase separation of excipients during lyophilization: Effects on protein stability.* J. Pharm. Sci., 1997. **86**(11): p. 1198-1203.

107.   Schebor, C., Burin, L., Buera, M.P., Aguilera, J.M., and Chirife, J., *Glassy state and thermal inactivation of invertase and lactase in dried amorphous matrices.* Biotechnol. Prog., 1997. **13**(6): p. 857-863.

108.   Hinrichs, W.L., Prinsen, M.G., and Frijlink, H.W., *Inulin glasses for the stabilization of therapeutic proteins.* Int. J. Pharm., 2001. **215**(1-2): p. 163-174.

109.   Eriksson, H.J., Hinrichs, W.L., van Veen, B., Somsen, G.W., de Jong, G. J., and Frijlink, H.W., *Investigations into the stabilisation of drugs by sugar glasses: I. Tablets prepared from stabilised alkaline phosphatase.* Int. J. Pharm., 2002. **249**(1-2): p. 59-70.

110.   Yannarell, D.A., Goldberg, K.M., and Hjorth, R.N., *Stabilizing cold-adapted influenza virus vaccine under various storage conditions.* J. Virol. Methods, 2002. **102**(1-2): p. 15-25.

111.   Bieganski, R.M., Fowler, A., Morgan, J.R., and Toner, M., *Stabilization of active recombinant retroviruses in an amorphous dry state with trehalose.* Biotechnol. Prog., 1998. **14**(4): p. 615-620.

112.   Allison, S.D., Molina, M.C., and Anchordoquy, T.J., *Stabilization of lipid/DNA complexes during the freezing step of the lyophilization process: The particle isolation hypothesis.* Biochim. Biophys. Acta., 2000. **1468**(1-2): p. 127-138.

113.   Molina, M.C., Armstrong, T.K., Zhang, Y., Patel, M.M., Lentz, Y.K., and Anchordoquy, T.J., *The stability of lyophilized lipid/DNA complexes during prolonged storage.* J. Pharm. Sci., 2004. **93**(9): p. 2259-2273.

114.   Carpenter, J.F., and Crowe, J.H., *An infrared spectroscopic study of the interactions of carbohydrates with dried proteins.* Biochemistry, 1989. **28**(9): p. 3916-3922.

115.   Widera, G., Johnson, J., Kim, L., Libiran, L., Nyam, K., Daddona, P.E., and

Cormier, M., *Effect of delivery parameters on immunization to ovalbumin following intracutaneous administration by a coated microneedle array patch system.* Vaccine, 2006. **24**(10): p. 1653-1664.

116.   Alarcon, J.B., Hartley, A.W., Harvey, N.G., and Mikszta, J.A., *Preclinical evaluation of microneedle technology for intradermal delivery of influenza vaccines.* Clin. Vaccine Immunol., 2007. **14**(4): p. 375-381.

117.   Zhu, Q., Zarnitsyn, V.G., Ye, L., en, Z., Gao, Y., Pan, L., Skountzou, I., Gill, H.S., Prausnitz, M.R., Yang, C., and Compans, R.W., *Immunization by vaccine-coated microneedle arrays protects against lethal influenza virus challenge.* Proc. Natl. Acd. Sci., 2009. **106**(19): p. 7968-7973.

118.   Koutsonanos, D.G., del Pilar Martin, M., Zarnitsyn, V.G., Sullivan, S.P., Compans, R.W., Prausnitz, M.R., and Skountzou, I., *Transdermal influenza immunization with vaccine-coated microneedle arrays.* PLoS ONE, 2009. **4**(3): p. e4773.

119.   Martin, J.F., *Vaccines in the developing world: looking for new solutions.* Vaccine, 1999. **17**(S3): p. S113-S115.

120.   Hausdorff, W.P., *Prospects for the use of new vaccines in developing countries: cost is not the only impediment.* Vaccine, 1996. **14**(13): p. 1179-1186.

121.   World Bank, *Investing in health.* World Development Report, 1993.

122.   Aylward, B., Kane, M., McNair-Scott, R., and Hu, D.H., *Model based estimates of the risk of human immunodeficiency virus and hepatitis B virus tarnsmission through unsafe injections.* Int. J. Epidemiol, 1995. **24**(2): p. 446-452.

123.   World Health Organization, *State of the world's vaccines and immunization, Geneva.* Unpublished document (WHO/GPV/96.04), 1996.

124.   World Health Organization, *Immunization in practice: Module 3, The cold chain.* Geneva: WHO, 2004.

125.   Galazka, A., Milstien, J., and Zaffran, M., *Thermostability of vaccines.* WHO

document ref. (WHO/GPV/98.07). Geneva:WHO, 1998.

126.   Dimayuga, R., Scheifele, D., and Bell, A., *Effect of freezing on DPT and DPT-IPV vaccines, adsorbed.* Can. Commun. Dis. Rep., 1995. **21**(11): p. 101-103.

127.   Mihomme, P., *Cold chain study: danger of freezing vaccines.* Can. Commun. Dis. Rep., 1993. **19**(5): p. 33-38.

128.   Prausnitz, M.R., Gill, H.S., and Park, J.H., *Microneedles for drug delivery,.* Modified Release Drug Delivery, vol. 2, ed. M.J. Rathbone, Hadgraft, J., Roberts, M.S., and Lane, M.E. 2008, New York: Informa Healthcare.

129.   Sivamani, R.K., Liepmann, D., and Malbach, H.I., *Microneedles and transdermal applications.* Expert Opin. Drug Deliv., 2007. **4**(1): p. 19-25.

130.   Glenn, G.m., Kenney, R.T., Ellingsworth, L.R., Frech, S.A., Hammond, S.A., and Zoeteweij, J.P., *Transcutaneous immunization and immunostimulant strategies: capitalizing on the immunocompetence of the skin.* Expert. Rev. Vaccines, 2003. **2**(2): p. 253-267.

131.   Glenn, G.M., Taylor, D.N., Li, X., Frankel, S., Montemarano, A., and Alving, C.R., *Transcutaneous immunization: A human vaccine delivery strategy using a patch.* Nat. Med., 2000. **6**: p. 1403-1406.

132.   Karande, P., Jain, A., Ergun, K., Kispersky, V., and Mitragotri, S., *Design principles of chemical penetration enhancers for transdermal drug delivery.* Proc. Natl. Acd. Sci., 2005. **102**(13): p. 4688-4693.

133.   Sinico, C., and Fadda, A.M., *Vesicular carriers for dermal drug delivery.* Expert Opin. Drug Deliv., 2009. **6**(8): p. 813-825.

134.   Mikszta, J.A., Dekker III, J.P., Harvey, N.G., Dean, C.H., Brittingham, J.M., Huang, J., Sullivan, V.J., Dyas, B., Roy, C.J., and Ulrich, R.G., *Microneedle-based Intradermal delivery of the anthrax recombinant protective antigen vaccine.* Infect. Immun., 2006. **74**(12): p. 6806-6810.

135.   Gardeniers, H.J.G.E., Luttge, R., Berenschot, E.J.W., de Boer, M.J., Yeshurun,

S.Y., Hefetz, M., van't Oever, R., and van den Berg, A., *Silicon micromachined hollow microneedles for transdermal liquid transport.* J. Microelectromech. Syst., 2003. **12**(6): p. 855-862.

136. Verbaan, F.J., Bal, S.M., van den Berg, D.J., Groenink, W.H.H., Verpoorten, H., Luttge, R., and Bouwstra, J.A., *Assembled microneedle arrays enhance the transport of compounds varying over a large range of molecular weight across human dermatomed skin.* J. Control. Release, 2007. **117**(2): p. 238-245.

137. Sullivan, S.P., Murthy, N., and Prausnitz, M.R., *Minimally invasive protein delivery with rapidly dissolving polymer microneedles.* Adv. Mater., 2008. **20**: p. 933-938.

138. Kolli, C.S.a.B., A.K., *Characterization of solid maltose microneedles and their use for transdermal delivery.* Pharma. Res., 2008. **25**(1): p. 104-113.

139. Park, J.H., Yoon, Y.K., Choi, S.O., Prausnitz, M.R., and Allen, M.G., *Tapered conical polymer microneedles fabricated using an integrated lens technique for transdermal drug delivery.* IEEE Trans. Biomed. Engin., 2007. **54**(5): p. 903-913.

140. Choi, S.O., Rajaraman, S., Yoon, Y.K., Wu, X., and Allen, M.G., *3-D Metal patterned microstructure using inclined UV exposure and metal transfer micromolding technology.* Solid-State Sensor, Actuator, and Microsystems Workshop, 2006.

141. Keitel, W.A., Atmar, R.L., Cate, T.R., Petersen, N.J., Greenberg, S.B., Ruben, F., and Couch, R.B, *Safety of high doses of influenza vaccine and effect on antibody responses in elderly persons.* Arch. Intern. Med., 2006. **166**(10): p. 1121-1127.

142. Gorse, G.J., Keefer, M.C., Belshe, R.B., Matthews, T.J., Forrest, B.D., Hsieh, R.H, Koff, W.C., Hanson, C.V., Dolin, R., Weinhold, K.J., Frey, S.E., Ketter, N., and Fast, P.E., *A dose-ranging study of a prototype synthetic HIV-1MN V3 branched peptide vaccine. The National Institute of Allergy and Infectious Diseases AIDS Vaccine Evaluation Group.* J. Infect. Dis., 1996. **173**(2): p. 330-339.

143.   Martanto, W., Moore, J.S., Couse, T., and Prausnitz, M.R., *Mechanism of fluid infusion during microneedle insertion and retraction.* J. Control. Release, 2006. **112**(3): p. 357-361.

144.   Davidson, A., Al-Qallaf, B., Das, D.B., *Transdermal drug delivery by coated microneedles: Geometry effects on effective skin thickness and drug permeability.* Chem. Engin. Res. Des., 2008. **86**(11A): p. 1196-1206.

145.   Gill, H.S., Denson, D.D., Burris, B.A., and Prausnitz, M.R., *Effect of microneedle design on pain in human volunteers.* Clin. J. Pain, 2008. **24**(7): p. 585-594.

146.   Schwartz, E., Shlim, D.R., Eaton, M., Jenks, N., and Houston, R., *The effect of oral and parenteral typhoid vaccination on the rate of infection with Salmonella typhi and Salmonella paratyphi A among foreigners in Nepal.* Arch. Intern. Med., 1990. **150**(2): p. 349-351.

147.   Toews, D.W., *A communitywide needle/syringe disposal program.* Am. J Public Health, 1995. **85**(10): p. 1447-1448.

148.   Ekwueme, D.U., Weniger, B.G., and Chen, R.T., *Model-based estimates of risks of disease transmission and economic costs of seven injection devices in sub-Saharan Africa.* Bull. World Health Organ. , 2002. **80**(11): p. 859-870.

149.   Smalls, L.K., Wickett, R.R., and Visscher, M.O., *Effect of dermal thickness, tissue composition, and body site on skin biomechanical properties.* Skin Res. Technol., 2006. **12**(1): p. 43-49.

150.   Ryu, H.S., Joo, Y.H., Kim, S.O., Park, K.C., and Youn, S.W., *Influence of age and regional differences on skin elasticity as measured by the Cutometer.* Skin Res. Technol., 2008. **14**(5): p. 354-358.

151.   Williams, J., Fox-Leyva, L., Christensen, C., Fisher, D., Schlicting, E., Snowball, M., Negus, S., Mayers, J., Koller, R., and Stout, R., *Hepatitis A vaccine administration: comparison between jet-injector and needle injection.* Vaccine, 2000. **18**(18): p. 1939-1943.

152.   Simonsen, L., Clarke, M.J., Schonberger, L.B., Arden, N.H., Cox, N.J., and

Fukuda, K., *Pandemic versus epidemic influenza mortality: a pattern of changing age distribution.* J. Infect. Dis., 1998. **178**(1): p. 53-60.

153.   Plotkin, S.A., (Ed.), *Mass vaccination: Global aspects - Progress and obstacles*, ed. Springer. 2006, Berlin Heidelberg, New York.

154.   *Centers for Disease Control and Prevention (CDC), Vaccine preparation and disposal.* Vaccine Storage and handling Toolkit: p. 1-7.

155.   Chen, D., Endres, R.L., Erickson, C.A., Weis, K.F.,McGregor, M.W., Kawaoka, Y., and Payne, L.G., *Epidermal immunization by a needle-free powder delivery technology: immunogenicity of influenza vaccine and protection in mice.* Nat. Med., 2000. **6**: p. 1187-1190.

156.   Harper, S.A., Fukuda, K., Cox, N.J., and Bridges, C.B., *Using live, attenuated influenza vaccine for prevention and control of influenza: supplemental recommendations of the Advisory Committee on Immunization Practices (ACIP).* MMWR Recomm. Rep., 2003. **52**(RR13): p. 1-8.

157.   DeMerlis, C.C., and Schoneker, D.R., *Review of the oral toxicity of polyvinyl alcohol (PVA).* Food Chem. Toxicol., 2003. **41**(3): p. 319-326.

158.   Levine, M.M., *Can needle-free administratin of vaccines become the norm in global immunization?* Nat. Med., 2003. **9**: p. 99-103.

159.   Howard, A., Mercer, P., Nataraj, H.C., and Kang, B.C., *Bevel-down superior to bevel-up in intradermal skin testing.* Ann. Allergy Asthma immunol., 1997. **78**(6): p. 594-596.

160.   Baxby, D., *Smallpox vaccination techniques; from knives and forks to needles and pins.* Vaccine, 2002. **20**(16): p. 2140-2149.

161.   Mahalingam, S., Damon, I.K., and Lidbury, B.A., *25 years since the eradication of smallpox: why poxvirus research is still relevant.* Trends. Immunol., 2004. **25**(12): p. 636-639.

162.   Nicolas, J.F., Guy, B., *Intradermal, epidermal and transcutaneous vaccination: from immunology to clinical practice.* Expert Rev. Vaccines, 2008. **7**(8): p.

1201-1214.

163.   Widera, G., Austin, M., Rabussay, D., Goldbeck, C., Barnett, S., Chen, M., Leung, L., Otten, G.R., Thudium, K., Selby, M.J., and Ulmer, J.B., *Increased DNA vaccine delivery and immunogenicity by electroporation in vivo.* J. Immunol., 2000. **164**: p. 4635-4640.

164.   Selby, M., Goldbeck, C., Pertile, T., Walsh, R., and Ulmer, J., *Enhancement of DNA vaccine potency by electroporation in vivo.* J. Biotech., 2000. **83**(1-2): p. 147-152.

165.   Sun, Y., Carrion, R. Jr., Ye, L., Wen, Z., Ro, Y.T., Brasky, K., Ticer, A.E., Schwegler, E.E., Patterson, J.L., Compans, R.W., and Yang, C., *Protection against lethal challenge by Ebola virus-like particles produced in insect cells.* Virol., 2009. **383**(1): p. 12-21.

166.   Ge, J., Deng, G., Wen, Z., Tian, G., Wang, Y., Shi, J., Wang, X., Li, Y., Hu, S., Jiang, Y., Yang, C., Yu, K., Bu, Z., and Chen, H., *Newcastle disease virus-based live attenuated vaccine completely protects chickens and mice from lethal challenge of homologous and heterologous H5N1 avian influenza viruses.* J. Virol., 2007. **81**(1): p. 150-158.